Image Analysis Using Fuzzy Mathematical Morphology: Advances and Applications

by

Muffaddal D. Ghadiali, BEng (Hons)

A thesis submitted for the Degree of Master of Philosophy
in the Department of Electronic Engineering of the
Hong Kong Polytechnic University

Department of Electronic Engineering,
The Hong Kong Polytechnic University

November 1996

To My Family

Preface

Contemporary computing systems are moving towards more intelligent machines capable of mimicking human perception and cognitive processes. This has attracted considerable interest towards computer and machine vision systems which have gained prominence, especially in the latter half of the century. The applications of computer vision are continually broadening in scope, fueled by the rising demand for systems with analytical and reasoning capabilities, coupled with the availability of powerful computing machines. Low level image processing techniques cater to the needs of automated vision systems by providing tools that can be used to process initially acquired information, in a manner that is useful to higher processes of the vision system.

The work presented in the course of this thesis is focused on one such image processing technique called mathematical morphology. Although the theoretical foundations that constitute the basic principles of mathematical morphology were established more than three decades ago, it has attracted considerable interest only in the past decade. The appeal of mathematical morphology lies in the intuitive manner in which all morphological operations are constructed and implemented. Understanding and realizing mathematical morphology based algorithms is quite intelligible even for the inexperienced as most operations are attuned with human intuition and thus easy to grasp. The research work undertaken during the tenure of the MPhil program, covered areas of academic interest as well as industry value. In terms of academic contribution, we propose new theoretical formulations which essentially forms the basis for the Fuzzy Pattern Spectrum. This is based on extending the foundations established thus far in the context of fuzzy mathematical morphology. From the perspective of application of these theoretical concepts to practical applications, we have designed and implemented algorithms such as the Vehicle License Plate segmentation and Tropical Cyclone segmentation algorithms, that can be implemented by economically feasible systems and offer viable performance. Additionally, the application of fuzzy pattern spectrum as a multi-level shape classifier and texture descriptor is demonstrated.

Acknowledgements

At the outset, I wish to express my sincere appreciation to my chief supervisor, Dr. Joe C. H. Poon and co-supervisor Professor Wan-Chi. Siu, for their support, encouragement and caring during the course of my graduate study. The endless hours of discussion and their unflinching dedication have endowed me with an experience I shall long cherish.

I also wish to express my gratefulness to the Research Degrees Committee of Department of Electronic Engineering, for extending the opportunity and the financial support for me to pursue a graduate degree in the Hong Kong Polytechnic University. Thanks are also due to all the faculty, my research colleagues (Mr. Gary Man, Mr Bity Chau, Mr. James Kwok and many others), laboratory technicians (Mr. W. W. Hong and Mr. Eric Tse) and undergraduate project students (Mr. Daniel Chow) for their assistance in many unaccountable ways.

In Indian culture, to express gratitude to one's family would mean expressing gratitude to oneself. As a token of my appreciation, I dedicate this thesis to all members of my family, for their constant encouragement, patience and support without which this effort may have been insurmountable.

Statement of Originality

The following contributions reported in this thesis are claimed to be original:

1. The Fuzzy Pattern Spectrum

We propose the novel concept of the fuzzy pattern spectrum, which essentially employs the mathematical basis proposed in the context of fuzzy mathematical morphology, in tandem with fuzzy set theoretic tools to determine the residues generated by a fuzzy erosion or a fuzzy opening. Thus, the fundamental advantage in employing the fuzzy pattern spectrum is that it provides the tools to quantify the spatial uncertainty which can be used directly in a decision making process, without compromising on the spatial information available within the image.

2. The Segmentation Algorithm for GMS Imagery

A novel feature extraction algorithm to segment tropical cyclones from Geo-stationary Meteorological Satellite (GMS) images has been designed. The underlying principle in designing such a system, was based on the distinction of features associated with tropical cyclones, while excluding those of unrelated cloud formations in the image. The designed algorithm, is in fact based on the intuitive approach used manually by a human expert and employs the tools of mathematical morphology to extract these two features. This algorithm can be expected to serve as part of a complete expert system to automatically locate or estimate tropical cyclone positions from an image and track possible movement in an automated tropical cyclone tracking system.

3. The fuzzy pattern spectrum as a novel texture descriptor

The drawback of the traditional pattern spectra is their inability to deal with the fuzziness in terms of image gray levels. The images need to be binarised to determine the residues and the resultant pattern spectra are highly sensitive to the thresholds in actual implementation.

The fuzzy pattern spectrum alleviates this problem by dealing with gray level images directly and quantifies the shape-size distributions in terms of fuzzy memberships.

Table of Contents

List Of Figures

List Of Tables

List of Publications and Submissions

International Journal Papers

1. M. D. Ghadiali, Joe C.H. Poon, W.C. Siu, "The fuzzy pattern spectrum as a texture descriptor", *Electronics Letters*, vol.32, no.19, pp.1772-1773, September, 1996.

2. M. D. Ghadiali, Joe C.H. Poon, W.C. Siu, "Multilevel Shape Representation and Classification using the Fuzzy Morphological Pattern Spectrum", submitted for possible publication in *Fuzzy Sets and Systems.*

3. M. D. Ghadiali, Joe C H Poon, W.C. Siu, "Segmentation of tropical Cyclones from GMS imagery using Mathematical Morphology", submitted for possible publication in *IEEE Transactions on Geoscience and Remote Sensing.*

International Conference Papers

1. Joe C H Poon, M. Ghadiali, G M Man, M S Lau, "A Robust Vision System for Vehicle License Plate Recognition using gray scale Morphology", *International Symposium on Industrial Engineering*, vol. 1, pp. 394-399, Greece, 1995.

2. M. D. Ghadiali, Joe C H Poon, "Adaptive image enhancement algorithms using non-liner techniques in the fuzzy property plane", *Applications of Digital Image Processing XIX (SPIE'96)*, Denver, USA, 1996.

Chapter One

INTRODUCTION

1.1 Overview and Scope of Research

The advent of powerful computing systems have made it feasible to realize automated machines and devices having levels of intelligence thought to be impractical earlier. Computer vision systems comprise one such area of research that has attracted tremendous interest for the in the latter half of the century and promises potential for a vast range of applications. This chapter presents an overview and establishes the foundations for the work presented in this monograph.

1.1.1 Digital Image Representation

Perhaps mankind's greatest achievement would be a creation that would equal or even surpass his own intellectual and cognitive abilities. Although this goal may seem unrealistic and is obviously far from being accomplished, computing systems have nevertheless become indispensable in everyday operations. At the beginning of this century, the "analytical engine" (the first theoretical proposition for a computing system) visualized by Charles Babbage would have taken an area over the size of a few football fields and thus was thought to be impossible to practically implement. As we approach the end of the century, microprocessors with a hundred times the computing power of the analytical engine can be packed into a silicon chip the size of a thumbnail.

As automated systems penetrate into every sphere of our daily lives, the demands for more "intelligent machines" has increased dramatically, fueled by the tremendous increase in the computing power available. Perhaps a key aspect of such an intelligent machine would be its vision system, which enables it to "see" and "understand" the environment around it. Though the human vision system is well understood in terms of its physiological organization, a complete machine vision system that parallels it's operation still far from realization. However some aspects of the human vision system have been successfully implemented to certain areas such as character and pattern recognition, with encouraging results (Gonzales, Woods [1992]). Computer vision and image processing system have been employed for applications ranging from bio-medical imaging to character and 3-dimensional object recognition (Russ, 1992). A typical machine vision system is usually made up of the sub-systems shown in Fig. 1.1. The image acquisition process is performed by any device that can be used to capture a natural scene to a digital image format, and usually include CCD cameras, scanners and so on.

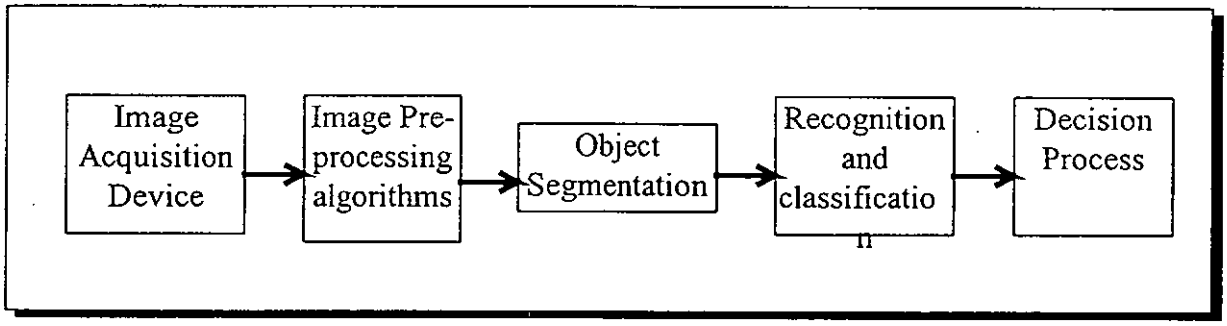

Figure 1.1: A generic representation of a Machine Vision System

Digital imaging can be broadly segmented into two categories. The low level processes, (which usually include image processing operations), are used to process pixel level information which is acquired from an image acquisition device such as a CCD camera. Low level image processing is used essentially to pre-process the raw image so that it can be useful to higher level processes. An instance of a typical low level process could be a simple order statistical or morphological filter. In high level processing, the image information is used to extract and process characteristics which may not be directly apparent in the spatial domain representation. These process typically involve segmentation of objects or feature extraction. The high level processes perhaps surpass the capabilities of the human vision systems in certain instances. A

classic example of such a process is the Fourier transform, that describes the frequency content of an image and is a powerful tool in image processing, which is not intuitive to the human vision process (Russ, 1992). The results from higher level processes are then used by decision algorithms, such as in an expert system. Our focus will be primarily on the techniques related to mathematical morphology, where we present some new developments and applications in this thesis.

1.1.2 Investigation Background

Mathematical morphology (Serra, 1987)or image algebra has attracted considerable interest in the image processing research since its initial inception about three decades ago. As its name indicates, mathematical morphology has sought to quantify the fundamentally intuitive, though mathematically elusive concepts of structure, shape and form. Mathematical morphology draws its concepts from a branch of stochastic geometry known as Minkowski algebra (Matheron, 1975). The usefulness of mathematical morphology stems from the fact that it perceives an image in terms of its features and geometric topology rather than an abstruse signal, thus providing tools that are more in tune with our cognitive processes. Mathematical morphology has been proved to be useful in diverse applications that require feature extraction algorithms (useful in image segmentation) and in constructing shape descriptors that can be used in object classification or pattern recognition (Sternberg, 1986).

One of the current areas of related research has been the development of fuzzy mathematical morphology, based on incorporating concepts from the Fuzzy Set theory, (as proposed by L Zadeh, and which is perceived as a generalized interpretation of the classical set theory). Fuzzy mathematical morphology provides a cognitive tool to deal with *spatial uncertainty* or *fuzziness* in image features and characteristics such as shapi*ness* or edgi*ness*. Traditional morphology is in fact perceived as a subset of its fuzzy representation where morphological *fitting* is enhanced to the *degree of fitting*. In essence, fuzzy mathematical morphology provides an indispensable tool for dealing with the inherent vagueness or ambiguity in certain objects or images features. Rather than replace traditional operations, the

fuzzy operators can be employed in tandem with their non-fuzzy (or crisp) counterparts to provide the right blend of usability and simplicity.

1.1.3 Research framework

The scope of the research work presented in this thesis encompasses theoretical aspects as well as applications related to practical image processing problems. The theoretical constituent covers recent advances in mathematical morphology, with a focus on developments related to fuzzy mathematical morphology. Subsequently, we present new propositions that use contemporary research as its core basis. The application of these theoretical concepts to real world problems are discussed in the latter half, with an aim to practically realize automated systems with potential industrial value. The research process was initiated with an investigation of contemporary approaches in morphological image analysis. The first objective pursued was predominantly academic in nature, specifically in the context of fuzzy mathematical morphology. The aim was to employ the axioms so far developed in extending its theoretical ideas, which would be significant in terms academic value. To this effect, we have developed the theoretical foundation for the novel concept of the Fuzzy Pattern Spectrum and have consequently demonstrated its applicability as a shape classifier and texture descriptor. The application of the fuzzy pattern spectrum as a texture classifier has been published as a brief journal letter.

The subsequent work was aimed at solving real world problems with an emphasis on applicability of the theoretical foundations developed thus far. The approach was to apply the theoretical tools in feature extraction and shape classification problems. Completed research investigation has included the development of a robust vehicle license plate segmentation system which has been presented at an international conference. The research work related to the automatic segmentation of Tropical cyclones and tropical storms from remote sensed Geo-stationary Meteorological Satellite images is also under review for Journal submission. The nature of the problem was to design a feature extraction algorithm to segment tropical cyclones from Geo-stationary Meteorological Satellite (GMS) images. The underlying principle in designing such a system, was based on the distinction of features associated with tropical cyclones, while excluding those of unrelated cloud formations in the image. The designed algorithm, is in fact based on the intuitive approach used manually by a human expert and

employs the tools of mathematical morphology to extract these two features. This algorithm is expected to serve as part of a complete expert system to automatically locate or estimate Tropical cyclone positions and possible movement on a real time basis.

1.2 Thesis Outline

The thesis has been organized into six chapters. An introduction to mathematical morphology, basic morphological operations and its historical background are presented in chapter two. Chapter three introduces the extension of traditional mathematical morphology to its fuzzy interpretation and investigates the contemporary research work related to fuzzy mathematical morphology thus far, which essentially formed the basis of our research propositions. The applications of traditional as well as fuzzy mathematical morphology in solving real world problems are presented in terms of the vehicle license plate segmentation and tropical cyclone extraction algorithms in chapter four. The theoretical basis, qualitative analysis and applications of the Fuzzy Pattern Spectrum as shape and texture descriptor are discussed in chapter five. Finally, chapter six discusses the propositions for future research directions and concluding remarks.

Chapter Two

PRINCIPLES OF MATHEMATICAL MORPHOLOGY

2.1 Mathematical Morphology - a primer

The theory of Mathematical Morphology evolved from the need to interpret simplistic ideas of object form and structure from a mathematical perspective. The following sections present an introduction to the fundamental concepts of mathematical morphology, and its usefulness in image analysis.

2.1.1 An intuitive understanding of shape, form and structure

The concepts of *shape, structure* and *form* are fairly intuitive to the human understanding of objects, structures, patterns and so on. Nonetheless, it has proved to be a challenge to translate this simplistic perception of common objects and features into a quantified representation that is appropriate for processing by a machine having limited intelligence. As a case in point, how does one isolate *square-like* shapes or objects in a cluttered scene? Is it possible to extract *lines* and *circles* from complex, noisy images without using some form of an extemporaneous solution? The problem may seem trivial at first, but proves to be much too abstract for a pragmatic realization. The crux of this predicament lies in its difficulty to formulate a generic methodology without employing an ad hoc approach which inevitably proves to be the stumbling block. In essence, what one needs are some mathematical means or a set of tools to translate the intuitive and abstract concepts of shape and structure into quantifiable entities.

Morphology is a generic term used in diverse disciplines ranging from biological to the physical sciences. It essentially relates to the development or quantification of shapes, structures or organisms. Mathematical morphology is a tool used to explicate the humanistic notions of form and shape, with the aim to establish a methodology to quantify these abstract, albeit intuitive concepts. By utilizing some simple tools of Euclidean set theory (namely set intersection, union, translation and complement), mathematical morphology purveys a tangible interpretation of the ideas of *shape* and *form*.

2.1.2 The historical background

Mathematical morphology or image algebra finds its roots in a branch of stochastic geometry known as Minkowski algebra. The work was initiated in the early 1960s by two researchers Georges Matheron [1975] and Jean Serra [1987], then at the Paris School of Mines in Fontainbleu, France. Their interest was initially in the areas of mineralogy and petrology, the aim being to characterize the properties of certain elements, such as permeability of porous materials like soil and rocks, by understanding their underlying geometric form and structure. Later, investigators including Sternberg [1986], Haralick [1987] extended the morphological filtering concepts initially designed for sets to functions. The long series of interactions between theory and implementation resulted in the monograph by Serra [1987], that became the origin for morphological filtering axiomatics. Though Matheron's and Serra's works established the theoretical basis for mathematical morphology, to the practicing engineer what was needed was a more simplified exposition. It was essential that the underlying concepts be presented in a manner that would be easily grasped by researchers who may not have in depth knowledge of stochastic geometry, random sets and lattice theory. Such tutorials, by Maragos [1987], Vincent [1992], et al were aimed primarily at presenting concepts from an application oriented perspective, without delving into the theoretical specifics. It took over three decades from the initial developments for the theoretical foundations to be employed in diverse engineering areas such as medical imaging, analysis of remote sensed imagery and feature extraction from complex images.

In recent years, there has been considerable interest in the relatively new area of fuzzy mathematical morphology (Dougherty [1992], Bloch [1993]) which seeks to combine traditional morphological filtering concepts and fuzzy set theoretic ideas to gain an understanding into the spatial ambiguity or fuzziness in image features. In conclusion, it seems that there was a significant lag in the application of the initial developments to practical realizations. Perhaps, this can be attributed to the exponential growth and availability of computing resources to successfully implement the theoretical axioms in useful real time implementations.

2.1.3 Morphological Filtering concepts

Mathematical morphology perceives images as an Euclidean sets. Thus, all classical set operations can effectively be used to operate on and transform this set. An image can be imagined to be analyzed using a random probe that quantifies the geometric meaning of a shape and its structure. This probe is called the *structuring element*, in the terminology of mathematical morphology. An image can be transformed and analyzed using structuring elements which are in fact smaller sets (or images) in themselves. The structuring element is similar to a kernel, template or moving window used in various other image processing techniques. The fundamental difference between structuring elements and kernels or moving windows is the flexibility in terms of its size and shape and the location of its origin or *hot-spot*. It should be noted that kernels or moving windows are invariably square matrices, with origins implicitly placed at their geometric centers. This difference may appear trivial at first glance, but proves to be a determining factor in distinguishing morphological operators from other techniques. The question that comes to mind is, how does one define these parameters (namely, size, shape and origin) of the structuring elements? This obviously is based on what shape, feature or characteristic one wishes to extract or segment. Thus, it is the designers outlook to appropriately select the parameters for a structuring element such that the end result will be as close to the one required. Nevertheless, this does not prove to be a daunting task since the design process is fairly intuitive.

2.2 Morphological Operations

The operations used in mathematical morphology essentially combine min-max algebra to image analysis problems. These concepts are adopted from a derivative of stochastic geometry, termed Minskowski Algebra, wherein a random probe is used to analyze geometric parameters.

2.2.1 Minkowski Algebra

We begin the discussion of morphological operation by defining some basic set operations. The translation of a set A by a vector x $(x \in \mathbb{R}^2)$ is defined as

$$A_x = A + x = \{ a + x : a \in A \} \qquad \textit{Eqn. 2.1}$$

Thus we assume x as a vector which shifts all elements of the set A. The following Fig 2.1 demonstrates the above idea. Now, the Minkowski addition of two sets A and B, can be shown using the Eqn. 2.1 as follows

$$A \oplus B = \cup \{ A + x : x \in B \} \qquad \textit{Eqn. 2. 2}$$

Thus, the Minkowski addition is simply the union of all translations of a set by each element of another set.

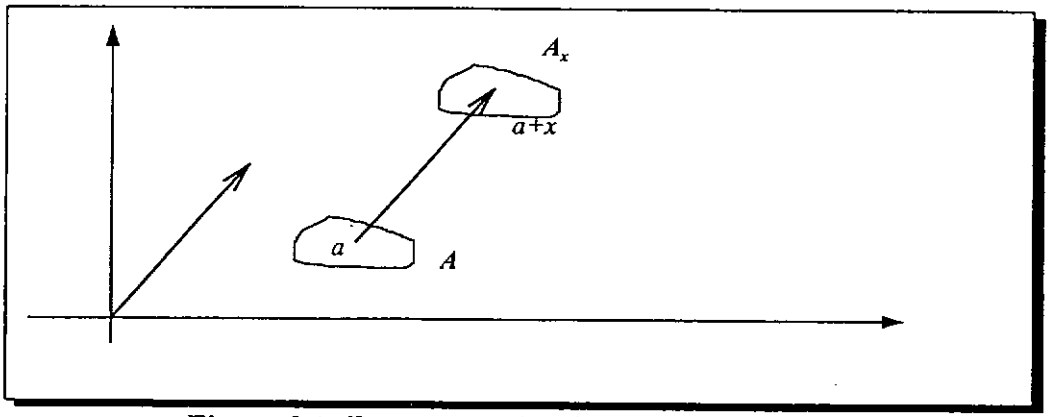

Figure 2.1: Representation for the Minkowski addition

In this vein, we can now define the Minkowski subtraction between sets A and B, which is simply the intersection of the translates of A by all elements of B. Thus,

$$A \ominus B = \cap \{A + x : x \in B\} \qquad \textit{Eqn. 2. 3}$$

These two operations discussed above have certain fundamental properties based on their stated definitions. The most immediate property from Eqn. 2.1, is *translation invariance* which provides that the Minkowski operation can be applied before or after translation of the set, bearing the same result. *Commutativity* and *associativity* provide for the fact that the order or sequence of operation do not affect the end result, thus,

$$A \oplus B = B \oplus A \qquad \textit{Eqn. 2. 4}$$

$$(A \oplus B) \oplus C = A \oplus (B \oplus C) \qquad \textit{Eqn. 2. 5}$$

2.2.2 Basic Morphological Operators

The most basic of morphology operations is *erosion*. Erosion serves as a *marker* for the locations at which the translate of the structuring element completely *fits* inside the image. Thus erosion of an image S by a structuring element E ($E \subseteq \mathbb{R}^I$) is denoted as

$$S \ominus E = \{x \in E \mid E_x \subseteq S\} \qquad \textit{Eqn. 2.6}$$

where $\mathcal{T}(S; x)$ denotes the translate of image S by $x \in E$

Alternatively erosion can be perceived as the intersection of all the image translates, with each translation corresponding to an element of the structuring element. Mathematically, we have

$$S \ominus E = \cap \mathcal{T}(S; x) \qquad \textit{Eqn. 2.7}$$

The dual operator of erosion is dilation, which is the union of the translates of the structuring element for each point at which its origin lies within the image feature. Dilation can thus be defined in the following ways.

$$S \oplus E = \{x \in \mathbb{R}^I \mid E^C \cap S \neq \varnothing\} \qquad \textit{Eqn. 2.8}$$

$$S \oplus E = \cup T(S;x) \qquad \text{Eqn. 2.9}$$

$$S \oplus E = (S^c \ominus (-E))^c \qquad \text{Eqn. 2.10}$$

The use of $(-E)$ indicates that dilation can be accomplished by complementing the image, eroding it with a reflection (flipping the structuring element about the two axes) of the original structuring element and finally complementing the result. It is to be noted that for a symmetrical structuring element with the origin at its center, the reflection is not needed.

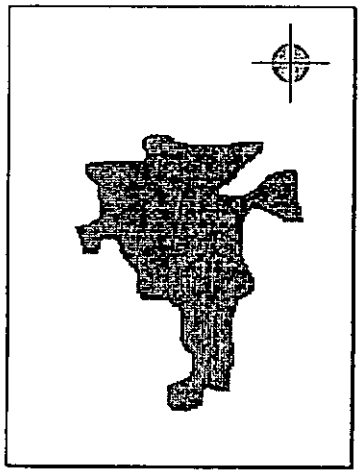

Figure 2.2: The Original Image - Island Profile

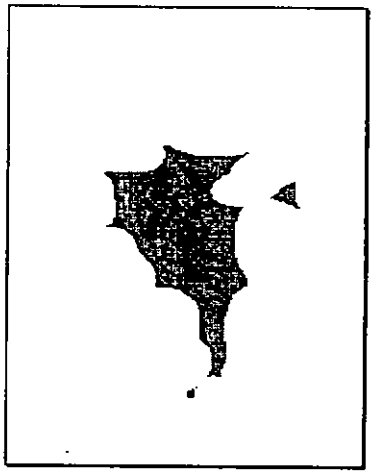

Figure 2.3: Erosion by a disk shaped structuring element

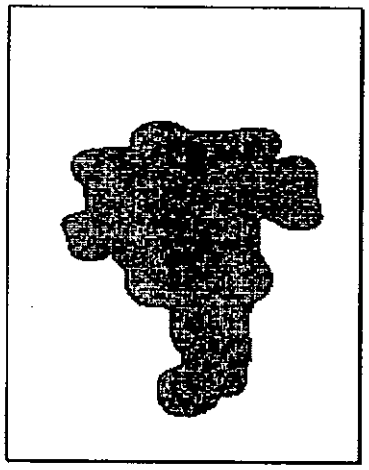

Figure 2.4: Image Dilated using the disk structuring element

The above three images show erosion and dilation of a binary image by a disc shaped structuring element with its origin at the center of the disc (Fig. 2.2 top right). As seen above, erosion causes shrinking of the image by eliminating the features that do not lie within the support of the structuring element (Fig. 2.3). Dilation causes expansion of the image, fills the intrusions and smoothes the edges of the image(Fig. 2.4). The basic morphological operators were defined for binary images and structuring elements only, however the scope has been extended using the concepts of multi-leveled functions to extend these operators to gray scale images and structuring elements. Erosion (dilation) have the following properties.

- *translation invariance* i.e., $S_x \oplus E = (S \oplus E)_x$ and $S_x \ominus E = (S \ominus E)_x$
- *increasing* i.e., $S \subseteq T$ then $(S \oplus E) \subseteq (T \oplus E)$ and $(S \ominus E) \supseteq (T \ominus E)$

For the discrete digital case we consider an image pixel to be a tuple $(x,y) \in \mathbb{Z}^+$ where x and y represent the row and column co-ordinate of each pixel. To implement a binary erosion (binary structuring element and image) the structuring element is translated to each pixel in the image and the result is a white pixel if *all* pixels within the structuring element support are white, else it is black. In the case of dilation the structuring element is translated to each pixel in the image in similar fashion. The result is a white pixel if *at least* one pixel within the structuring element support is white, else it is black.

2.2.3 Extending the concepts to functions

Any signal having d-dimensions can be represented mathematically by a function of d independent variables. If this signal assumes only two values (bi-level), it is termed as a *set* in $\mathbb{R}^d$. Such is the case for a binary image, which will assume two values, namely black and white. When a signal assumes more than one value (multi-leveled), it is termed as a *function* in $\mathbb{R}^1$, which is the case for gray scale images. Thus, for the purpose of processing we shall deal with 2-D sets and functions exclusively.

The basic morphological operations presented for binary images are extended to multi-level images, using the concepts of the Umbra transformation [Sternberg,1986]. The umbra $U(f)$ of a function f: is defined as

$$U(f) = \{ (x,t) \in D \times V : f(x) \geq t \} \qquad \text{Eqn. 2.11}$$

Thus the umbra of a function is defined as consisting of all points that occupy the space below the graph of f to -∞, within the domain D and range V.

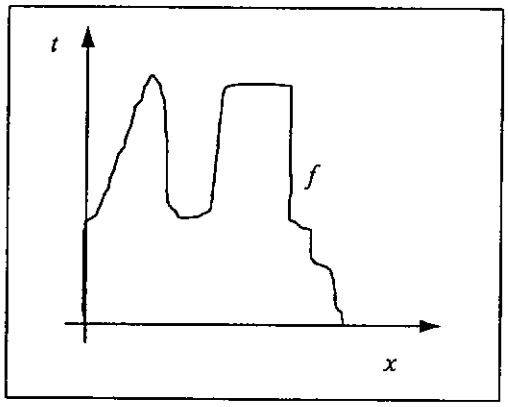

Figure 2.5: Graph of Multileveled function *f*

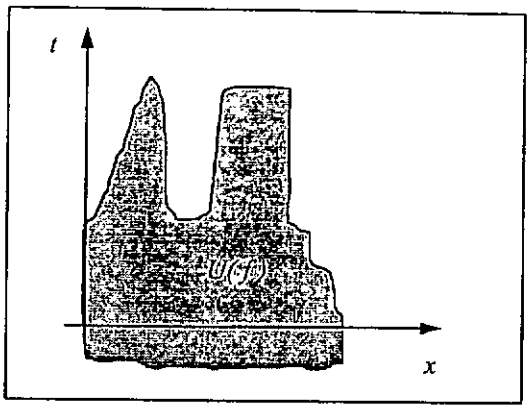

Figure 2.6: The Umbra of *f*, *U(f)*

This concept is demonstrated in the Fig.2.5 and Fig.2.6. Conversely, one can uniquely reconstruct the original function *f* by considering the suprema of all *t*, such that $(x,t) \in U(f)$. Thus

$$T[U(f)] = sup \{ t : (x,t) \in U(f). \} \qquad \text{Eqn. 2.12}$$

Using the above definition we can now define the morphological operations for multi-leveled functions. Gray scale erosion of function *f* by function *b* is defined as,

$$f \ominus b = T[U(f) \ominus U(b)] \qquad \text{Eqn. 2. 13}$$

And similarly, the gray scale dilation of function *f* by function *b* is defined as,

$$f \oplus b = T[U(f) \oplus U(b)] \qquad \text{Eqn. 2. 14}$$

The underlying physical meaning of the umbra is to essentially represent the function as a stack of binary sets piled one on top of the other. We can then apply the definition of binary erosion and dilation to obtain the dual operations for gray scale images. A gray scale image can be considered as a function *s*, of varying pixel intensities. Morphological operations are performed on such images using binary (*function-set* operations) or gray scale (*function-function*

operations) structuring elements. These operations are classified into the following groups based on the type of image and structuring element involved.

a) Function-Set operations:

$$(s \ominus E)(x) = inf \{f(y) \mid y \in E_x\} \qquad Eqn.\ 2.15$$

$$(s \oplus E)(x) = sup \{f(y) \mid y \in E_x\} \qquad Eqn.2.16$$

In the discrete (digital) case the function-set erosion is computed by translating the binary structuring element E, to each pixel in the gray scale image s, and the result is the minimum of the image pixel intensities within the support of the structuring element. Dilation is simply the maximum of the image pixel intensities within the support of the structuring element.

b) Function-Function operations:

$$(s \ominus e)(x) = inf \{f(y) - e(x-y) \mid y \in E_x\} \qquad Eqn.2.17$$

$$(s \oplus e)(x) = sup \{f(y) + e(x-y) \mid y \in E_x\} \qquad Eqn.2.18$$

In the discrete (digital) case the erosion is computed by translating the gray scale structuring element to each pixel in the gray scale image and the result is the minimum of the pixel wise difference between the image pixel intensities and the support of the structuring element. The function-function dilation is implemented by calculating the maximum of the pixel wise sum between the image pixel intensities and the support of the structuring element.

2.2.4 Secondary Morphological Operators

Erosion and dilation can be used to derive secondary operators which provide powerful tools in terms of practical applicability. A cascade of erosion and dilation yields a useful transformation known as an *opening*, whereas the cascade of a dilation followed by an erosion is termed as a *closing*. The effect of closing is to fill up holes and intrusions in the image structure,

whereas opening is useful in isolating or eliminating smaller features, while preserving the general structure in the image. Opening ($\circ$) and closing ($\bullet$) are expressed as

$$S \circ E = (S \ominus E) \oplus E) \qquad Eqn.\ 2.19$$

$$S \bullet E = (S \oplus E) \ominus E) \qquad Eqn.\ 2.20$$

Openings and closings have been used extensively in algorithms to eliminate redundant features and to merge others based on the processing needs.

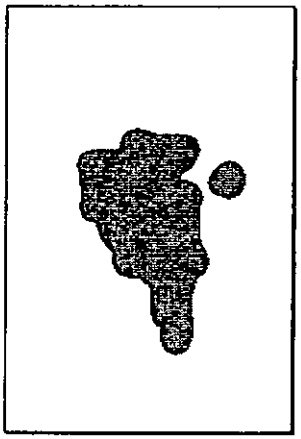

Figure 2.7:The morphological Closing

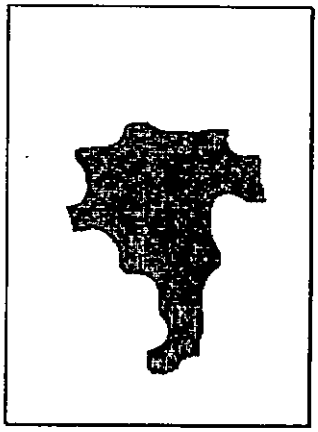

Figure 2.8: The morphological Opening

Openings (closings) have the following properties

translation invariance i.e., $S_x \circ E = (S \circ E)_x$ and $S_x \bullet E = (S \bullet E)_x$;

increasing i.e., if $S \subseteq T$ then $(S \circ E) \subseteq (T \circ E)$ and $(S \bullet E) \subseteq (T \bullet E)$;

anti-extensivity (extensivity) i.e., $(S \circ E) \subseteq E$ and $(S \bullet E) \supseteq S$;

idempotence i.e., $((S \circ E) \circ E) = (S \circ E)$ and $((S \bullet E) \bullet E) = (S \bullet E)$;

Since openings (closings) are increasing (anti-extensive), they essentially preserve the relation of subsethood between objects opened (closed) by the same structuring element.

Idempotence is a powerful property that guarantees the convergence of the opening. In this sense, an image which is opened by a given structuring element remains unchanged after the initial opening. Thus, if an image A is opened by a structuring element B, it remains unchanged for subsequent openings by B, and is called *B-open*. Additionally, if there is a second structuring element C, such that $C \subseteq B$, then opening any *B-open* image will result in no change in the image. The same properties hold true for the morphological closing in a dual fashion.

An interesting paradigm to understand the conceptual underpinnings of mathematical morphology can be seen in the theory of *cellular automata*, which consists of evolution or degeneration of *cells* based on certain criteria in relation to their neighborhoods. In essence, mathematical morphology formalizes these criteria by representing neighborhoods as structuring elements and the subsequent operations within these neighborhoods, (which inherently embody elimination or generation) in terms of morphological operators such as erosion or dilation.

2.3 Morphological Transformations

Using the secondary operators one can further construct useful transformations. Of the many possible, we discuss only a few relevant to succeeding discussions.

2.3.1 The Top-Hat Transformation

The top-hat transform consists of the image difference between the original image and its opened result. It is implemented by determining the difference between the opened image and the original image before processing. The resultant of the top-hat is that regions that have been filtered out by the opening are preserved. Thus regions of spatial domains smaller than the structuring elements will be visible in the top-hat transformed image. Mathematically, we can represent the top-hat transformation as,

$$Tophat\ (A,B) = A - A \circ B \qquad \textit{Eqn. 2.21}$$

The original Lenna image (Fig. 2.9) and its top-hat transformed image (Fig. 2.10) are shown below. The opening was implemented using a digital disk shaped structuring element of ten pixels diameter.

Figure 2.9: The original Lenna image

Figure 2.10: The result of a top-hat transformation

As can be seen from the images above, the result of the top-hat transformation is to enhance the peaks while suppressing the smooth, low frequency regions. It can be perceived as rolling a ball on the intensity plot of the image and removing all regions not covered by the ball. In essence, the final result of the top-hat transform is based on the size of the structuring element employed for the opening. In later chapters, we shall demonstrate the use of the top-hat transform to isolate certain features of interest from a given image.

2.3.2 The Bottom-Hat Transformation

The dual of the top-hat transform is the bottom hat transform or the valley detector defined by

$$Bothat(A,B) = A - A \bullet B \qquad Eqn.\ 2.22$$

The bottom-hat transform is simply the difference between the closed image and the original. Consequently, the closing minus the original image is a bottom-hat transform.

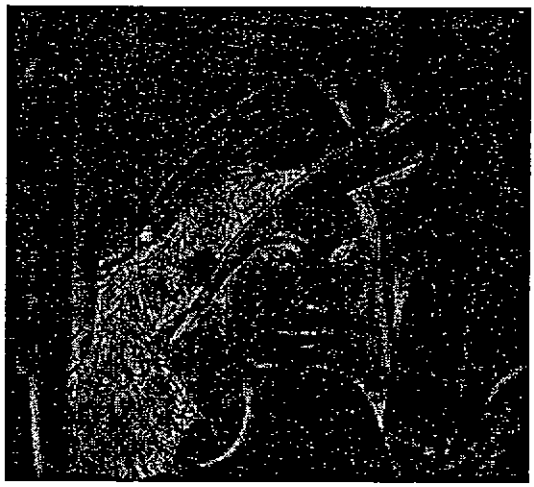

Figure 2.11: The result of a bottom-hat transformation

The bot-hat transformation of the original Lenna image by a digital disk of 10 pixels diameters is as shown above in Fig. 2.11. In the bot-hat transformation the resultant image preserves regions that have been filled up due to the closing. In terms of the rolling ball paradigm, it is similar to rolling the ball beneath the image surface and preserving regions within which the ball does not fit.

2.3.3 The Hit-or-Miss Transformation

The *hit-or-miss* transform is the adaptation to mathematical morphology of the technique of template matching used for object detection. The hit-or-miss uses a pair of disjoint structuring elements $D = (E, F)$[1] which are complementary within a specified window. The choice of size and shape of the structuring element pair is based on the features of object to be extracted. The hit element E detects all objects that minimally *fit* into it, by performing a simple binary erosion. The miss element F, on the other hand, eliminates all the objects that *do not fit* within the hollow support region of the structuring element. The results of the hit and miss operation are combined to give a the location of the object to be detected.

[1] $E \cap F = \varnothing$

$$S \circledast D = (S \ominus E) \cap (S^c \ominus F)$$

It should be noted that the hit-or-miss transform can be used for binary sets only, and has no equivalent operation in gray-scale morphology[2].

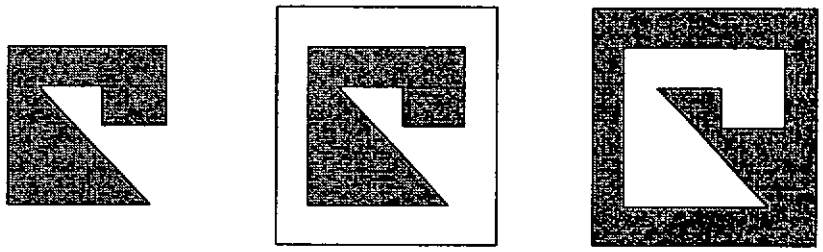

Figure 2.12: (a) Image Object (b) Hit element (c) Miss element

The above figure shows the binary object to be detected in Fig. 2.12(a), and the corresponding hit structuring element Fig. 2.12(b) and miss structuring element Fig. 2.12(c). It is obvious that the hit and miss structuring elements must be carefully designed to achieve the desired results. Moreover, this technique is sensitive to the variations in the image and the presence of noise may result in false detection or no detection at all.

2.3.4 Morphological Gradient

The morphological gradient consists of the difference between the dilated and eroded result of a given image. In essence the morphological gradient enhances the edges in an image. Fig. 2.13(a) and (b) shows the dilated and eroded result respectively of the original Lenna image by a structuring element disk of 10 pixels diameter. The morphological gradient is determined by the pixel wise difference of the dilated and eroded images, as shown in Fig. 2.11(c).

[2] This is one of the drawbacks resolved in fuzzy mathematical morphology

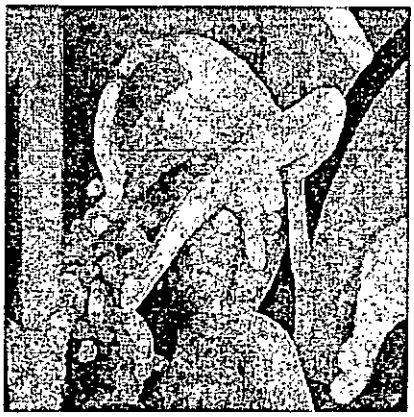

(a)Lenna image - Dilated

(b)Lenna image - Eroded

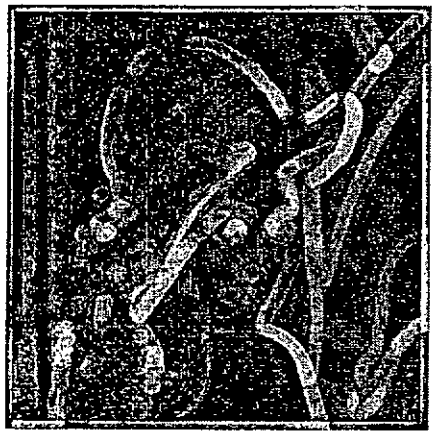

(c) The morphological gradient

Figure 2.13

Mathematically, the morphological gradient is denoted as

$$\nabla S = (S \oplus E) - (S \ominus E) \qquad \textit{Eqn. 2.23}$$

Amongst other useful morphological transformations are the morphological skeleton, morphological shape decomposition, watershed transforms and so on.

2.4 Implementation of Morphological operations

In the final section we discuss some algorithms for implementation of morphological operators and a brief overview of common hardware realization techniques. The algorithms

presented here are intended to demonstrate the design of programs used in implementing morphological operations.

2.4.1 The Morphological Erosion

The morphological erosion is computed based on how the structuring element is actually defined. For a binary structuring element each pixel belonging to the structuring element can be defined as "1", while not belonging as "0". To enable definitions of irregular, non-convex structuring element, certain pixels are defined as don't cares, denoted by "-1". The following is a short program pseudocode designed to calculate the set and function erosion for structuring elements for any shape, size and location of origin. The image and the structuring element pixels may be processed as arrays or streams based on the nature of the processing.

```
function Binary - Binary Erosion
Begin Image column scan
        Begin Image row scan
        s = stelem;  { first element in structuring element }
        result = 1;      { result TRUE at first }
Begin structuring element row scan
                if (s >= ZERO)  { active structuring element pixel }
                        temp = In { get image pixel }
                        if ( In = WHITE) then
                                Next structuring element pixel
                        Else
                                result = BLACK
                        Break structuring elements scan
                        Next SE element
        End of row scan
        Out = result'
        End of image column scan
        End of image row scan
End of Binary - Binary Erosion
```

Morphological (function-set) erosion of a gray-level image with a binary structuring element involves a slightly more complex implementation. The image and structuring element representations are the same as the earlier pseudocode.

```
function Gray scale - Binary Erosion
Procedure
Begin Image column scan
        Begin Image row scan
        s = stelem;  { first element in structuring element }
        result = WHITE;      { result is maximum at first }
Begin structuring element row scan
                if (s >= ZERO)  { active SE element }
                        temp = In { get image pixel }
                        if ( In > BLACK) then
                                result = Minimum (temp, result)
                                Next structuring element pixel
                        Else
                                result = BLACK
                        Break structuring elements scan
                        Next structuring element pixel
        End of row scan
        Out = result'
        End of image column scan
        End of image row scan
End of Gray scale - Binary Erosion
```

The function-function erosion is implemented by calculating the minimum of the pixel wise difference between the image pixel intensities and the support of the structuring element. The pseudocode remains the same as the implementation for function set erosion, the difference being in the manner the final result is calculated. In terms of computational requirements, the function-function erosion is the most computation intensive as each structuring element pixel represents a differencing operation.

```
function Gray scale - Gray scale Erosion
Begin Image column scan
        Begin Image row scan
        s = stelem;  { first element in structuring element }
        result = WHITE;      { result is maximum at first }
Begin structuring element row scan
                if (s >= ZERO)  { active SE element }
                        temp = In { get image pixel }
                        if ( In > BLACK) then
                                result = In - s
                                result = Minimum (temp, result)
                                Next structuring element pixel
                        Else
                                result = BLACK
```

Break structuring elements scan
Next structuring element pixel
End of row scan
Out = result'
End of image column scan
End of image row scan
End of Gray scale - Binary Erosion

2.4.3 Hardware Implementation Issues

An active area of research within mathematical morphology has been the implementation of morphological operations using fast algorithms and architectures so that they can be useful in real-time applications. Due to the large sizes and varying shapes of structuring elements, morphological operation can be extremely intensive in terms of computational requirements.

An advantage of morphological operations being applied in local neighborhoods is that they are highly suitable for parallel architectures. In general, most of the implementations can perform morphological operations larger than the neighborhood size by utilizing sequential neighborhood operation, but are yet limited in terms of the types of morphological operations that can be actually performed. Of recent interest has been the use of systolic array design (Djuntan et al[1994]). Instead of the conventional approaches based on cellular logic, the systolic array design makes use of the idea of generalized binary convolutions. The result is a gain in speed, design simplicity, reduced number of processor elements and suitability for VLSI implementation.

Commercially available hardware, such as the MVC 150/40 computation environment is one implementation that offers real-time morphological processing modules. These devices offer operation speeds of less than 7.5 msec for 512 x 512 images with 128 gray levels. Such implementations can be tailored to suit the application needs due to the flexibility in the range of operations and the specifications of the structuring elements.

2.4.4 Conclusion

The essence of this chapter has been to establish theoretical basis which forms the foundation of mathematical morphology. The effect of fundamental morphological operators such as erosion, dilation opening and closing have been demonstrated using simple examples. Additionally, some tertiary operations were discussed, which are essentially built using primitive morphological operators. In the following chapter we continue the discussion to more contemporary developments in mathematical morphology. The focus of the following chapters will be predominantly on developments related to combining the fuzzy set theoretic approach to traditional morphological operators.

Chapter Three

FUZZY SETS AND MATHEMATICAL MORPHOLOLGY

3.1 Fuzzy Sets and Image analysis

Mathematical morphology and Fuzzy Sets find common ground in the fact that both are essentially based on classical set theory. The combination of the tools of the fuzzy set theory to traditional morphological operations, gives "fuzzy" morphological operators that show some interesting properties. In this chapter we discuss theoretical as well as practical underpinnings resulting from the incorporation of fuzzy set theoretic concepts to morphological operators.

3.1.1 The Fuzzy Set theory

The Fuzzy Set theory, as proposed by L Zadeh [1965], is seen as a generalized interpretation of the classical set theory. In classical set theory (also termed as the *crisp set theory*) the membership (or the belonging) of each element relative to a set can be specified by a characteristic function which assigns a value of either 1 or 0, thereby dichotomizing the elements as members or non-members of the given set. As opposed to this, the fuzzy set theory proposes to determine the *degree* to which an element belongs to a particular set, hence the characteristic function (or *membership grade*) may take any value between in the interval [0, 1]. The underlying idea in the theory of fuzzy sets was to incorporate the human cognitive process, into the mathematical framework. In the words of Zadeh, "...mathematics of fuzzy or cloudy quantities which are not describable in terms of probability distributions."

The set of "*tall people*" is in itself an ambiguous concept. How does one define "*tall*", and hence establish the basis for classification? It is obvious that there is no universal classification mechanism that can give a unique answer.

The root of this problem lies in the ambiguity of the meaning of *tall*. The definition of *tall* may well be dependent on either the age group, sex, nationality or perhaps on all these parameters. Thus the set in itself is "fuzzy", with no rigid boundaries that can purvey a clear distinction between what can or cannot be considered *tall*. The fuzzy set theory attempts to solve this problem by assigning memberships to elements (or person) based on the height, sex, etc. The membership degree denotes our *belief* as to how likely a given candidate can be perceived to be tall. This is in accordance with the human cognitive notion of common ideas which do not have distinct dividing lines or Boolean logic based decision. Example of one such membership function could be the one shown in Fig. 3.1. The vertical axis represents the degree of membership of the element x represented on the horizontal axis. Thus in our case, the x-axis represents the parameter of height, while $\mu(x)$ (y-axis), represents the degree to which a certain candidate can be classified as *tall*. It is obvious that the actual function may vary based on the nature of the particular set in question.

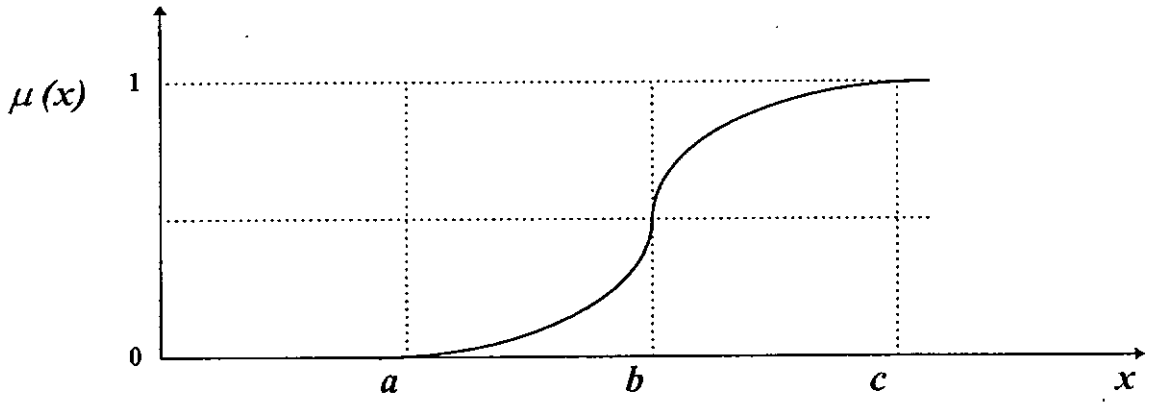

Figure 3.1: A typical fuzzy membership function

Consequently, larger the value of the membership grade, higher the possibility of that element belonging to the particular set. In the universe of discourse X, we can thus define the membership grade μ_A of element x to the fuzzy set A as

$$\mu_A(x) : X \rightarrow [\,0,\,1\,] \qquad \textit{Eqn. 3.2}$$

The basic fuzzy set operations in terms of their membership functions are defined as follows

union	$\mu_{A \cup B}(x) = max\ \{\ \mu_A(x),\ \mu_B(x)\ \}$
intersection:	$\mu_{A \cap B}(x) = min\{\ \mu_A(x),\ \mu_B(x)\ \},$
difference:	$\mu_{A/B}(x) = min\ \{\ \mu_A(x),\ 1 - \mu_B(x)\ \}$
complement:	$\mu_A^{c}(x) = 1 - \mu_A(x)$
algebraic sum:	$\mu_{A+B} = \mu_A(x) + \mu_B(x) - \mu_A(x) \cdot \mu_B(x)$
bounded sum:	$\mu_{A \oplus B}(x) = min\ \{\ 1,\ \mu_A(x) + \mu_B(x)\ \}$
bounded difference:	$\mu_{A \ominus B}(x) = max\{\ 0,\ \mu_A(x) + \mu_B(x) - 1\ \}$

It should be noted that even though probabilities and fuzzy memberships share the same evaluation space of [0,1], the point of departure lies in the fact that probabilities do not allow the any scope for *ignorance.* It is the concepts (definition of the sets) that are in themselves vague or fuzzy. Hence, it follows that the sum of all probabilities must equal unity. However fuzzy memberships have no such restrictions. In the universe of discourse X, we can thus define the membership grades μ of N elements $x_1 \ldots\ldots x_N$ to the fuzzy set A as

$$A = \cup\, \mu_i \,/\, x_i \qquad \textit{Eqn. 3.3}$$

3.1.2 Images - The fuzzy set theoretic perspective

The relationship between a fuzzy set and an image does not seem obvious at first glance. However, if we perceive the image as a set (which is incidentally also the morphological approach) the relationship becomes more distinct. An image can be interpreted as an array of

fuzzy singletons, and its local or global properties such as brightness, shape, edges can in effect be represented in terms of fuzzy membership grades (Goetcherian[1980]). The representation of an image of dimensions M x N ($M = \{m_j \mid j = 1...J\}$, $N=\{n_k \mid k = 1...K\}$), with L discrete gray levels in the fuzzy domain is denoted as

$$X = \cup\cup p_{mn} / x_{mn} \qquad \textit{Eqn. 3.4}$$

where p_{mn} $(0 \leq p_{mn} \leq 1)$ is the representation of the extent to which a given pixel x_{mn} $(0 \leq x_{mn} \leq L)$ posses a specific property. This property may be defined based on the nature of the application. The fuzzy set thus constructed based on this property is the *fuzzy property plane.*

3.2 Mathematical Morphology and the Fuzzy Set theory

3.2.1 Background

Recent work in this field has sought to augment the scope of traditional morphology (based on the classical crisp set theory) by applying the tools from the fuzzy set theory in order to gain an understanding into the *spatial uncertainty* (or *certainty*) knowledge base. Fuzzy mathematical morphology is thus an innovative combination of two popular techniques, the fuzzy set theory and morphological image analysis. The meeting point of these two techniques is that mathematical morphology is based on the classical set theory, which is conceived as a subset of the fuzzy theory.

The intuitively fundamental notion of *hard fitting* which forms the basis of morphology is extended to *degree of fitting.* A theoretical background for such a *fuzzy morphology* has been established by Dougherty et al [1993], and Bloch et al[1994]. There are diverse methods to arrive at a fuzzy morphology, simply due to the numerous functions to resolve the morphological fitting criteria to a fuzzy membership grade. Fuzzy mathematical morphology provides new operations on images that introduce spatial uncertain information which can be useful in decision processes linked to pattern recognition.

3.2.2 Need for Fuzzy Mathematical Morphology

In terms of the requirement of a fuzzy mathematical morphology, as far as practical applications are concerned, the traditional morphological erosion servers as a classic example. Erosion is basically employed to serve as a *marker* of the locations that satisfy the specified criteria. This marker is essentially bi-valued, indicating whether the specified structuring element fits or does not fit within the specific region. The hit-or-miss transform uses erosion in this vein, to determine the locations at which the structuring element pair *fit* inside and outside of image or object. As far as the practical applicability of this technique is concerned, it is obvious that this method is extremely sensitive to scale variation, shape tilt and noise, often resulting in misclassification or no detection at all. The reason being that classical erosion offers a limited evaluation space of $\{0,1\}$, resulting in the above condition.

Fuzzy mathematical morphology seeks to determine to what *extent* a shape belongs to a certain class by relaxing the evaluation space to [0, 1]. Consequently, in gray scale morphology we do not have a similar hit-or-miss transform equivalent operator. This problem is overcome by employing the fuzzy hit-or-miss transform (based on the fuzzy erosion) and thus be used to determine the fuzzy degree of fit.

3.2.3 Constructing a Fuzzy Mathematical Morphology

Several works have established the underlying theory for fuzzification of mathematical morphology operations and yet preserving its basic properties. Investigations have presented various approaches to provide the complete background theory that can be used to fuzzify all morphological operations. The conventional approach is to develop an *indicator for set inclusion* that will determine the degree to which a fuzzy set is a subset of another fuzzy set. This indicator, known as the *index function*, is of importance in formulating a fuzzy mathematical morphology where analysis of images is inherently dependent on the notion of *set inclusion.* There have been a variety of propositions for such a function, primarily due to the many ways for determining operations on functions equivalent to union and intersection, wherein the functions take values in the range [0,1].

As in any other mathematical formulation, the prevalent technique is to postulate axioms which should be satisfied by the index function, and develop a specific mathematical form for such an indicator. The necessary and sufficient conditions, under which the mathematical formulations will give rise to the required characterizations of index function, can then be specified. Albeit the fundamental theory of fuzzy mathematical morphology is well-developed in terms of characterizations of fuzzy Minkowski algebra, perhaps the theory is still lacking. Specifically, in the sense that work in the areas of a fuzzy granulometric theory, investigation of other image algebra resulting from modifying the constraints of the index function, translation invariant mappings and τ-openings are under investigation. From the variety of techniques developed, an appropriate definition can be adopted depending on the effects desired and the required properties.

3.3 Contemporary research work

The following sections discusses the current state-of-the-art in the context of research related to Fuzzy mathematical morphology. We discuss the works of research groups and present a comparative idea of the methodologies adopted by each group.

3.3.1 Dougherty, Sinha et al

The approach proposed by Dougherty et al[1993], is based on establishing the theoretical basis for the notion of set inclusion. The fundamental concept of subsethood or simply fitting has been extended using fuzzy set theoretic tools. Their approach is to formulate a set inclusion indicator or index function. Such an indicator is based on the concept that it satisfies certain axioms, which are in accordance with the general properties of traditional or crisp morphological operations.

The basis of their approach is founded on two key features. First, they provide an alternative generalization, one that offers the preservation of the traditional morphological erosion as a marker of fits within a binary image. They employ the traditional modeling of gray

scale images as fuzzy sets, by means of a mapping of pixel intensities (gray scale values) to fuzzy memberships. Thus, in effect a white pixel assumes membership 1, while black assumes 0, and all other gray levels mapped in the interval [0, 1]. Essentially, they denote the degree of belonging of each pixel to the given image. The fitting criteria is similarly mapped to fuzzy memberships, 1 denoting a complete fit whereas other values correspond to the degree of fitting. The exact mathematical representation of this fitting criteria is based on the choice of the index function employed.

The second aspect is the manner in which one can define such an indicator for set inclusion, that characterizes the morphological fitting criteria. The idea is to formulate a generalized interpretation, such that in the case of binary realizations is also preserved, essentially for {0, 1}. In this sense fuzzy mathematical morphology, is actually a complete generalization of traditional binary and gray scale morphologies, both of which are special cases of the fuzzy interpretations. The above formulation could well have been pursued in a non-fuzzy manner. However, this would miss the basic notion of modeling a fuzzy fitting that preserves the general fuzzy extensions of traditional mathematical morphology.

The mathematical formulation initially assumes that images are fuzzy subsets of the Cartesian or Euclidean grid, and a point (pixel) is considered as a fuzzy singleton. This assumption does not differ from the traditional manner in which the fuzzy set-theoretic approach is employed in image processing. The point of departure however lies in the fact that the fuzzy memberships are not merely used to replace traditional operators by their fuzzy counterparts, but to extend the morphological criteria of subset hood in terms of fuzzy fitting criteria. This is achieved using the indicator for set inclusion, which is essentially the mapping of two fuzzy sets (the image and the structuring element) to another fuzzy set (the degree of fitting). This indicator for set inclusion I, is defined thus,

$$I : [0,1] \times [0,1] \rightarrow [0,1] \qquad \textit{Eqn. 3.5}$$

The necessary and sufficient conditions for such an indicator I,in order that it may preserve the traditional morphological properties are specified by the following nine axioms:

1. $I(A,B) = 1 \Leftrightarrow A \subseteq B$

3. $I(A,B) = 0 \Leftrightarrow \{ x:\mu_A(x) = 1 \wedge \mu_B(x) = 0 \} \neq 0$

3. $B \subseteq C \Rightarrow I(A,B) \leq I(A,C)$

4. $B \subseteq C \Rightarrow I(C,A) \leq I(B,A)$

5. $I(-A,-B) = I(A,B)$ *and* $\forall x \in U,\ I(A,B) = I[T(A;x), T(B;x)]$

6. $I(A,B) = I(A^c, B^c)$

7. $I(B \cup C, A) = min[I(B,A), I(C,A)]$

8. $I(A, B \cap C) = min[I(A,B), I(A,C)]$

9. $I(A, B \cup C) \geq max[I(A,B), I(A,C)]$

The general postulation (Sinha, Dougherty, 1993]) for such an indicator, which satisfies the above axioms is given by the following formula

$$I(A,B) = \inf \min [1, \lambda(\mu_A(x)) + \lambda(1 - \mu_B(x))] \qquad Eqn.\ 3.6$$

In terms of practical interpretation of this formulation, the definition of λ will ascertain the criteria for determining the membership grade of the resultant morphological operation. The membership grade specifies the extent to which the eroded region lies *under* the structuring element. The following equations are some formulations that can satisfy the condition for λ: $[0,1] \rightarrow [0,1]$

$$\lambda_n = 1 - xn \qquad \forall\ n \geq 1 \qquad Eqn.3.7(a)$$

$$\lambda_n = (1 - x) / (1 + nx) \qquad \forall\ 0 \geq n \geq 1 \qquad Eqn.3.7(b)$$

$$\lambda_n = ((1/1 + xn) - x/2)) \qquad \forall\ n \geq Ln(3)/Ln(2) \qquad Eqn.3.7(c)$$

The value of n determines the noise sensitivity of the index function. As the value of n is increased, the index function becomes increasingly susceptible to noise. It essentially determines the extent to which the object and the noise can be distinguished.

Using the definition stated in Eqn. 3.7*(a)* for the indicator function, we can thus define the *fuzzy erosion* $\mathcal{E}$, of a fuzzy set $\mathcal{A}$ by a fuzzy structuring element $\mathcal{B}$ (with $n = 1$) as

$$\mu_{\mathcal{E}(\mathcal{A},\mathcal{B})} = inf\ min\ [\ 1,\ 1 + \mu_{\mathcal{A}}(x) + \mu_{T(\mathcal{B},x)}(x)\ ] \qquad Eqn.\ 3.8$$

Subsequently, the fuzzy dilation $\mathcal{D}$, can then be defined as

$$\mu_{\mathcal{D}(\mathcal{A},\mathcal{B})} = sup\ max\ [\ 0,\ \mu_{\mathcal{A}(x)} + \mu_{T(\mathcal{B},x)}(x) - 1\ ] \qquad Eqn.\ 3.9$$

It should be understood that the process of fuzzification of morphological operators is not simply to represent traditional crisp operations by merely fuzzifying the operators and operands themselves. This would mean a simple mapping from the crisp set operation to a fuzzy interpretation. The reasoning behind selecting the indicator for set inclusion is to model the fitting paradigm in morphology in an intrinsically fuzzy manner.

3.3.2 Bloch, Maitre

The propositions of the French group consisting of Bloch and Maitre [1994] appeared at about the same time as Dougherty et al. Their approach was based on the fundamental methods for decision making based on probabilities, the fuzzy set theoretic approach and the evidence theory. They suggested that the notion of spatial localization uncertainty is unavoidable due to the image formation process itself which may be dependent on the acquisition device and method, non-ideal impulse response, imperfect frame-scene registration and so on.

They argued that traditional mathematical morphology is not equipped to correctly manage uncertainty bounds and reliable detection simultaneously because of the inherent nature of the morphological structuring element. The coarse nature or the inflexibility in the way one can design the structuring element results in the limitation placed on to what extent one can express the knowledge uncertainty. Thus their basis was to adopt the fuzzy set theoretic approach is due to its inherent flexibility and their implication to pattern recognition.

The categorized fuzzy operations based on the definition of the image and structuring element either of which could be fuzzy or crisp.

The first case is a fuzzy image η dilated by a binary structuring element B, which is simply constructed from the α - cut set of η dilated by B, thus:

$$d_B(\eta) = \int d_B(\eta_\alpha)\, d_\alpha, \qquad \textit{Eqn. 3.10}$$

The actual computation of the fuzzy dilation at any element x of the fuzzy image will thus be denoted as

$$d_B(\eta)(x) = \sup\, \eta(y) \qquad \textit{Eqn. 3.11}$$

where $y \in B_x$

Considering a binary image X, dilated by a fuzzy structuring element ν can be obtained by the fuzzification over the structuring element ν, as follows,

$$d_\nu(X)(x) = \int d_{\nu\alpha}(X)(y)\, d_\alpha, \qquad \textit{Eqn. 3.12(a)}$$

Finally, we consider the fuzzy dilation of a fuzzy image η, by as fuzzy structuring element ν, similar to the sense of Dougherty et al's interpretation. Thus we have,

$$d_\nu(\eta)(x) = \int\int d_{\nu\alpha}(\eta)(x)\, d_\alpha d_\beta \qquad \textit{Eqn. 3.12(b)}$$

Thus for the computation of the fuzzy dilation, we have

$$d_\nu(\eta)(x) = \int \sup\, \eta(y)\, d_\alpha \qquad \textit{Eqn. 3.13}$$

The implication of the above definitions are that the global behavior of a fuzzy dilation is in agreement with the properties traditional morphological dilation, and in fact provide the general formulation for dilation of which the crisp operations are a subset. In terms of the intuitive understanding, membership values of those points are increased which were

considered "not surely" belonging to the fuzzy set which results in the propagation of local maxima within the specified neighborhood. The extension of the above concepts to construct fuzzy erosion would be simply to replace the maxima or supremum in the equation by the minima or infimum.

3.3.3 Maccarone, Di Gesu, et al

The approach adopted by Maccarone, Di Gesu, et al [1988] was predominantly ad hoc, based on formulating fuzzy set compatible operations, without a thorough analysis of the theoretical implications. It is to be noted that though they proposed various fuzzy morphological operators, not all are compatible with the general properties of traditional or crisp morphological operations.

In essence they proposed four different definitions of the fuzzy erosion[Maccarone et al, 1991], however their mathematical basis and their properties are not discussed, the intention being to provide a more pragmatic approach to specific image analysis problems. The fuzzy image and structuring element are represented as χ_f and χ_s respectively.

Minimum Erosion:

$$\chi_{f\ominus s} = min \{ 1 - |\chi_s(y) - \chi_f(y)| \} \qquad Eqn.\ 3.14$$

The term $1 - |\chi_s(y) - \chi_f(y)|$ is the complement of the symmetric difference between two fuzzy sets. If f is binary, the classical erosion results. This definition could however be restrictive if we have $|\chi_s(y) - \chi_f(y)| = 1$, and will then have the result of the erosion as zero which could be undesirable in some applications. This operator was experimentally shown to be useful in performing erosion on all image levels, with the structuring element having values equal to the maximum of the image gray level.

Averaged Erosion:

$$\chi_{f\ominus s} = 1 - \Sigma|\chi_s(y) - \chi_f(y)|\}/\ |s(x)| \qquad Eqn.\ 3.15$$

where |s(x)| is the cardinality of the structuring element. This definition provides a smoother erosion but is not compatible with traditional erosion in the case of binary images. The result of an averaged erosion is too uniform for a structuring element having extreme values. An improvement can be obtained by using intermediate valued structuring elements.

(Δ) -Delta Erosion:

$$\chi_{f\cdot s} = 1 - \Sigma \Delta(\chi_s(y) - \chi_f(y)) \; / \; |s(x)| \qquad \textit{Eqn. 3.16}$$

where $\Delta(x) = 0$ if $x<0$ else 1. This definition takes into account the possibility that the structuring element may be contained within the image. This operator results in all parts of the input image having values less than that of the structuring element being enhanced.

Exact Erosion:

$$\chi_{f\cdot s} = min \; \{ 1 - \Delta (\chi_s(y) - \chi_f(y)) \} \qquad \textit{Eqn. 3.17}$$

This definition corresponds to the classical representation if the image is binary, and also satisfies the possibility that the structuring element may be contained within the image. The exact erosion is similar to the Delta erosions without mediation in the erosion operation.

In general the authors have used the above proposed operators to perform low and medium level image analysis, consisting of edge detection, skeletonization and segmentation of multilevel images. They have also included a study of applications to astronomical image analysis using Fuzzy mathematical morphology.

3.3.4 De Baets, Kerre et al

The work by De Baets et al [1994], seems to disregard the fundamental basis of set inclusion as seen in the earlier mentioned approaches. Instead, their emphasis appears to be in formulation of gray scale morphological operations using a fuzzy set theoretic approach. The gray levels in an image are assumed to belong to the unit interval [0, 1], or scaled to this interval in. An n-dimensional image gray scale image is interpreted as a fuzzy set using a linear mapping. This is precisely the interpretation proposed initially by Goetcherian [1980], and in

essence misses the fundamental criteria of geometric subsethood which lies at the core of mathematical morphology.

The literature review presented in their works (De Baets et al, [1994]), thus does not cover the propositions by Dougherty et al and Bloch et al. They however have commented on the approach of Di Gesu et al, as "none of these definitions is a correct extension of the binary erosion".

3.3.5 Other research works

There have been other researchers who have proposed approaches which are essentially based on similar notions however differing in the specific formulation employed and implementation method used.

The approach by Wu Minjin[1994] associates mathematical morphology with order statistics, and the definitions of percentile operations are used to transform the Minskowski structural operators based on algebraic, geometric and statistical properties of fuzzy operators. The theoretical basis is established by analyzing the Fuzzy mathematical morphology thus constructed based on geometric morphological functions and extraction of morphological feature parameters. Application areas include analysis of metallographic and cell structure images.

Popev[1995] proposes an approach which employs the general framework proposed by Dougherty et al as the fundamental basis. The first axiom proposed by Dougherty et al is omitted for convenience and the technique used by Werman and Peleg is employed to analyze gray-tone images in the fuzzy domain.

3.4 Implementing fuzzy morphological operators

In this section we use some simple examples to demonstrate the practical implementation of the fuzzy erosion, dilation and opening and contrast them with their traditional crisp counterparts.

3.4.1 The Fuzzy erosion

Consider a noisy "T"- shaped object whose fuzzy memberships are denoted in the finite set $\mathcal{A}$, eroded by a fuzzy structuring element $\mathcal{B}$, with its origin located at the top-left corner of the matrix. The memberships in the matrices denote the degree of belonging of each pixel to the image and all memberships outside the image are assumed zero.

$$\mathcal{A} = \begin{bmatrix} 0.6 & 0.1 & 0.3 & 0.4 \\ 0.9 & 1.0 & 0.9 & 0.8 \\ 0.3 & 0.9 & 0.8 & 0.2 \\ 0.2 & 0.8 & 0.7 & 0.4 \\ 0.1 & 0.9 & 1.0 & 0.3 \end{bmatrix} \qquad \mathcal{B} = \begin{bmatrix} 0.9 & 0.9 \\ 0.9 & 0.9 \end{bmatrix}$$

Using the formulation of the indicator function for erosion *(Eqn. 3.7)*, we have the resultant fuzzy erosion as

$$\mathcal{E}(\mathcal{A},\mathcal{B}) = \begin{bmatrix} 0.2 & 0.2 & 0.4 & 0.1 \\ 0.2 & 0.9 & 0.3 & 0.1 \\ 0.3 & 0.8 & 0.3 & 0.1 \\ 0.2 & 0.8 & 0.4 & 0.1 \\ 0.1 & 0.1 & 0.1 & 0.1 \end{bmatrix}$$

The resulting erosion can be obtained by thresholding memberships below 0.8 to zero, to obtain the eroded image. It can be seen that as a contrast from the traditional erosion, the resultant of the fuzzy erosion gives the degree of erosion in the noisy shape. Outside the image, the background will have a constant membership of 0.1. This is a result of using the

indicator with a non-crisp ($\mu < 1$) structuring element. The practical implication of this can be interpreted as considering the eroded background having a membership value determined by the structuring element and the specific formulation of the index function. When we use a crisp structuring element ($\mu = 1$ *or* $\mu = 0$), the above erosion would be the same as the crisp case, and the memberships of the background would be zero.

3.4.2 Fuzzy Dilation

We now demonstrate the fuzzy dilation, of image $\mathcal{A}$, to be dilated by a fuzzy structuring element $\mathcal{B}$, using *(Eqn 3.8)*. We have

$$\mathcal{D}(\mathcal{A},\mathcal{B}) = \begin{bmatrix} 0.9 & 0.9 & 0.8 & 0.7 \\ 0.9 & 0.9 & 0.8 & 0.7 \\ 0.8 & 0.8 & 0.7 & 0.3 \\ 0.9 & 0.9 & 0.9 & 0.3 \\ 0.8 & 0.9 & 0.9 & 0.2 \end{bmatrix}$$

As seen from the above result, the consequent dilation is in line with the dilated result for a crisp operator. Practical applications of the above operators have been shown to have a considerable improvement in edge detection (morphological gradient), filtering union noise and shape detection applications.

3.4.3 Fuzzy Opening

The fuzzy opening $\mathcal{O}$, is demonstrated using a fuzzy erosion and dilation in a manner similar to its crisp counterpart, namely

$$\mathcal{O}(\mathcal{A},\mathcal{B}) = (\mathcal{D}(\mathcal{E}(\mathcal{A},\mathcal{B}),\mathcal{B}) \qquad \textit{Eqn. 3.18}$$

Thus, in terms of fuzzy erosion, we have

$$O(\mathcal{A},\mathcal{B}) = (\mathcal{E}[\mathcal{E}(\mathcal{A},\mathcal{B})]^c, -\mathcal{B})^c \qquad \textit{Eqn. 3.19}$$

It should be noted that the above relation shall be used in generating the fuzzy openings used in the consequent sections. Using the result from example 1, we have the following result

$$[\mathcal{E}(\mathcal{A},\mathcal{B})]^c = \begin{bmatrix} 0.8 & 0.8 & 0.6 & 0.9 \\ 0.8 & 0.1 & 0.7 & 0.9 \\ 0.7 & 0.2 & 0.7 & 0.9 \\ 0.8 & 0.2 & 0.6 & 0.9 \\ 0.9 & 0.9 & 0.9 & 0.9 \end{bmatrix}$$

As a result of complementing the image background will have a constant membership of 0.9. Eroding the above image with the structuring element $(-\mathcal{B})$, we have

$$\mathcal{E}([\mathcal{E}(\mathcal{A},\mathcal{B})]^c, -\mathcal{B}) = \begin{bmatrix} 0.9 & 0.9 & 0.7 & 0.7 \\ 0.9 & 0.2 & 0.2 & 0.7 \\ 0.8 & 0.3 & 0.2 & 0.8 \\ 0.8 & 0.3 & 0.3 & 0.7 \\ 0.9 & 0.3 & 0.3 & 0.7 \end{bmatrix}$$

The background will now have a constant membership of 1.0. This is because the structuring element has a membership of 0.9, which results in a complete fit.

Complementing the above we finally have the result of the fuzzy opening as the below

$$O(\mathcal{A},\mathcal{B}) = \begin{bmatrix} 0.1 & 0.2 & 0.4 & 0.1 \\ 0.2 & 0.9 & 0.8 & 0.1 \\ 0.3 & 0.8 & 0.8 & 0.2 \\ 0.2 & 0.7 & 0.7 & 0.3 \\ 0.1 & 0.7 & 0.7 & 0.1 \end{bmatrix}$$

The result is an opened image with the horizontal bar of the "T" removed due to the opening. The purpose of the above discussion was to demonstrate the effect of a fuzzy operation on an image with a certain amount of ambiguity due to the presence of noise.

Although the difference in the fuzzy opening operation as compared with its crisp transformation is rather subtle, its result is significantly different. The traditional crisp operation, with a flat structuring element of membership 0.9, would lead to the erosion of the noisy regions in the image.

3.4.4 Object extraction using Fuzzy Erosion

At the conclusion of the chapter, we demonstrate a simple example of the use of a fuzzy erosion in extracting an object from a noisy image The basic operation involves erosion of the image using a structuring elements represents the objects of interest. Erosion marks the location where there is a *hit* by the structuring element pair. In our experiments we use a *flat* (constant valued over its domain) structuring element with a membership grade of 0.75. Fig 3.1 shows a gray level intensity plot of the image containing six objects, from where we have to determine the location of the two squares with different gray levels. The noisy image is constructed by adding Gaussian noise and using a smoothing filter, and is shown in Fig 3.2. The result of a gray level set erosion by the structuring element defined above is shown in Fig 3.3. The two high peaks corresponding to the objects of interest, in addition to which the circular objects are also detected to some extent which may cause ambiguity. This result is however expected as traditional erosion does not aim to satisfy such criteria. The result of a fuzzy erosion shown in Fig 3.4, are the two peaks that determine the locations of the squares in the image.

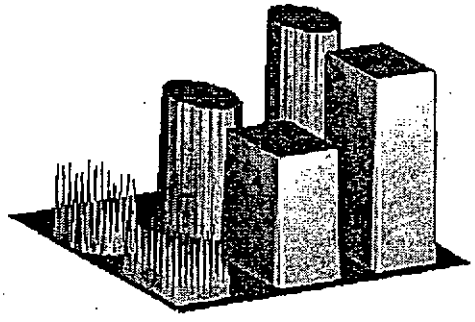

Figure 3.1: Original multilevel image

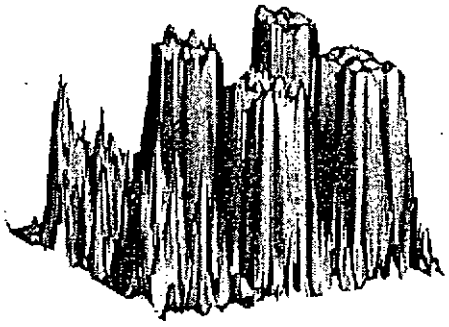

Figure 3.2: Original image with noise

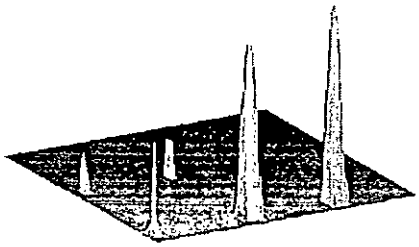

Figure 3.3: Traditional erosion result

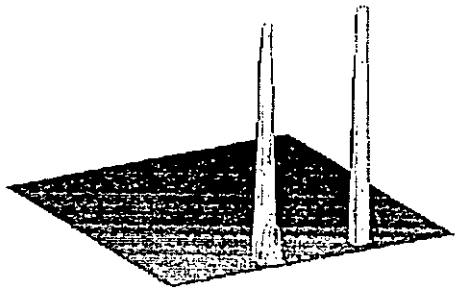

Figure 3.4: Fuzzy erosion result

3.4.5 Conclusion

The theme of this chapter was essentially to present the theoretical basis and demonstrate the need for fuzzification of traditional morphological operations. We have discussed some of the propositions for developing different fuzzy morphologies which have been proposed by various research groups over the past few years. The practical implications of the proposed approach by Dougerty et[1992] have been demonstrated by means of fuzzy membership matrices and a simple object extraction problem. The fundamental reason in adopting the propositions by Dougherty et al is the fact that the fuzzy morphological operations are in line with traditional operators n a non-fuzzy scenario. Moreover, the ease of implementation of these operators makes them the ideal choice for algorithm design. The fuzzy morphological operations discussed here form the basis of the fuzzy pattern spectrum and the feature segmentation algorithms to be presented in subsequent chapters. The following chapters are focused on applying the theoretical foundations thus far in real world applications, and serve to extend these conceptual ideas into practical solutions.

Chapter Four

APPLICATION OF MORPHOLOGICAL OPERATORS IN IMAGE SEGMENTATION

4.1 The Problem Domain - Image Segmentation

Image segmentation is a generic term used to describe operations that are used to extract, locate or differentiate certain features or characteristics from an image. A typical application of an image segmentation algorithm would be to extract certain objects from a complex or cluttered image, the result of which could be used for higher process such as an automatic vehicle navigation system.

4.1.1 Morphological Image Segmentation

Traditionally, mathematical morphology had been extensively used in image segmentation, to extract specific features of interest in an application. The usefulness of mathematical morphology lies in its ability to provide flexible tools in order to design a suitable algorithm to extract an object from a complex image. This chapter discusses real-world applications of traditional and fuzzy mathematical morphology operators in object segmentation problems. This algorithm design characterizes the manner in which a complex object, with a certain degree of feature ambiguity (or fuzziness) can be located (or its likelihood determined), fundamentally using the tools described in the previous chapters.

We initially discuss the application of traditional morphological operators in a vehicle license plate segmentation application, and fuzzy morphological operators in segmentation of tropical cyclones from satellite imagery. These algorithms are completely based on low-level morphological operations, supplemented by simple image addition, subtraction etc. The key feature in these applications is that each demonstrates the applicability of traditional as well as fuzzy morphological operators.

4.1.2 Problem Characteristics

Detection of vehicle license plate numbers is found to be useful in monitoring systems such as automated toll-pay systems, identification of stolen vehicles, travel time data provision or in parking lots. The design methodology in a comprehensive license number recognition system involves isolation of the license plate region from the input image and then detection of the license numbers. There have been many different approaches to the problem of vehicle license plate detection, such as the mathematical morphology method by Arregui, Mitxelena[1992] and the spatial frequency differential analytic methods Tanaka and Hwang[1991]. Perhaps, the most straight forward way would be the shape recognition technique proposed by Crimmins and Brown[1985], the concept being based on performing hit or miss transforms using different sizes of every possible character as a structuring element.

These approaches have the drawbacks of having intense computation demands in addition to which the results would be poor due to the distortion in images caused by noise, positioning of the camera and uncertainty in the features present in the background. Additionally, these methods are suited for images in well illuminated conditions and simple backgrounds. In cases where there is poor illumination, complex background, and extraneous noise their performance drops considerably. This places severe limitations on the image acquisition process, rendering them useless in practical systems.

The morphological segmentation algorithm developed was based on simple gray scale morphological operations. In concept the algorithm detects simple features in license plates such as horizontal lines, and spacing between characters, yet it does not place any specific restrictions on the input images. The robustness of this algorithm was demonstrated by using

images in noisy conditions and poor illumination. The uniqueness of this approach was that there were no special restrictions imposed on the input images. The algorithm showed an extremely good detection rate even with images which were fairly complex, in poor illumination, and noisy.

In the case of the segmentation of tropical cyclones, the problem is to extract an object which is abstract in the sense that features in a tropical cyclone are dynamic. There are no fixed criteria, as in the case of the earlier segmentation problem which could be defined in concrete terms. The essence of the problems is to design an algorithm that can extract the consistent features which characterize a typical tropical cyclone, without placing too many restrictions on the design parameters, that may make the implementation difficult to realize. To overcome these problems we use fuzzy morphological operations and structuring elements to tackle the inherent fuzziness and ambiguity. The later sections discuss the actual algorithm design and implementation of morphological operations used in these segmentation problems.

4.2 Segmentation of License Plates

The vehicle license plate segmentation is an interesting problem in the sense that for a practically viable system there have to be minimal restrictions placed on the system. The key aim while designing our system was to make the algorithm independent of the image complexity, which in turn makes it easy to implement using a PC and a conventional image acquisition device.

4.2.1 Basic Assumptions

The recognition of the vehicle license number by an automated system is a two step process consisting of segmentation of the region of interest, (the license plate region), from the image and then recognition of characters. We are concerned here primarily with the segmentation of the image. A character recognition system can be used in tandem to complete the license number recognition process. The following were the characteristics and factors that

were taken into account while developing the algorithm. The emphasis was placed on making the technique as independent as possible with respect to prerequisites of the image for successful detection.

1. The illumination condition of the image may vary as images are obtained in diverse ambient conditions.

2. The image will have a certain amount of background noise owing to the fact that it is taken from a natural scene.

4. The size of the license plate region or the area occupied by characters may vary from about 35 pixels to about 304 pixels in the image.

4. Characters may be distorted due to digitization noise, especially so in cases where the license plate region may be small.

5. The orientation of the license plate may be different for images, owing to the variation in the angle of vision. Hence, some amount of inclination should be tolerated.

6. The front license plates are white while the rear license plates are yellow, hence corresponding gray levels for the front license plates will be higher than that of the rear license plates.

4.2.2 Designing the Algorithm

The fundamental idea in designing the algorithm was to apply the intuitive manner in which the human cognition process isolated a license plate on a vehicle. This cognition process was then resolved into primitive steps leading to the ultimate recognition. Since morphological operators in themselves offer only low level operations, the primitives were used as a basis to develop the algorithm. Amongst these primitive features we extract only those that may be present rarely in other regions besides the license plate. Also, these features should not be affected considerably by noise and distortion, and should be size invariant within a certain range. We compared various character primitives such as corners, lines, enclosed or partially

enclosed areas and spacing between characters. The approach in our algorithm was based on detecting lines which are by far the most simple features. It was observed that these features can tolerate noise as well as a certain amount of inclination of the license plate due to the thickness of the character lines. Additionally, we also detect spacing between characters to further enhance the algorithm.

4.2.3 Description and Implementation Issues

The first step in the algorithm is to perform a top hat transform. This enhances details of the image and filters off the low frequency components in the image which are less likely to contain the region of interest. The next step is to detect spacing between characters. This is done by converting characters to rectangles by repeated dilation and minimization. This ensures that even inclined lines are also converted to rectangles. The spacing between the rectangles is then determined by filling the vertical space by closing and then subtracting from the original image to remove any noise the image is then opened by a vertical line.

The horizontal lines are detected by opening the original image by a horizontal line structuring element and then extended by performing a dilation so that they overlap with the spacing. It should be noted that vertical spacing and the horizontal lines are detected size invariantly by the algorithm. The location where the horizontal lines are adjacent to vertical spacing are determined by a minimum operation between them. The resulting image is then processed so that the gray level is directly proportional to the probability of the presence of the license plate region, and finally isolated points are eliminated.

The license plate region is obtained by thresholding the image obtained, so that the pixels are above the threshold level determined by the maximum pixel '*p*' in the image. In this region we search from '*p*' to its left and right for the first pixel with value 0, naming them '*a*' and '*b*' respectively. finally on line '*ab*' we search above and below it for each point on '*ab*' till a pixel with value 0 is obtained. the two searched areas are the license plate region. To get a better estimation of the license plate region in case where it is over detected we can use a simple post processing. This is done by selecting a thresholding level which cuts out the left most peak of the histogram of the license plate region determined from the previous step.

Thus the characters will be set to gray level 0 while the license plate background will be value 127. the characters can be filled by a closing operation, and the smoothing of boundaries is done by opening, thus the over detected regions are removed.

4.2.4 Mathematical Representations

Let the originally captured image be A, and structuring elements used in consequent processing steps denoted as below:

SQ_n - n x n square with central point as origin.

HL_n - n pixels of horizontal line, with mid point as its origin.

VL_n - n pixels of vertical line , with mid point as its origin.

The actual morphological and other simple image operations are implemented as described in the following steps:

1. Perform top-hat transform on input image A

$$B = HAT(A, SQ_4) \qquad Eqn.\ 4.1$$

2. Convert each character to a rectangle by repeated dilation and minimization

$$B' = B$$

Repeat

$$B' = Max((B' \oplus VL_3), (B' \oplus HL_3)) \qquad Eqn.\ 4.2$$

Twelve times

3. Detect spacing between characters

$$C = (B' \bullet HL_9 - B') \circ VL_7 \qquad Eqn.\ 4.3$$

4. Detect horizontal lines by opening

$$F = ((E \bullet SQ_{15}) - E) \oplus SQ_{15} \qquad Eqn.\ 4.4$$

5. Find regions where horizontal lines are adjacent to spacing

$$E = Min(C\ (D \oplus HL_5) \qquad Eqn.\ 4.5$$

6. Process E so that gray level is directly proportional to the probability of the presence of the license plate and eliminate isolated points.

$$F=((E \bullet SQ_{15}) - E) \oplus SQ_{15} \qquad Eqn.\ 4.6$$

7. Obtain license plate region by

a) Find maximum pixel (p) in F

b) Threshold F so that all pixels are above threshold level, to obtain result G

c) In G search from p to the left for the first pixel with value 0, call it a; similarly search to the right for a pixel b

d) In G, for each pixel on line ab, search upwards till a pixel with value 0 is obtained; similarly search downward

e) The two searched areas above are the license plate region.

8. From the histogram of gray level image A_G, with domain equal to $A \cap \bullet \{(x,y) : G(x,y)=1\}$ and $A_G(x,y)=A(x,y)$, find a threshold which cuts the leftmost peak of the histogram, and threshold A_G to obtain H

9. Fill characters excluding the outer dark region and smooth out the boundary by opening.

$$I = (((H \bullet HL_3) \bullet VL_3) \circ HL_7) \circ VL_7 \qquad Eqn.\ 4.7$$

4.2.5 System Description and Experimental Results

In order to test and implement the algorithm a software development platform was designed. The platform can be used to perform gray scale morphological operations such as opening, closing, image addition and subtraction, high and low pass filtering, thresholding and so on. The program can be used in two modes. The interactive mode allows the user to perform each operation individually and observe its effects, while the batch mode executes multiple instructions in a series as specified by the user in a batch file.

The algorithm simulations were implemented using an i486-processor based computer system running MS - DOS, as the main processing unit. To capture a video image from a camera to an 8 - bit gray level TIFF image format file, an image grabber was employed. The images were captured using a common CCD camera, without using any external illumination.

Our algorithm was tested with forty natural scene images of size approximately 400 x 200 pixels large with 128 gray levels. The actual license plate region ranged from 7x5 pixels to 19x16 pixels in area. In Hong Kong the license plate consists of two alphabets and four or less numerals, which can be placed in either below or on to right side of the alphabets. In some images the license plate was at a slight inclination, therefore the license plate region was not always rectangular in shape. The camera was focused on the license plate, however the distance between the camera and license plate varied for different images. The images were taken with different background including people, other vehicles, buildings, trees and so on. These conditions demonstrate the robustness of the algorithm.

(a) Originally Captured Image

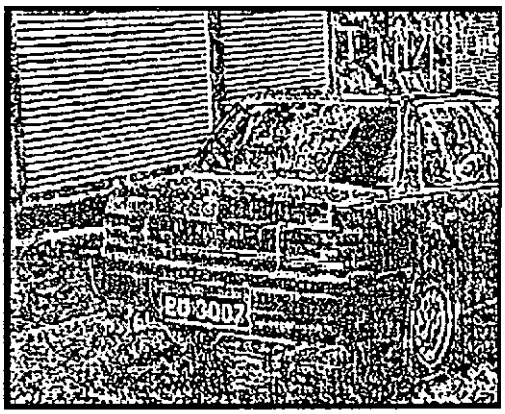

(b) Top Hat transformed image

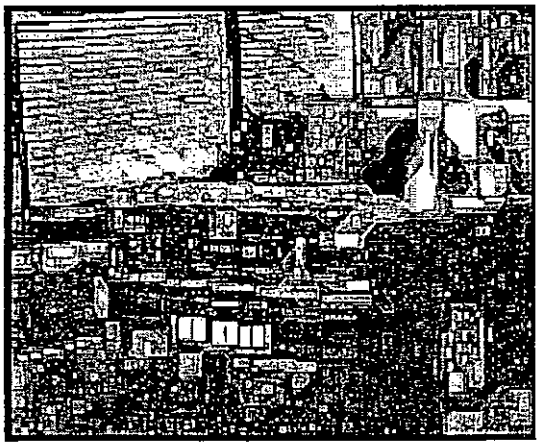

(c) Detection of Character Features

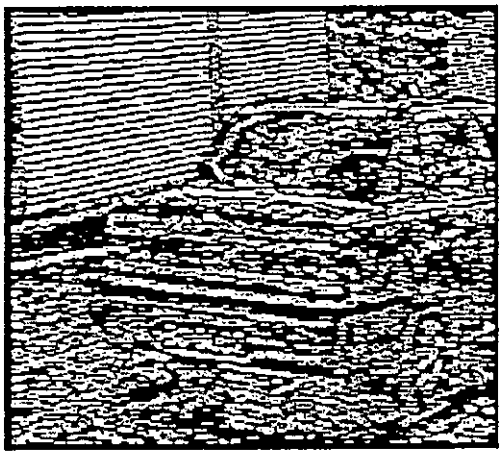

(d) Detection of Horizontal Lines

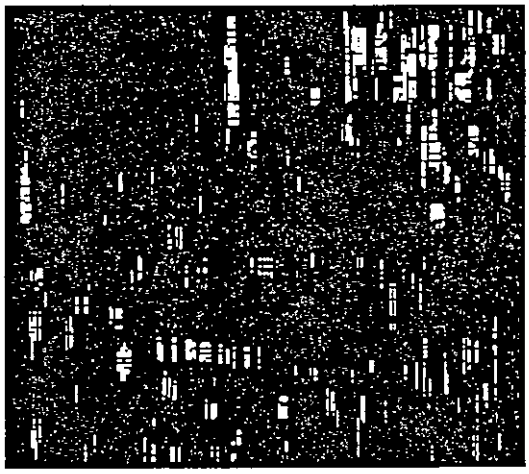

(e) Detection of Horizontal & Vertical Lines

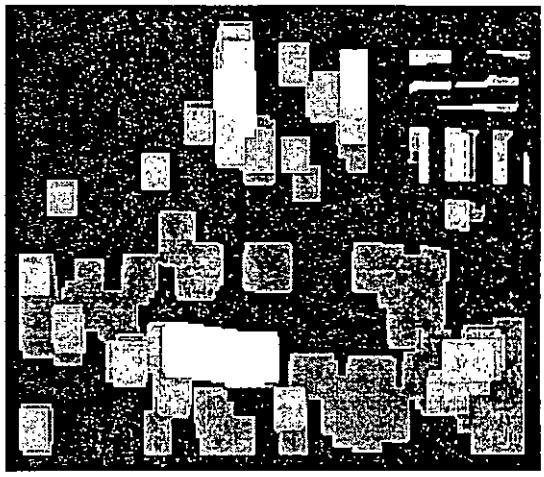

(f) Segmenting character regions

(g) Segmenting the LP region

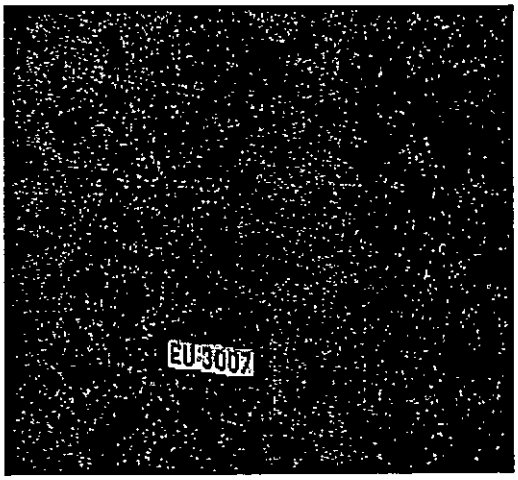

(h) Final Post-Processing

Figure 4.1: Processing steps of the vehicle License Plate segmentation algorithm

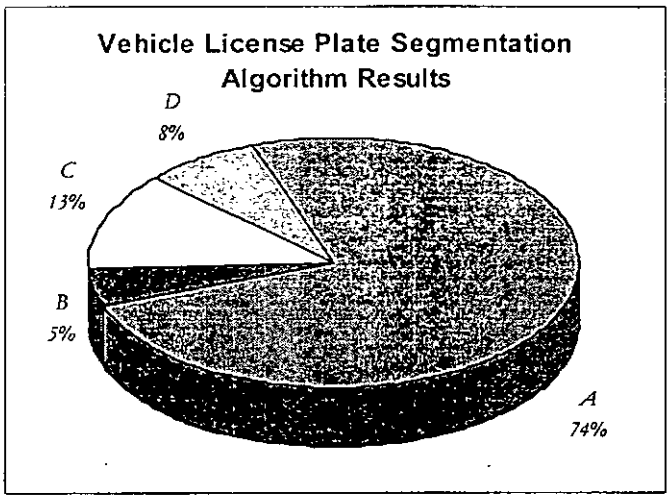

Figure 4.2: Detection results of the VLP algorithm

Category	Description
A	License plate properly segmented
B	License plate character partially obscured or over segmentation of area
C	Under segmentation
D	Wrong detection

(a) Original Image

(b) Segmented Result

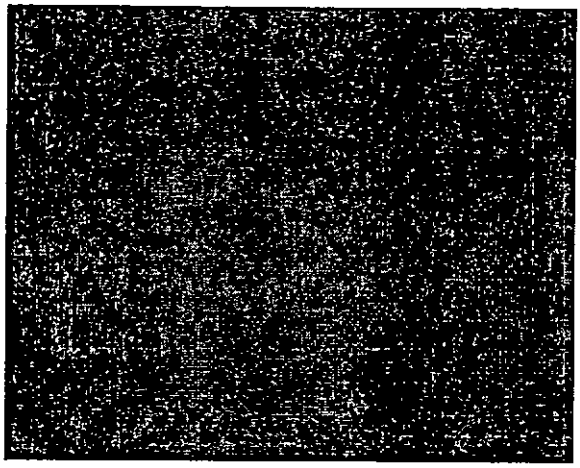

(c) Original Image with Blurring

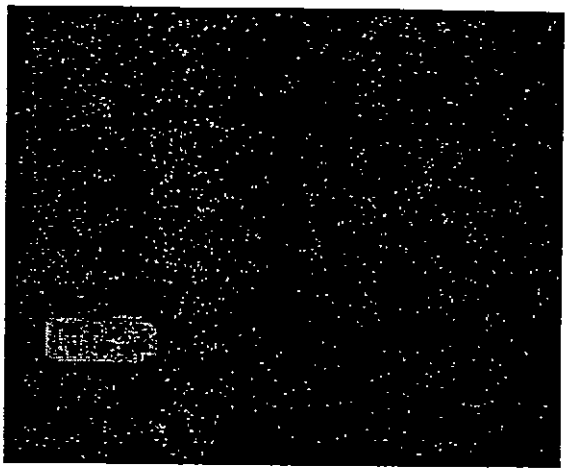

(d) Segmented Result

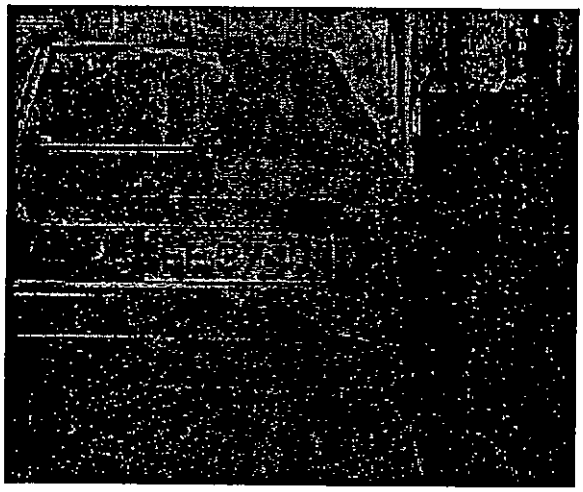

(e) Original Image with Poor Illumination

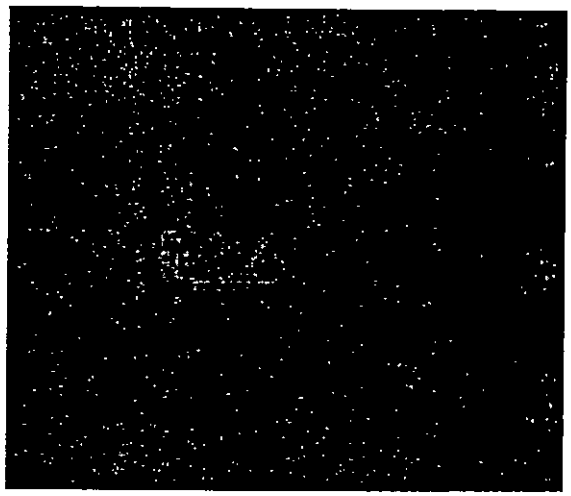

(f) Segmented Result

Figure 4.3: Test for robustness of the algorithm

4.3 Tropical cyclone segmentation from Satellite Imagery

The tropical cyclone segmentation problem differs from the VLP algorithm in the manner in which the features extraction criteria are defined. The two application serve as classic examples to demonstrate the advantages of traditional and fuzzy mathematical morphology for the applications perspective.

4.3.1 Tropical Cyclone tracking using GMS

A tropical cyclone is characterized as a non-frontal synoptic scale low-pressure weather system over tropical or sub-tropical waters with organized convection (thunderstorm activity) and definite cyclonic surface wind circulation (Montgomery, Farell [1993]). Tropical cyclones are one of many atmospheric circulation systems, which can be grouped and expressed in various scales of motion. The nomenclature of these atmospheric systems varies on the basis of their geographic location. In the western North Pacific and the China Seas, the most intense are termed as *typhoons*, which are equivalent to the *hurricanes* in the Atlantic and the eastern Pacific and *cyclones* in the Indian Ocean.

To avoid complication, throughout our discussion we shall use the generic term *tropical cyclone* to reference such atmospheric systems. In general terms, a mature tropical cyclone is an atmospheric disturbance consisting of a moist, convective, centrally located, rotary mass. The central region is considerably denser than its surroundings. Along the periphery are convective clouds and precipitation regions which form curved or spiral bands. The combination of these two features exhibit a symmetrical pattern with a circular or elliptical wall cloud around a central region of relatively calm and cloud free area called the eye. Based on its intensity (wind speed) and state of activity, they are classified as tropical depression, tropical storm, severe tropical storm and tropical cyclone. Our algorithm is designed specifically for segmenting tropical cyclones, as the features are distinctly visible at this stage.

From its position above the earth, the GMS surveys the eastern hemisphere once every hour. This temporal resolution is a significant advantage over polar orbiters which normally are capable of only two passes in a day. A complete scan of the earth takes approximately 25 minutes. In the resulting imagery, each pixel represents 1.24 km in VS (Visible spectrum, day-time only) and 5 km in IR (Infra-red spectrum). During the scan, data are transmitted to the CDAS (Command and Data Acquisition Station), where it is processed and raw data broadcast immediately to ground stations. The subsequent imagery is used to generate a track map based on the path of the tropical cyclone. By means of track maps, the data can be utilized in future estimation and prediction.

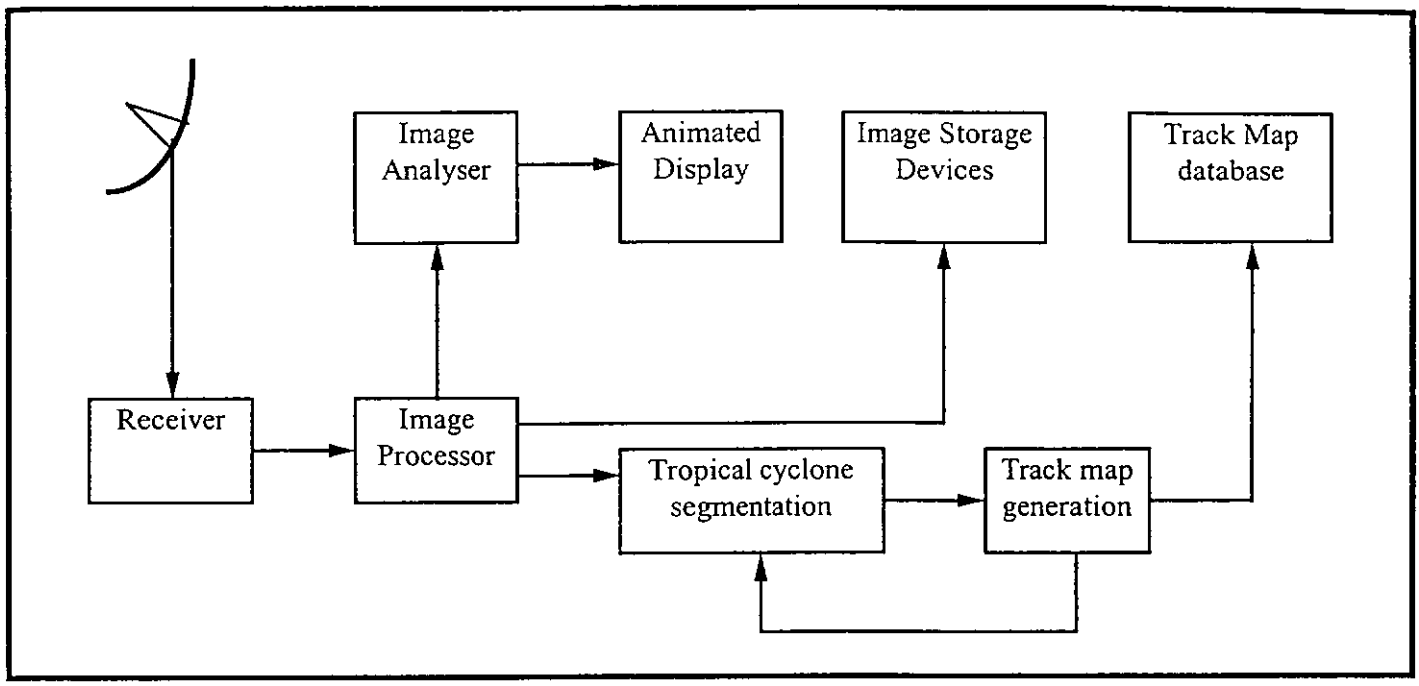

Figure 4.4: A complete GMS imaging system

4.3.2 Initial Assumptions of the Segmentation Algorithm

The algorithm design parameters are based on certain *a priori* assumptions with respect to the characteristics of the images. The intent is to achieve a higher rate of segmentation of tropical cyclones as opposed to the irregular atmospheric cloud formations. In a given image the actual region occupied by the tropical cyclone must cover at least 10% of the entire image size. This is essentially to limit the algorithm to reasonable limits in terms of processing requirements. There are no assumptions about the location of tropical cyclone, which can be present anywhere within the image region. Hence, the complete image must be processed. The image is initially enhanced using histogram equalization to maintain standard intensity levels between images. To have an acceptable segmentation results, the maximum number of tropical cyclones likely to be present in a single image is limited to two. This however is not a significant constraint as the final segmentation result may be acceptable even for images having more than two tropical cyclones. The final results will be dependent on the actual number of tropical cyclones and the general characteristics of the image Finally, to ensure that the tropical

cyclone is not obscured or partially cut-off, it is assumed that each tropical cyclone will have both its features (central core region and peripheral winds) clearly visible in the image.

4.3.3 Design philosophy and Algorithm description

The proposed technique can be considered as being implemented in two steps. The first step is to isolate the central rotary mass that appears as circular cloud formation and then we have to determine the presence of peripheral spiral wind patterns in the outer band. To determine the optimum parameters for designing the structuring element shape and sizes we use a training set of five test images which are representative of the general images. This step is performed only at the developmental stage in the algorithm design process to determine the optimum parameters for the structuring elements shapes and sizes for each operation. These parameters are then used for all subsequent segmentation operations. On the basis of the results in training set, a set of structuring elements are defined for each stage of processing. For instance, to extract the peripheral wind bands we have a set of three structuring elements of different sizes. In the actual segmentation process, the optimum structuring element is determined dynamically from the set based on the nature of the specific features in the given image. To implement such intelligent selection of structuring elements we have used *pixel count values*. The image is processed once with each structuring element from the pre-defined set and the structuring element with the optimum pixel count value is finally employed. The pixel count value is pre-set for each operation and is determined from the training prototype set. To eliminate or preserve certain features in the image, we use image masks, which are essentially binary images generated from previous processing steps. To generate some of these masks we have used fuzzy morphological operations, and employed the memberships with preset α-cut values to set the binary thresholds.

The foremost step uses a fuzzy closing to smooth larger features in the images. This also fills up the eye region and other discontinuities within the core of the tropical cyclone and the intensity variation in each connected region is minimized. The next step is to use fuzzy opening to eliminate small features and enhance the larger circular cloud formations. The structuring element employed in the fuzzy opening is designed using the assumption regarding the tropical

cyclone size. As the result of the fuzzy opening, we now have memberships which are used to construct an image mask (using the α-cut set). The resultant mask is termed as the core mask. The subtracted image mask will remove large circular features and limit our region of interest to these regions only, as only these regions can enclose the tropical cyclone core.

The second phase of the algorithm uses a top-hat transformation of the original image. This serves to enhance the regions which have smaller features and considerable variance in spatial intensity. The top-hat transformed image is again histogram equalized to ensure standard intensity levels. As it can be seen from the result, the spiral wind patterns are enhanced. Using the core mask and its dilated representation as masks on the top-hat transform, we isolate the peripheral band region. The subsequent step is to extract the peripheral spiral cloud patterns. Since these features can be closely approximated using diagonal shaped fuzzy structuring elements having positive and negative slopes. As these features are quite ambiguous in nature we use a fuzzy opening with structuring elements of different lengths. Initially we open the images with the largest structuring element from the set which has been determined on the basis of the training images. The two opened images (one for each of the structuring elements, positive and negative slopes) are combined by a simple *or*ing. A pixel count value is taken to determine if the selected structuring elements are too large for the particular case. If it is below the value determined *a priori* from the training test images, the next smaller structuring elements are chosen and the process repeated iteratively till the pixel count value exceeds the pre-set value. Thus we dynamically choose the optimum structuring elements based on the nature of the peripherally located spiral cloud formations for each particular image. The resultant image is then closed to eliminate discontinuities in the periphery regions and an opening is used to remove smaller unwanted regions. The structuring element for these two operations is a circular disk which has a fixed size for all images since we perform only image enhancement and not a feature extraction. The next operation is to dilate the resultant region by a disk shaped structuring element to have a connected and enlarged peripheral band region. This generates the peripheral mask and completes the second stage of our algorithm.

In the concluding step, we need to combine the results of the two operations to determine locations of the tropical cyclones from all other possible regions. This is determined by the elimination of all the regions that do not satisfy the required conditions, namely the

presence of the circular core and the peripheral spiral cloud formations. To make the algorithm flexible enough to segment more than one tropical cyclone from a given image, we need to consider each unconnected region separately. The initial image mask (obtained from the first fuzzy opening step) is eroded with a disk shaped structuring element to generate an unconnected *seed* for each region. Each seed is now processed independently, by dilation with large disk shaped structuring element. This encompasses the probable region around the core which has the most likelihood of the presence of peripheral clouds. This dilated image is then *and*ed with the result of the previous step, and the pixel count is determined. If the pixel count exceeds the preset value, we can preserve the seed region (as it is the tropical cyclone region), else it is rejected. For each region we repeat this process iteratively, and the resultant image is the final core region mask. The tropical cyclone segmentation mask is obtained by oring the peripheral mask with the core region mask, and closing with a disk to smooth discontinuities. The segmented image is obtained by *and*ing the original image and the segmentation mask.

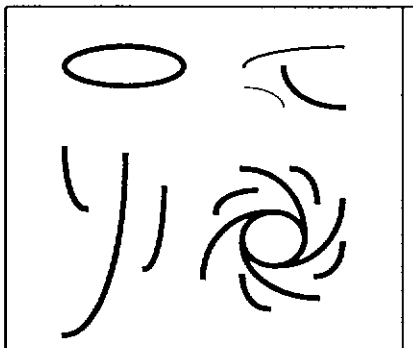

Fig. 4.5 a

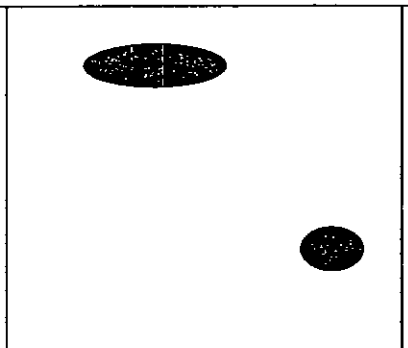

Fig. 4.5 b

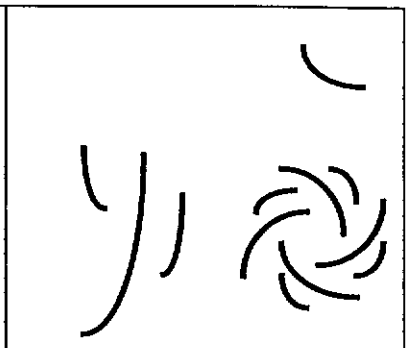

Fig. 4.5 c

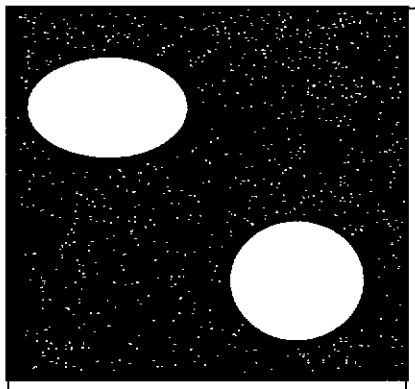

Fig. 4.5 d

Fig. 4.5 e

Fig. 4.5 f

Fig. 4.5 g

Fig. 4.5 h

Fig. 4.5I

Figure 4.5: A schematic of the Tropical Cyclones segmentation algorithm design

4.3.4 Implementation Pseudocode and Mathematical Representation

The above description is presented in the form of pseudocodes to represent the segmentation algorithm in terms of the morphological operations described in the previous section. The steps in the algorithm are indicated by representing morphological and other image operations along with the shapes and sizes of the structuring elements used at each stage.

Symbol Key:

$A, B, \ldots$	= *image matrices*
SD_x	= *Disk shaped structuring element with diameter* x
SP_x	= *Diagonal structuring element with positive slope and length* x
SN_x	= *Diagonal structuring element with negative slope and length* x
M_x	= *Image mask* x
R_x	= *Connected region* x
$Alpha_x$	= *Fuzzy alpha cut at* x
HEq	= *Histogram Equalization*
$Count\ (X)$	= *Function to determine pixel count of image matrix* X
PC_x	= *Calculated pixel count at* x
PT	= *A priori determined minimum pixel count values*

Begin Segmentation algorithm

Image size normalization and histogram equalization;

A = *Load Matrix(Original image);*

$B = O\,(\,C\,(A, SD_5\,), SD_{35}\,)\,;$

$M_1 = Alpha_{0.7}\,(B\,);$

$C = HEq\,(TopHat\,(A, SD_5\,));$

$D = Mask\,((M_1 \oplus SD_{30}\,), C\,);$

$E = Mask\,(D, M_1);$

Repeat

$$F = \mathrm{OR}\,(O\,(E, SP_x), O\,(E, SN_x\,)\,);$$

$PC_x = Count\ (F);$

Until $(PC_x > PT_1);$

$M_2 = ((F \bullet SD_5) \circ SD_5);$

$H = (M_1 \ominus SD_{15});$

For each connected region (R_x) *in* H

$S_x = (R_x \oplus SD_{40});$

$T_x = AND\ (S_x, M_2);$

$PC_x = Count\ (T_x);$

If $(PC_x > PT_2)$ *then* $R_x =$ *White else* $R_x =$ *Black ;*

$K = OR\ (K, R_x);$

Next R_x

$M_3 = OR\ (M_1, M_2);$

$L = (M_3 \bullet SD_{20});$

Segmented Result $= Mask\ (L, A);$

End Segmentation algorithm;

4.3.5 Algorithm Implementation issues

The above described algorithm has been realized on a SUNSparcStation-20 (CPU: TMS390Z55, clock 60 MHz, 131072K RAM). Prior to processing, the images were histogram equalized and normalized to a resolution of 250 x 200 pixels with 256 gray levels. The average user CPU times recorded for the most significant operations are shown in Table 4.1. The processing time for simple image operations such as *or*ing, *and*ing and masking is usually less than 0.5s. The total processing time required to implement the algorithm is approximately 50-60 seconds, varying on the nature of the images. From the characteristics of the acquisition process it is obvious that the processing time for real time implementation of the algorithm is well within the specified limitations.

Operation	SE Size and Shape	Average User CPU Time (Sec)
Fuzzy Closing	5 pixel diameter disk	0.6
Fuzzy Opening	35 pixel diameter disk	32.0
Binary Dilation	30 pixel diameter disk	6.0
Top-hat	5 pixel diameter disk	0.5
Fuzzy Opening	5 pixel length diagonal	0.9
Fuzzy Opening	7 pixel length diagonal	1.2
Binary Closing	20 pixel diameter disk	3.2

Table 4.1: Processing times for the Tropical Cyclone segmentation algorthim

4.3.6 Simulation Results

The above algorithm was tested with a varied set of images including imagery having two tropical cyclones in one image. The test set consists of imagery representative of general conditions associated with the GMS imagery. The images for key segmentation steps to be shown consist of single and multiple tropical cyclones. Fig *4.6a* shows the GMS image (resized and histogram equalized) of tropical cyclone Gertie on 20th December 1995. The result of a fuzzy closing is shown as Fig. *4.6b*, and the enhanced peripheral wind region is shown in the top-hat transformed image, as Fig. *4.6c*. The image in Fig. *4.6c* is fuzzy opened with diagonal structuring elements and *or*ed resulting in isolation of the peripheral wind region as shown in Fig. *4.6d*. The combination of the core and peripheral regions results in the final mask of Fig. *4.6e*. The final segmentation result can be seen in Fig . *4.6f*.

The second image set, starting with Fig *4.7a*, shows a GMS visible image, with two tropical cyclones Wilda and Verne on 23rd October 1994. There are three distinct regions in this image, and we may also note the irregular cloud formation to the right. The result after the

initial fuzzy opening is shown in fig *4.7b* and the top-hat transform is shown in *4.7c*. The extracted peripheral regions are seen in Fig *4.7d*, and the final mask generated is shown in Fig *4.7e*, with *4.7f* as the result of the segmentation.

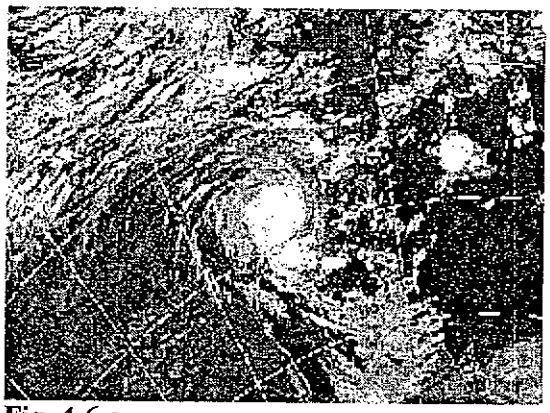

Fig. 4.6 a

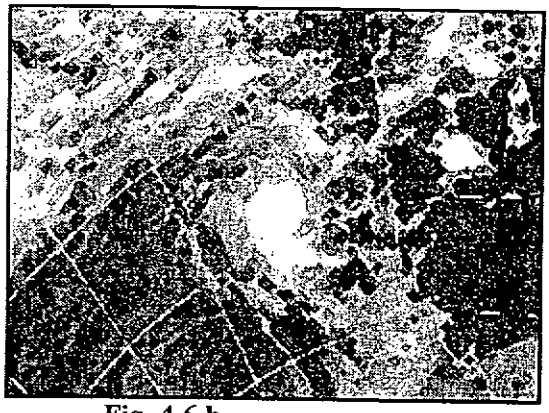

Fig. 4.6 b

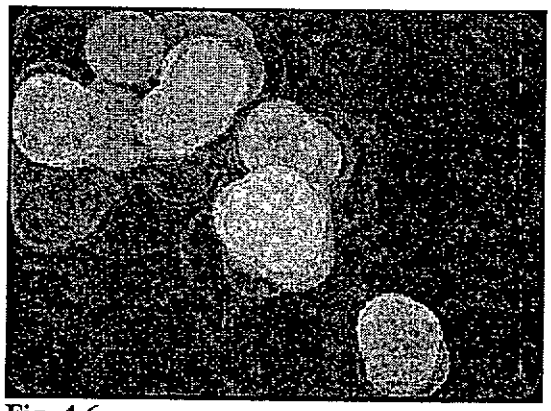

Fig. 4.6 c

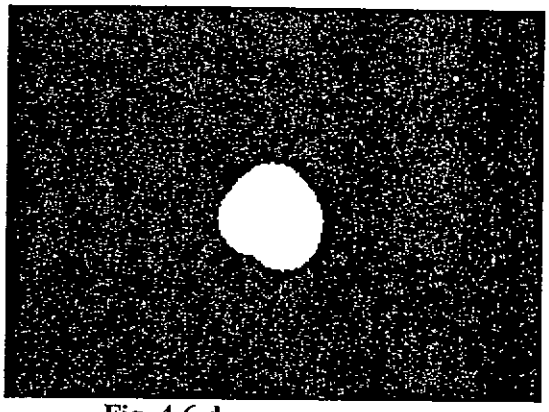

Fig. 4.6 d

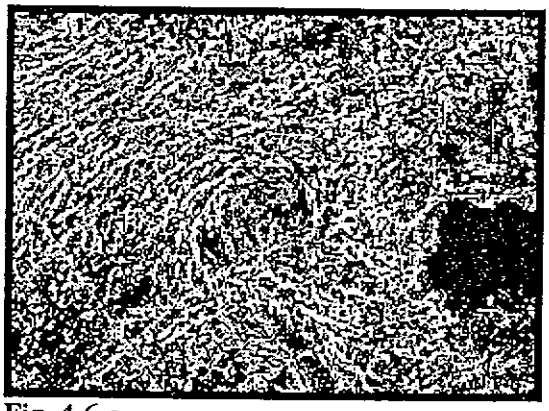

Fig. 4.6 e

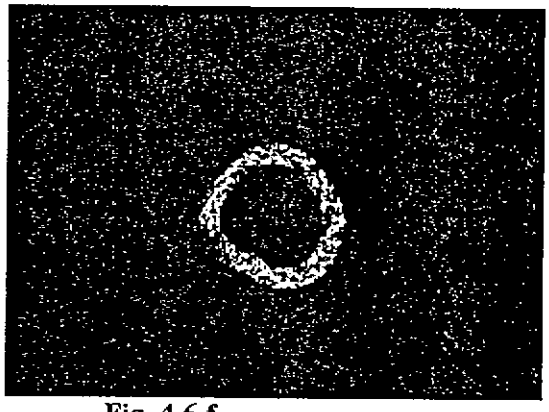

Fig. 4.6 f

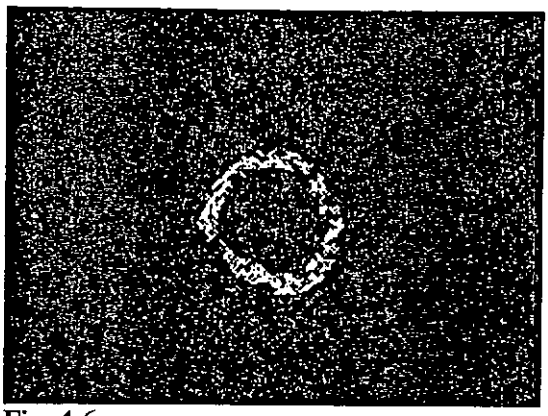

Fig. 4.6 g

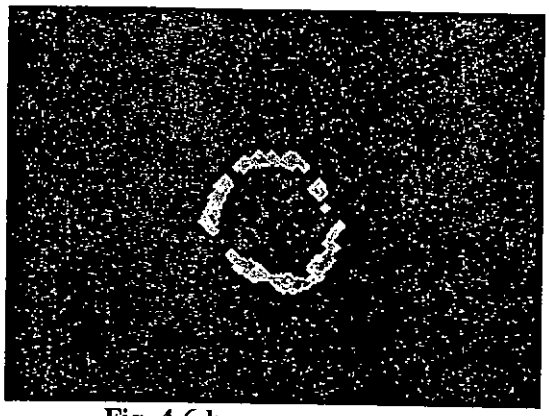

Fig. 4.6 h

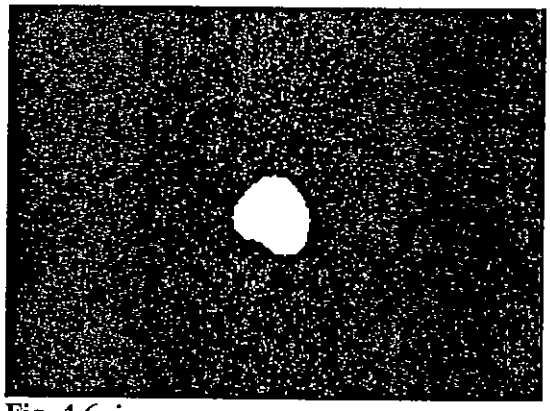

Fig. 4.6 i

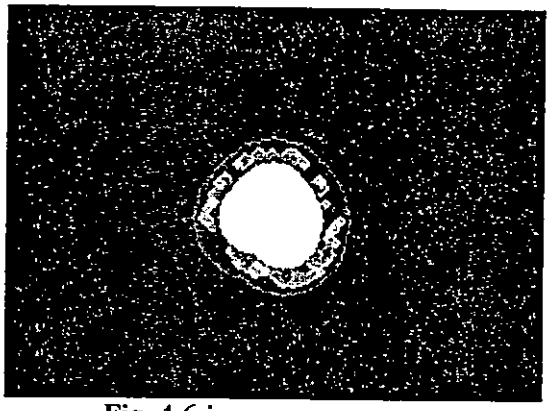

Fig. 4.6 j

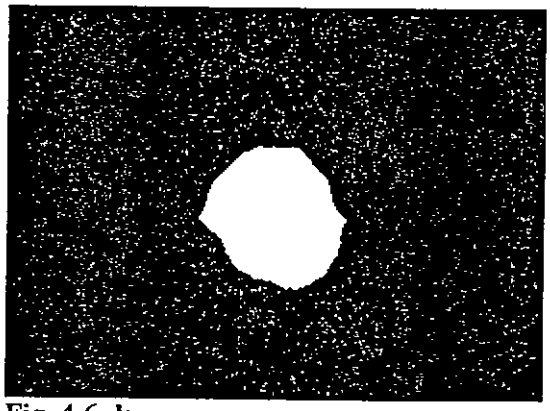

Fig. 4.6 k

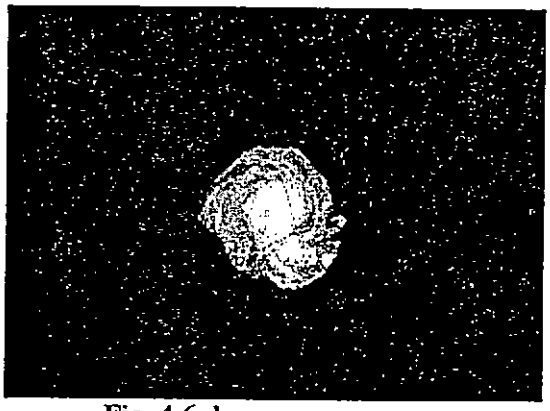

Fig. 4.6 l

Figure 4.6: Processing steps in the Tropical Cyclone extraction algorithm

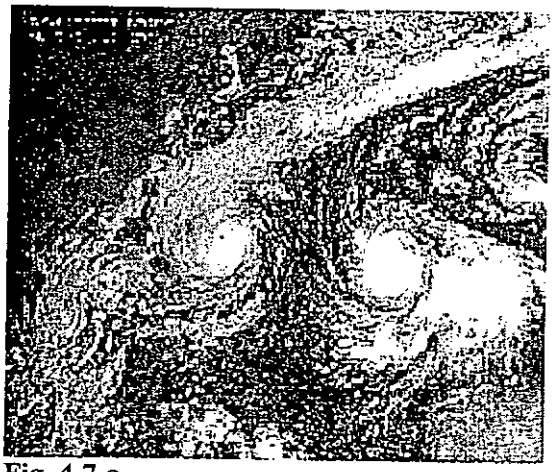

Fig. 4.7 a

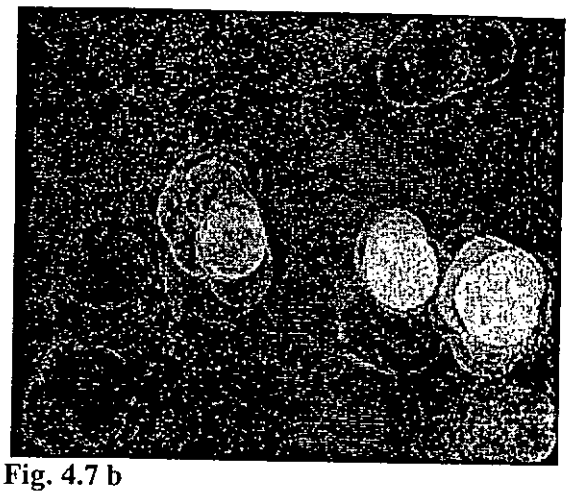

Fig. 4.7 b

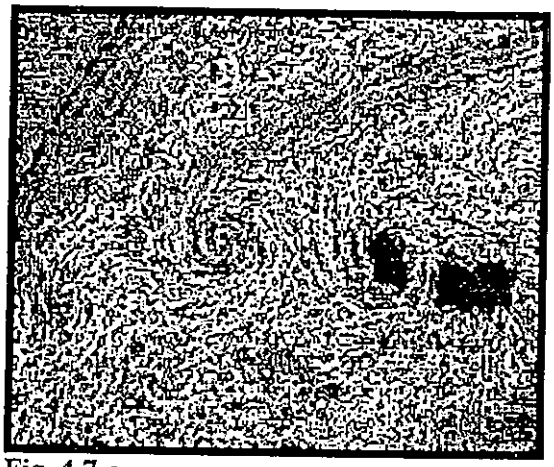

Fig. 4.7 c

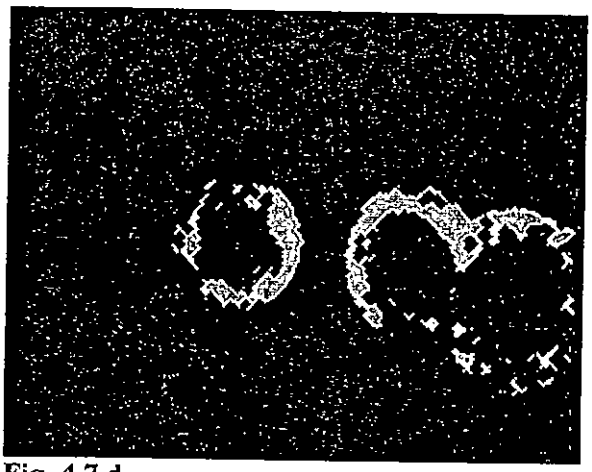

Fig. 4.7 d

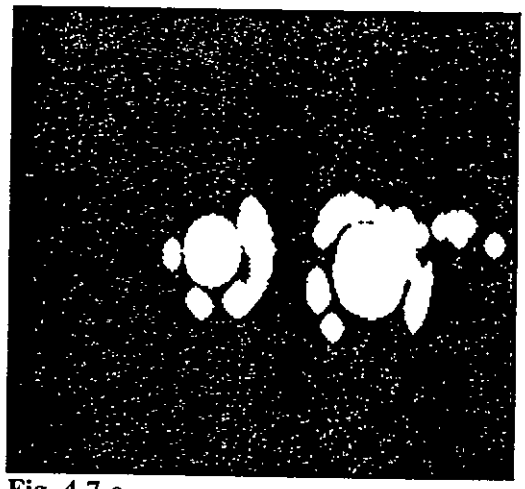

Fig. 4.7 e

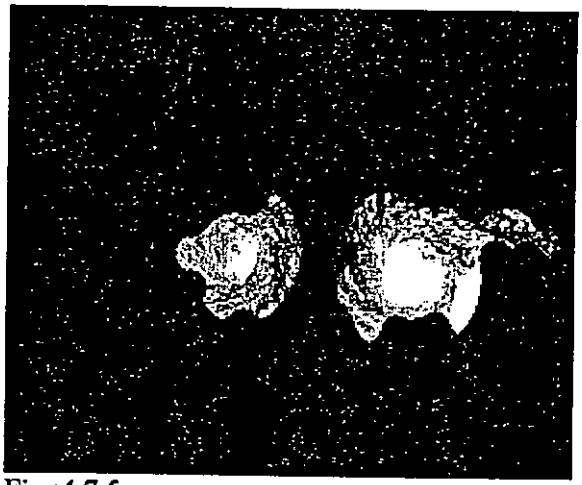

Fig. 4.7 f

Fig 4.7: Processing steps -Image with two Tropical Cyclones

4.4 Enhancements and Future directions

4.4.1 Summary of Results

This chapter presented algorithms which were based on traditional and fuzzy mathematical morphology, designed to solve image segmentation problems. The proposed algorithms were tested with varied image sets, and consequent experimental results are seen to be comparable to those of manual operation within the specified constraints. The overall computing requirements are low as the implementation is entirely based on some efficient and simple morphological operations. Furthermore, some operations can be implemented in parallel, as the algorithm is basically designed to extract features independently, hence these processing steps can be executed simultaneously.

The results of processing images using the algorithms designed for the vehicle license plate extraction and tropical cyclone segmentation indicate the algorithms to be fairly accurate, although within the specified limitations. Both the approaches use assumptions which are intuitive and draw heavily upon the human cognition process. In terms of real-time implementation considerations, the proposed algorithms have been shown to be effectively implemented on standard systems, and hence can be realized in cost effective implementations.

4.4.2 Future avenues for development

The fact that these methods are purely low-level approaches and do not use any conditional parameters, indicate that better segmentation results can be possible by including information from other sources. For instance in the tropical cyclone tracking system an algorithm can be designed to limit the region of interest. This follows from the fact that once the tropical cyclone is segmented from the initial image, the subsequent images can be reduced to only the possible areas of movement. Other enhancements include an introduction of some post processing steps such as image smoothing to improve segmentation results. Additionally, requirement on the tropical cyclone size can be relaxed (at the expense of computation speed) by varying the structuring elements sizes and using the same process iteratively. It should be noted that since this algorithm forms part of an expert system, there will be a certain amount

of *a priori* information available such as the likelihood of occurrence (such as, time of year) and the possible regions. The algorithm for tropical cyclone segmentation can be used for detection of other cloud formations by simple modifications to the structuring elements and morphological operations.

Similarly, the vehicle license plate segmentation algorithm, albeit developed for vehicle license plate detection, can be used in other applications involving detection of labels, name-plates, serial numbers and so on. Being based on the detection of features present in characters, it can be applied to other recognition problems as well without any significant modification to the main algorithm. In order to supplement the robustness of the algorithm and minimize false detection, the algorithm could be enhanced to detect additional features present in the license plate region. These features could include inner side of corners, which could be detected using the hit or miss transform with suitable structuring elements. Additionally, the hit or miss transform could be also used to detect fully or partially enclosed areas with varying sizes of structuring elements. A combination of these methods would increase the robustness of the algorithm hence placing fewer constraints on the image requirements.

Another avenue for further development is implementation of the algorithms in terms of hardware realization. In case of the tropical cyclone segmentation algorithm, the processing time is quite sufficient, due to the inherent lag in the time of acquisition of subsequent images. However, the vehicle license plate segmentation algorithm would require a faster processing speed as the corresponding image capture rate could be much higher. As these algorithm are based solely on simple morphological operations and image addition, subtraction and masking, they can be effectively implemented in hardware which would significantly reduce the processing time, an important factor to be considered in real time recognition systems. Techniques based on piplined architectures or systolic arrays can be effectively used to implement the algorithm as they take advantage of the recursive nature of morphological transformations.

4.4.3 Conclusion

This chapter has primarily focused on the application of morphological operators in real world applications. The intent has not only been to demonstrate the applicability of morphology in practical image segmentation problems but also to contrast the conventional and fuzzy operators in terms of their practical usefulness. In the next chapter we adopt a theoretical vein and present new developments in terms of extending the fundamental notions of fuzzy mathematical morphology to establish the theoretical basis for the fuzzy pattern spectrum.

Chapter Five

THE FUZZY PATTERN SPECTRUM

5.1 Morphological Pattern Spectrum

The fundamental concept of shape-size filtering was proposed initially by Matheron[1975], where image features or their granularity could be quantified using multi-scaled morphological operators. We extend the basic notions using the tools of fuzzy mathematical morphology to generate the Fuzzy Pattern Spectrum.

5.1.1 The principal concepts

Morphological operations are ideal for understanding the features related to shape and size in an image. An extension of basic morphological operations such as erosion or opening can be used in cascades to generate "shape-size" descriptors. This methodology is based on determining the residual of the eroded or opened image to construct distributions that quantify the measure of a given feature. Traditionally these descriptors have been termed as the *pattern spectrum*(Maragos, [1989]) or *pecstrum* (Anasstassopoulos et al[1991]). The pattern spectrum quantifies the distribution of a specific shape in an image. In a sense, the pattern spectrum can be considered analogous to the Fourier spectrum, with the difference being that one quantifies the shape whereas the other provides an insight into the frequency distribution of the signal.

Matheron [1978] and Serra [1986] have initially proposed the opening as a shape-size classifier based on the *granulometric* distribution. The basic idea is to employ morphological openings as tools to generate shape-size descriptors that determine up to what scale a given shape exists in an image. A structuring element B can generate a multi-scale family of

structuring elements of the form $nB = B \oplus B \oplus B .... \oplus B$ (n-times, n = 0,1,2....). Thus, if B is convex, B represents the shape and n the scale. A family of multi-scale openings $\{X \circ nB\}$ where B is the generator is denoted by

$$X \circ nB = [(X \ominus B) \ominus B \ominus B .... \ominus B) \oplus B \oplus B \oplus B .... \oplus B] \quad n\text{-times} \qquad \textit{Eqn. 5.1}$$

The opening will eliminate all objects with shape B and size n in the image such that for finite images at $n = k$, that is,

$$X \circ kB = \varnothing \qquad \textit{Eqn. 5.2}$$

The pattern spectrum is constructed by measuring the size distribution *(residue)* after opening for each n. From the formal mathematical definitions of the pecstrum for M dimensional sets and functions proposed by Pitas et al[1992], we summarize the definitions for functions only (as is relevant to the subsequent discussion) as shown below.

5.1 Representation for functions (discrete)

For a discrete M-dimensional function $f \in \mathbb{R}^M$, we can define the pecstrum

$$P(n) = \frac{-d\,/\,dn\left[Mes\left(f_{ng}\right)\right]}{Mes(f)} \qquad \textit{Eqn. 5.3}$$

where: $n \in [o, -\infty]$; g is a continuous convex function with its umbra $U(g)$ a subset of $\mathbb{R}^{M+1}$; f_{ng} denotes the morphological function-function opening by structuring element ng, and $Mes(f) = \int\int\int .. \int f(x_1, x_2, .., x_M) dx_1 dx_2 .. dx_M$.

5.2 Representation for functions (continuous)

For a discrete M-dimensional function $f \in \mathbb{R}^M$ we can define the pecstrum

$$P(n) = \frac{\left[Mes\left(f_{ng}\right)\right] - \left[Mes\left(f_{(n+1)g}\right)\right]}{Mes(f)} \qquad \textit{Eqn. 5.4}$$

where: $n \in \mathbb{Z}^+$; g is a discrete convex function, whose support is a compact subset of $\mathbb{E} \in \mathbb{Z}^{M+1}$; f_{ng} denotes the morphological function-function opening by structuring element ng; and $Mes(f) = \sum_{x_1} \sum_{x_2} \dots \sum_{x_m} f(x_1, x_2, \dots, x_M)$

The pattern spectra denoted in the above representations can in fact be determined from the histograms of the images for each opening transform with respect to the original image (Haralick et al [1992]).

5.2 The Fuzzy Pattern spectrum (FPS)

5.2.1 The fundamental notions

The traditional morphological pattern spectrum is fundamentally based on analyzing image subsets which a constructed by using iterative erosions or openings. The key philosophy in degenerating an image is to eliminate redundant objects or features that do not satisfy a pre-determined criteria. This process can be considered analogous to a sieving mechanism. The "grains" in this process represent the objects or features and the "sieve" or filter represents the set of morphological operations.

Conceptually, this methodology does not emphasize the actual implementation process in which the residue after each erosion or opening can be measured. This problem is aggravated in the case of gray scale images where the measurement of each residue after the morphological operation can be critical to the finally generated pattern spectra. Of course one could argue that a suitable "threshold" criteria could be ascertained to determine the residue at each step of the iteration. But this would essentially compromise on the image information(since, by nature the process is heuristic) and would consequently put the reliability of such an algorithm to question. Essentially, what is required is a tool that deals with image ambiguity directly, rather than to leave the decision process to a pre or post processing operation. In fact, in the initial arguments by Dougherty and Sinha [1992], this is the fundamental criteria for the requirement of a fuzzy mathematical morphology.

In order to generate a fuzzy pattern spectrum, we essentially employ the mathematical basis proposed in the context of fuzzy mathematical morphology, in tandem with fuzzy set theoretic tools to determine the residues generated by a fuzzy erosion or a fuzzy opening. Thus, the fundamental advantage in employing the fuzzy pattern spectrum is that it provides the tools to quantify the spatial uncertainty which can be used directly in a decision making process, without compromising on the spatial information available within the image.

5.2.1 Formal definitions

Let us now formally propose our Fuzzy Pattern Spectrum in the context of the fuzzy operations as described above. For a continuous M-dimensional crisp function f, its fuzzy representation $\mathfrak{I}$ can be obtained by using a fuzzifier ϕ such that $\phi : \mathbb{R} \rightarrow [0, 1]$, and thus we have $\phi : f \rightarrow \mathfrak{I}$. Similarly, we have the fuzzification of the crisp structuring element b, $\phi : b \rightarrow \beta$. Thus, we have the fuzzy pattern spectrum for the continuous case denoted by

$$P(n) = \frac{-d / dn\left[Mes\left(\mathfrak{I}_{n\beta}\right)\right]}{Mes(\mathfrak{I})} \qquad \textit{Eqn. 5.5}$$

where: $n \in [o, -\infty]$; β is a continuous convex function with its umbra $U(\beta)$ a subset of $\mathbb{E} \in \mathbb{R}^{M+1}$; $\mathfrak{I}_{n\beta}$ denotes the *fuzzy morphological opening* by structuring element $n\beta$ and $Mes(\mathfrak{I}) = \int\int\int..\int \mu(x_1)dx_1$ denotes the area of the fuzzy set

For a discrete M-dimensional function $\mathfrak{I} \in \mathbb{R}^M$, we can define the pecstrum

$$P(n) = \frac{\left[Mes\left(\mathfrak{I}_{n\beta}\right)\right] - \left[Mes\left(\mathfrak{I}_{(n+1)\beta}\right)\right]}{Mes(\mathfrak{I})} \qquad \textit{Eqn. 5.6}$$

where: $n \in \mathbb{Z}^+$; β is a discrete convex function whose support is a compact subset of $E \in \mathbb{Z}^{M+1}$; $\Im_{n\beta}$ denotes the fuzzy morphological opening by structuring element $n\beta$ and $Mes(\Im) = \sum_{x_1} \sum_{x_2} \ldots \sum_{x_M} \mu(x_1, x_2 \ldots, x_M)$

5.2.3 Advantages of the Fuzzy Pattern Spectrum over Conventional Approaches

In the practical implementation of the fuzzy pattern spectrum, we need to determine the α-cut *a priori* in order to compute *Mes(ℑ)*. This is usually determined empirically based on the nature of images and noise. The cut at level α of a fuzzy set A with the characteristic function μ_A and is defined as follows:

$$A_\alpha = \{x : \mu_A \geq \alpha\}, \qquad \alpha \in [0,1] \qquad \textit{Eqn. 5.7}$$

The above α-cut determines the measure after a fuzzy opening. This measure (for each n) is termed as the *fuzzy opening residue* ($\aleph'_n$), that is,

$$\aleph'_n = \left[Mes(\Im_{n\beta})\right] - \left[Mes(\Im_{(n+1)\beta})\right] \qquad \textit{Eqn. 5.8}$$

It is obvious that by varying α we can in effect modify $\aleph'_n$, and thereby the fuzzy pattern spectrum. This essentially depends on the nature of the images in question. In contrast to the traditional pattern spectra based on the crisp morphological opening, this presents a significant advantage while employing the fuzzy morphological operator since there is no dual parameter to $\aleph'_n$.

To elucidate the above idea, an example of the calculation of $\aleph'_n$ is shown. We employ the result from the example of the fuzzy opening discussed earlier. In this case, we shall only determine $\aleph'_1$ which in effect is the residue calculated after the first opening of the fuzzy set A, with the structuring element B as shown earlier. From the resultant opening, we now determine the fuzzy opening residue for $n=1$.

$$\aleph_1 = \left[Mes\left(\Im\right)\right] - \left[Mes\left(\Im_\beta\right)\right] \qquad \textit{Eqn. 5.9}$$

In calculating the areas of the fuzzy sets after opening, namely $Mes(\Im)$ (the original image) and $Mes(\Im_\beta)$ (the resultant of the first opening), we need to determine the value of α. Assume that we select $\alpha = 0.5$, we shall have the original and result of the opened image matrix as below,

$$\mathcal{A} = \begin{bmatrix} 0.6 & 0.0 & 0.0 & 0.0 \\ 0.9 & 1.0 & 0.9 & 0.8 \\ 0.0 & 0.9 & 0.8 & 0.0 \\ 0.0 & 0.8 & 0.7 & 0.0 \\ 0.0 & 0.9 & 1.0 & 0.0 \end{bmatrix} \qquad O(\mathcal{A},\mathcal{B}) = \begin{bmatrix} 0.0 & 0.0 & 0.0 & 0.0 \\ 0.0 & 0.9 & 0.8 & 0.0 \\ 0.0 & 0.8 & 0.8 & 0.0 \\ 0.0 & 0.7 & 0.7 & 0.0 \\ 0.0 & 0.7 & 0.7 & 0.0 \end{bmatrix}$$

and consequently we have the calculated value of $\aleph_1$ as:

$$\aleph_1 = [Mes(\mathcal{A})] - [Mes(\mathcal{A}_\beta)]$$

$$\aleph_1 = 11 - 8$$

$$= 3$$

If we select $\alpha = 0.8$, we shall have the original $\mathcal{A}$ and result of the opened image matrix as below,

$$\mathcal{A} = \begin{bmatrix} 0.0 & 0.0 & 0.0 & 0.0 \\ 0.9 & 1.0 & 0.9 & 0.8 \\ 0.0 & 0.9 & 0.8 & 0.0 \\ 0.0 & 0.8 & 0.0 & 0.0 \\ 0.0 & 0.9 & 1.0 & 0.0 \end{bmatrix} \qquad O(\mathcal{A},\mathcal{B}) = \begin{bmatrix} 0.0 & 0.0 & 0.0 & 0.0 \\ 0.0 & 0.9 & 0.8 & 0.0 \\ 0.0 & 0.8 & 0.8 & 0.0 \\ 0.0 & 0.0 & 0.0 & 0.0 \\ 0.0 & 0.0 & 0.0 & 0.0 \end{bmatrix}$$

and we have the calculated value of $\aleph_1$ as

$$\aleph_1 = [Mes(\mathcal{A})] - [Mes(\mathcal{A}_\beta)]$$

$$\aleph_1 = 9 - 4$$

$$= 5$$

Thus, for one opening itself, we have different values $\aleph'_n$. This serves as a clear advantage in determining the optimum parameters based on the nature of images. Though the selection of α is heuristic, it can be determined based on the nature of noise or distortion expected in the images. The other values of $\aleph'_n$ can subsequently be calculated after each successive opening and the fuzzy pattern spectrum thus constructed. Although the above example may risk simplification of the actual determination of $\aleph'_n$, it strives to demonstrate the underlying idea in using fuzzy openings and α-cuts.

5.2.5 A qualitative analysis

To explain the meaning of the fuzzy pattern spectrum, we use a texture image to interpret variations in spectra with relation to specific image features. The idea is to employ a test image to generate the fuzzy pattern spectrum with relates to specific image features. In fact the technique shown here is effectively used in a texture classification scheme discussed later.

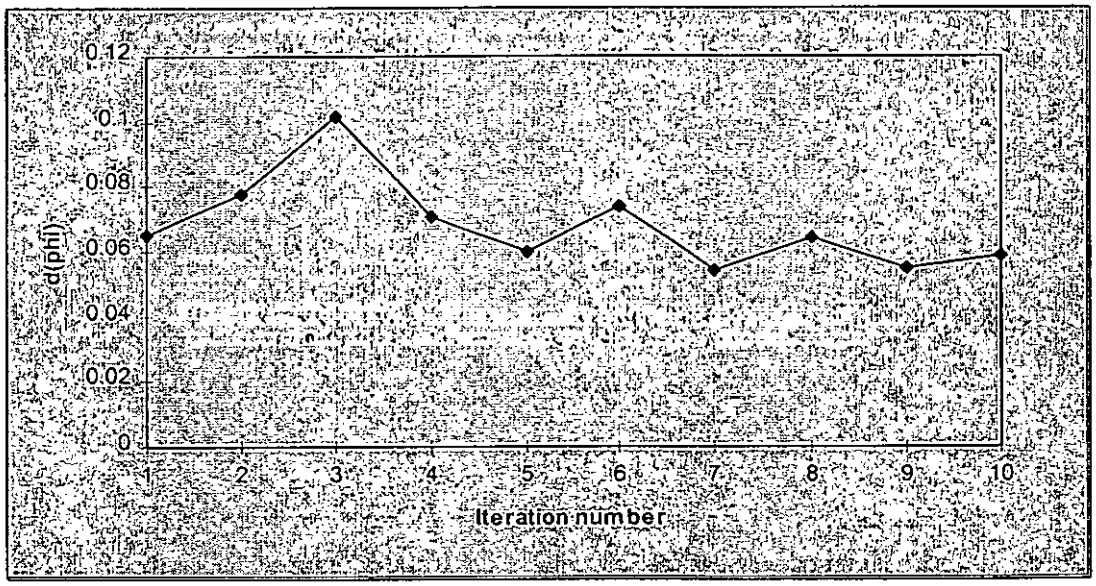

Figure 5.1 : The fuzzy pattern spectrum for a sample Brodatz texture

The fuzzy pattern spectrum shown in Fig. 5.1 has been constructed using a test texture image of coffee beans. To generate the above distribution we process the image with a series of

ten fuzzy erosions, beginning with a structuring element of diameter three pixels, which is dilated by itself after each successive erosion. At each iteration we measure the value of the fuzzy pattern spectrum by using Eqn. 5.8 shown earlier, with the value of n ranging from 0 to 10 (for a total of ten erosions). As described earlier *d(phi)* is determined by normalizing the residue after each fuzzy erosion. In our case we use the alpha cut set with $\alpha = 0.3$.

In the fuzzy pattern spectrum shown in Fig 5.1 each peak represents a significant erosion in image features, as the size of the structuring element in incrementally increased. The initial peak represents elimination of smaller features that are present in the image. It should be noted that the initial peak is largest of all, indicating the presence of a scarce number of small sized particles in the image. The subsequent peaks are less accentuated than the initial, showing that there is a consistent presence of larger features in the test image. This is precisely the case as seen in from the actual images. As the iterative erosion is stopped after a fixed number, the distribution does not represent all values up to convergence. It should be noted that the distribution is fairly even as we approach the end of the iterative process. This indicated that the image features do not vary considerably in terms of their sizes, which is in accordance with the observed results.

Needless to mention, the above qualitative explanation does not necessarily provide a comprehensive method to interpret any random shape-size distribution. In essence what is portrayed in the above explanation is a generic method to arrive at such interpretations for fuzzy pattern spectra. Later section will discuss spectra of various test images which are used in image and texture classification.

5.3 Properties of the fuzzy pattern spectrum

5.3.1 Relationship to traditional Pecstrum

In this section, we discuss some of the properties of the fuzzy pattern spectrum. It can be seen that most relations that hold true for the fuzzy opening are directly applicable to the fuzzy pattern spectrum.

5.3.2 Translation invariance:

The fuzzy morphological opening is invariant under translation, and hence we have

$$T_y[FPS(x)] = FPS[T_y(x)] \qquad \textit{Eqn. 5.10}$$

5.3.3 Rotation invariance

In general, the fuzzy pattern spectrum is variant under rotation. However, for a rotationally symmetric (isotropic) structuring elements, rotation invariance holds true. Thus, for a symmetrical Euclidean disc of finite support, rotation invariance is possible. This property has in fact been employed by Anastassopoulos et al[1991], to determine the degree of rotation of an object using asymmetrical structuring elements.

5.3.4 Non - invertibility

As the fuzzy pattern spectrum provides a non-unique representation, the original signal is not recoverable using its fuzzy pattern spectrum alone. Thus, the fuzzy pattern spectrum cannot in itself be used as a complete shape reconstruction system.

5.3.5. Area of the fuzzy pattern spectrum

In the case of the traditional pattern spectrum, the area under a finite image is always unity. Thus, we have

$$\sum_{n=0}^{+\infty} P(n) = 1 \qquad \textit{Eqn. 5.11}$$

However, for the fuzzy pattern spectrum, the above will *not* hold true, except for $\alpha = 0$. Thus, we have

$$\left.\begin{aligned} \sum_n \aleph_n \neq \sum_n Mes(\Im) \\ \sum_n Mes(\Im) \neq 1 \end{aligned}\right\} \forall\, \alpha \neq 0 \qquad \textit{Eqn. 5.12}$$

This is a direct result of the α - cuts determining the fuzzy opening residue, and is a significant departure from its non-fuzzy representation.

5.4 Applications of the fuzzy pattern spectrum

In this final section, we demonstrate the applicability of the proposed fuzzy pattern spectrum as a shape classifier and a texture descriptor, based on the results derived thus far. The first experiment demonstrates the use of the fuzzy pattern spectrum as a tool for shape classification whereas the latter applies to generating descriptors for textures.

5.4.1 Multilevel object recognition

Traditionally, in a multilevel shape recognition problem using pattern spectrum based morphological approaches, the key to a successful recognition rate has been the approach used to deal with spatial uncertainty. The limitations of the crisp pattern spectrum are evident in such a problem as the final result is entirely dependent on the criteria which are determined ad hoc. We essentially demonstrate the use of the fuzzy pattern spectrum to preserve the image characteristics while determining the pattern spectra. In our experiments, we initially used a prototype set of known images and the fuzzy pattern spectrum as a classifier for noisy shapes.

The prototype set consisted of four multilevel images (Annulus, T-shape, Star and Plane) having mutually unique fuzzy pattern spectra. The original images (figures 5.2a, 5.4a, 5.6a, 5.8a) were used to determine the residues after multi scale fuzzy openings (figures 5.2(b-g), 5.4(b-f), 5.6(b-j), 5.8(b-h). The multi scale fuzzy openings were implemented by using (digital) disk shaped structuring elements of increasing diameters. The figures showed a gradual reduction of the image area until the image residues were reduced to zero. The test set consisted of similar images which were scaled, rotated, translated and blurred by a 3x3 blurring mask (figures 5.3a, 5.5a, 5.7a, 5.9a). Blurring introduced fuzziness in the images in terms of edge ambiguity. Since structuring elements used were circular discs which are isotropic, rotation invariance was maintained. The multi scale openings of the test images are shown in figures 5.3(b-g), 5.5(b-f),

5.7(b-j), 5.9(b-h). The resultant fuzzy openings of the test set varied from the original set in terms of the pixel memberships as a direct result of the blurring of image edges. The criteria for determining the measure of variation in the fuzzy pattern spectrum for each image were calculated using the MAD (mean absolute difference) between the two image sets concerned. We define the MAD for the two fuzzy pattern spectra (FPS_1 and FPS_2) at n as follows:

$$MAD_n = \frac{\sum_{n=0}^{N-1} |FPS_1(n) - FPS_2(n)|}{N} \qquad Eqn.\ 5.13$$

Tables 5.1-4, show the resultant MAD between the fuzzy pattern spectrum of the test image sets and the original image sets and the classification results based on it. In determining the fuzzy opening residue, we used the α-cut sets with $\alpha = 0.6$ based on the type of distortion expected in the images. The maximum gray levels in the images were $\mu = 1.0$ and the minimum $\mu = 0.0$.

Table: 5.1: Resultant MAD for Annulus image

	MAD between FPS for Test Image - **Annulus**				
n	**Annulus**	**J-shape**	**Star**	**Plane**	**Result**[3]
5	0.0	1.0	200	6.0	B
9	0.0	2.5	135	131.0	B
13	0.0	4.3	128.6	134.0	B
17	0.0	59.5	112.7	134.75	A
21	0.0	81.6	127.2	133.0	A
25	0.0	91.3	138.1	124.1	A
29	0.0	91.3	122.8	124.1	A
33	0.0	91.3	135.7	124.1	A

Table 5.2: Resultant MAD for J-shaped image

[3] A = Correct classification
B = Result ambiguous i.e. more than one MSE < δ

	MAD between FPS for Test Image J-Shape				
n	Annulus	J-shape	Star	Plane	Result
5	1.0	0.0	200	4.0	B
9	2.5	0.0	135	132.5	B
13	4.3	0.0	126	132.3	B
17	59.5	0.0	134.5	121.2	A
21	81.6	0.0	178.6	156.2	A
25	91.3	0.0	204.3	140.1	A
29	91.3	0.0	179.5	140.1	A
33	91.3	0.0	206.2	140.1	A

Table 5.3: Resultant MAD for Plane image

	MAD between FPS for Test Image - Plane				
n	Annulus	J-shape	Star	Plane	Result
5	6.0	4.0	195.0	0.0	B
9	131.0	132.5	195.0	0.0	A
13	134.0	132.3	137.3	0.0	A
17	134.75	121.2	121.0	0.0	A
21	133.0	156.2	108.6	0.0	A
25	124.1	140.1	135.0	0.0	A
29	124.1	140.1	120.1	0.0	A
33	124.1	140.1	154.2	0.0	A

Table 5.4: Resultant MAD for Star image

	MAD between FPS for Test Image - Star				
n	Annulus	J-shape	Star	Plane	Result
5	200	200	0.0	195.0	B
9	135	135	0.0	195.0	A
13	128.6	126	0.0	137.3	A
17	112.7	134.5	0.0	121.0	A
21	127.2	178.6	0.0	108.6	A
25	138.1	204.3	0.0	135.0	A
29	122.8	179.5	0.0	120.1	A
33	135.7	206.2	0.0	154.2	A

In our specific examples, to determine correct recognition, the following criteria was used,

$$MAD_{0.6} < \delta \qquad \textit{Eqn. 5.14}$$

where δ is the pre-determined minimum error threshold for the specific recognition task. In our experiments, we selected $\delta = 50.0$. The value of δ is determined using the training set, and is based on the relative variation in shape between the images sets under consideration.

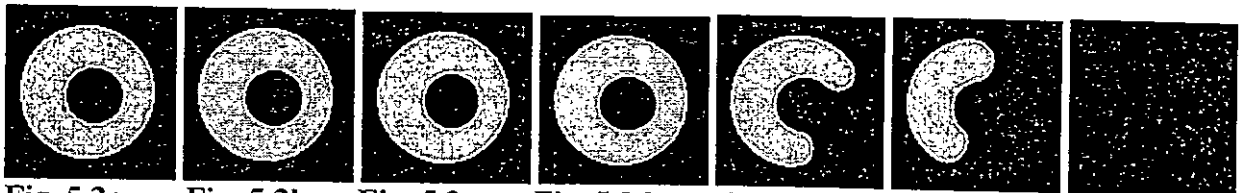

Fig. 5.2a Fig. 5.2b Fig. 5.2c Fig. 5.2d Fig. 5.2e Fig. 5.2f Fig. 5.2g

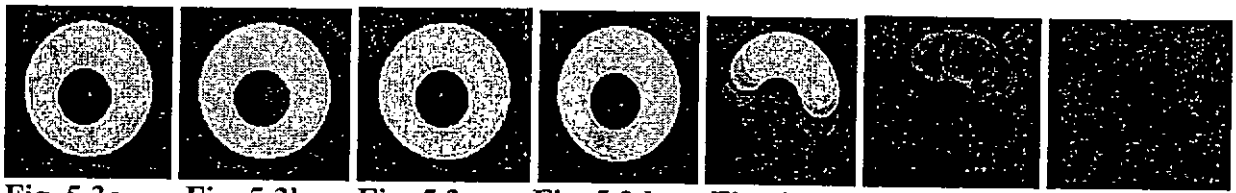

Fig. 5.3a Fig. 5.3b Fig. 5.3c Fig. 5.3d Fig. 5.3e Fig. 5.3f Fig. 5.3g

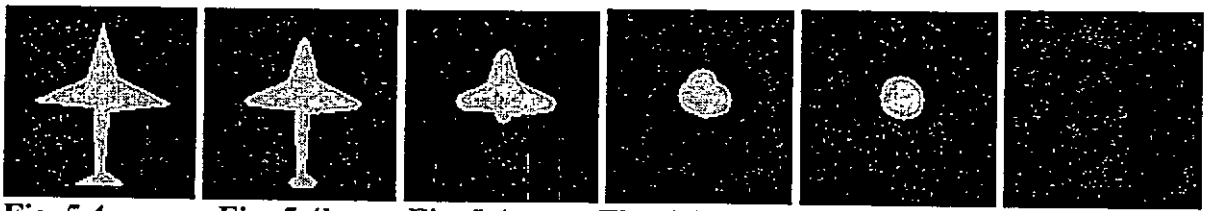

Fig. 5.4a Fig. 5.4b Fig. 5.4c Fig. 5.4d Fig. 5.4e Fig. 5.4f

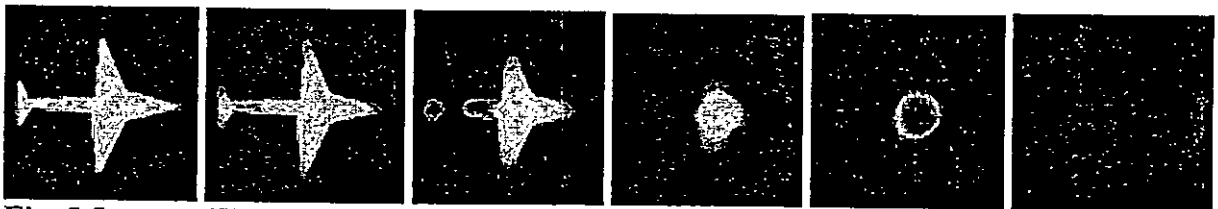

Fig. 5.5a Fig. 5.5b Fig. 5.5c Fig. 5.5d Fig. 5.5e Fig. 5.5f

Fig. 5.6a Fig. 5.6b Fig. 5.6c Fig. 5.6d Fig. 5.6e Fig. 5.6f Fig. 5.6g Fig. 5.6h Fig. 5.6i Fig. 5.6j

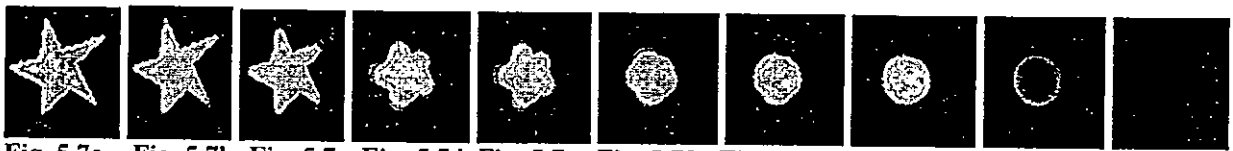

Fig. 5.7a Fig. 5.7b Fig. 5.7c Fig. 5.7d Fig. 5.7e Fig. 5.7f Fig. 5.7g Fig. 5.7h Fig. 5.7i Fig. 5.7j

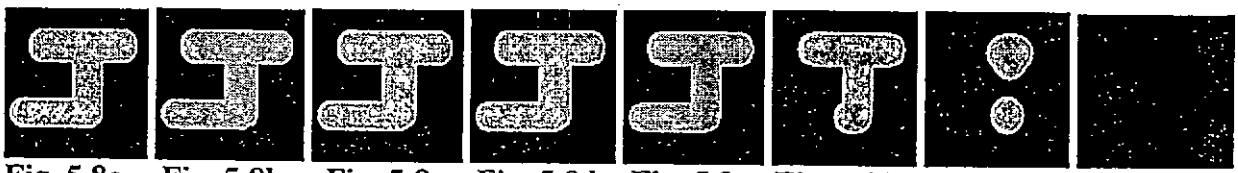

Fig. 5.8a Fig. 5.8b Fig. 5.8c Fig. 5.8d Fig. 5.8 Fig. 5.8f Fig. 5.8g Fig. 5.8h

Fig. 5.9a Fig. 5.9b Fig. 5.9 Fig. 5.9d Fig. 5.9e Fig. 5.9f Fig. 5.9g Fig. 5.9h

From the results observed in the Tables 5.1-5.4, it is clear that correct classification of a known object can be determined using the fuzzy pattern spectrum for all values of n provided $\aleph_n$ is appropriately selected based on the α-cuts, which are empirically determined. In the above results, for small values of n, there is a possibility of ambiguity in the classification process due to limitations of the square digital grid. For disks having small radii it is difficult to approximate an exact Euclidean disc in the discrete digital representations which may lead to the above phenomenon. This does not seem to present a serious drawback. In practical applications, a decision cannot be made based only on a single opening residue. In general the complete fuzzy pattern spectrum has to be used for determining the MADs.

5.4.2 Texture descriptor

In this section we discuss the fuzzy pattern spectrum as a novel descriptor for texture classification.. The experiment is performed on gray scale texture images to demonstrate its effectiveness in quantifying spatial uncertainty in images, wherein a classification accuracy of 94% is achieved.

The drawback of the traditional pattern spectra in texture classification is their inability to deal with the fuzziness in terms of image gray levels. The images need to be binarised to determine the residues and the resultant pattern spectra are highly sensitive to the thresholds in actual implementation. The fuzzy pattern spectrum alleviates this problem by dealing with gray level images directly and quantifies the shape-size distributions in terms of fuzzy memberships. In the practical implementation of the fuzzy pattern spectrum, we need to specify the α-cut which determines the value of $\aleph_n$. This presents a significant flexibility since there is no dual parameter to $\aleph_n$ in crisp pattern spectra. Though the selection of α is heuristic, it is dependent

on the actual number of erosions employed. The value of α must however be greater than zero, since $\mu = 0$ is the image background.

The application of the fuzzy pattern spectrum for texture representation and classification is demonstrated using an unsupervised classification approach. Five texture sets (D4, D20, D64, D74 and D95) were scanned from the Brodatz album[1968] at 300dpi to 256 gray level images with 256 x 256 pixel resolution. The fuzzy pattern spectrum for each image was calculated using 10 fuzzy erosions by disk shaped isotropic structuring elements, the first being a disk of diameter 3 pixels, and the rest obtained by iterative dilation of the initial structuring element by itself. Eroded results for one prototype texture (D20) are shown in Fig. 5.10. The prototype set consisted of five texture images as shown in Fig. 5.11, and their respective fuzzy pattern spectra of are as shown in Figure 5.12. The test set comprised of 50 unknown images, 10 from each texture set. The fuzzy pattern spectrum of one such test set (texture D4) are shown in Figure 5.12. The distance between the fuzzy pattern spectrum of each image in the test set and the five prototypes was calculated using the sum of absolute differences and then classified based on the minimum distance criterion. The classification results are shown in Table 5.5. The actual fuzzy pattern spectrum values generated for each of the ten test set images for texture D20 (Rattan texture image) are shown in Table 5.6.

From the set of 50 test images, 47 were correctly classified and the average error margins (average of the distance between the classification result and correct texture) for wrongly classified textures were less than 0.04. It is believed that these results could be improved using a larger number of erosions. The simulations were performed on a SparcStation2 (mem: 49152K cpu: SUNW, Sun4/75) and the user CPU times were approx. 80 seconds to generate the fuzzy pattern spectrum for each image.

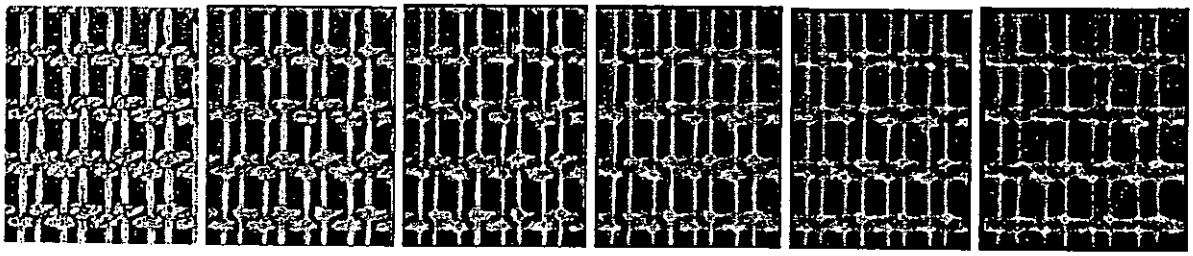

(a) (b) (c) (d) (e) (f)

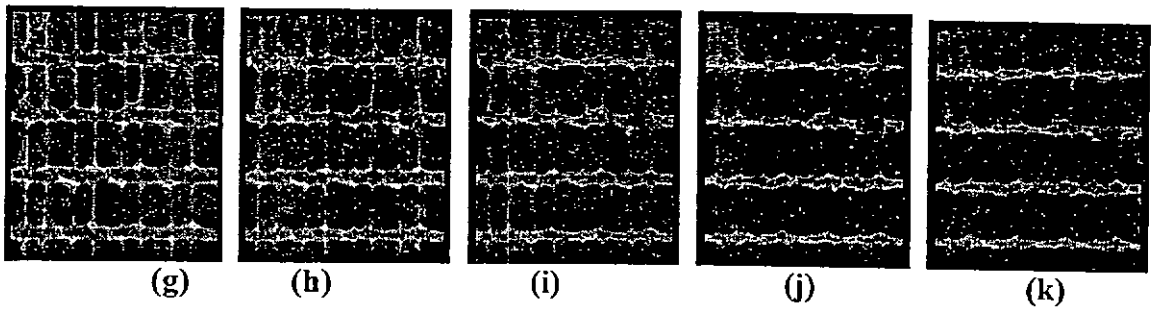

Figure 5.10: The (a) original Brodatz texture D20, and results after erosions by disk shaped structuring elements of diameters (b) 3, (c) 5, (d) 7, (e) 9, (f) 11, (g) 13, (h) 15, (i) 17, (j) 19 and (k) 21 respectively.

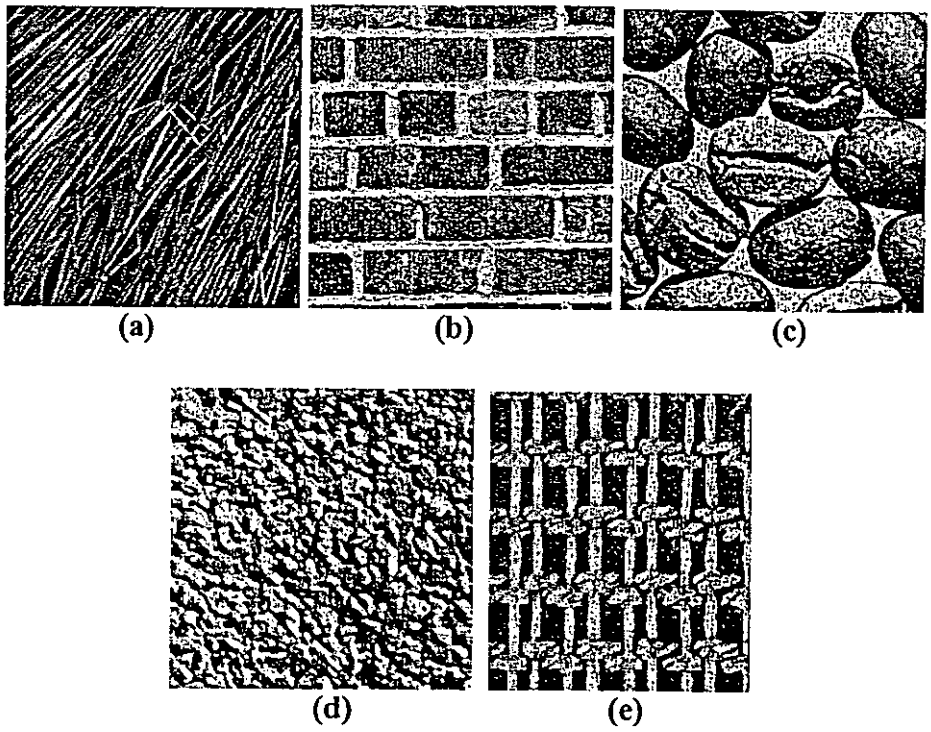

Figure 5.11: The original Brodatz texture (a) D4, (b) D64, (c) D74, (d) D95, (e) D20

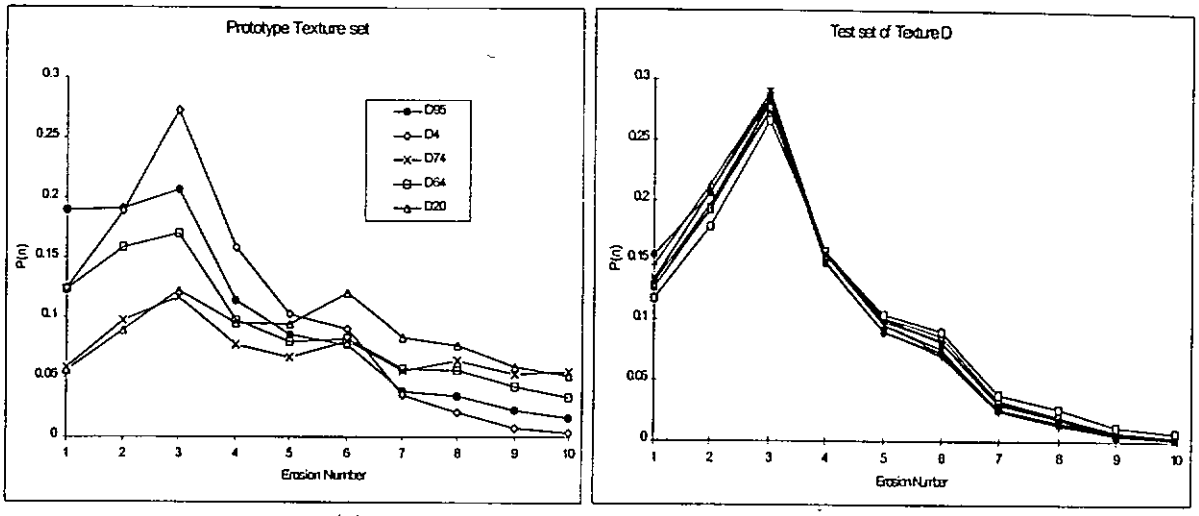

(a) (b)

Figure 5.12: A comparison of the FPS (a) of the prototype texture set and (b) the test set of texture D4. Erosion numbers 1 to 10 represent erosions by disks of diameters 3 to 21 respectively.

Table 5.5: Texture Classification Results

Texture type	Correct Classification	Wrong Classification	Average Margin of Error
D4	10	0	0
D20	10	0	0
D64	8	2	0.03
D74	10	0	0
D95	9	1	0.02

Table 5.6: The fuzzy pattern spectrum values for texture D20

	Rattan 1	Rattan 2	Rattan 3	Rattan 4	Rattan 5	Rattan 6	Rattan 7	Rattan 8	Rattan 9	Rattan 10
Erosion 1	0.1289	0.1074	0.0864	0.1029	0.0907	0.0753	0.1019	0.0774	0.0893	0.0994
Erosion 2	0.1786	0.1565	0.1377	0.1632	0.1333	0.1235	0.1432	0.1239	0.1274	0.1439
Erosion 3	0.2057	0.1835	0.1633	0.1904	0.1536	0.1395	0.1624	0.1381	0.1438	0.1599
Erosion 4	0.1056	0.1040	0.0957	0.1053	0.0935	0.0902	0.0963	0.0849	0.0896	0.0967
Erosion 5	0.0818	0.0827	0.0774	0.0767	0.0773	0.0764	0.0794	0.0695	0.0750	0.0804
Erosion 6	0.0760	0.0801	0.0756	0.0696	0.0822	0.0810	0.0781	0.0724	0.0779	0.0787
Erosion 7	0.0448	0.0543	0.0529	0.0447	0.0562	0.0550	0.0541	0.0503	0.0571	0.0530
Erosion 8	0.0412	0.0533	0.0540	0.0455	0.0576	0.0539	0.0525	0.0537	0.0597	0.0548
Erosion 9	0.0280	0.0412	0.0438	0.0336	0.0452	0.0430	0.0405	0.0428	0.0455	0.0425
Erosion 10	0.0204	0.0331	0.0406	0.0287	0.0432	0.0410	0.0357	0.0414	0.0398	0.0356

5.4.4 Conclusion and future directions

In this chapter we have introduced the concept of a fuzzy morphological pattern spectrum based on an intrinsically fuzzy morphological operations. It is envisaged that the proposed applications of the fuzzy pattern spectrum based approach could be used as a sub-system in a complete pattern recognition system for object extraction from complex images. It is obvious that the fuzzy pattern spectrum cannot be used in itself as a complete recognition system in practical applications, essentially due to its non-unique representation However this is not the intent here either. Albeit within a limited framework, the fuzzy pattern spectrum is shown to be a robust shape classifier and texture descriptor. In essence, the fuzzy pattern spectrum provides an understanding of the shape-size distribution within the scope of decision making, which is vital in a pattern recognition process.

In terms of its application to real world problems, we demonstrate the fuzzy pattern spectrum as a classifier for simple multilevel shapes having a certain amount of fuzziness or ambiguity from the training set. Additionally we demonstrate its use as a texture descriptor which would prove invaluable in cataloguing texture databases since it provides concise descriptors which can be matched easily, giving an efficient search and storage mechanism. The accuracy of descriptors can be enhanced by using fuzzy openings which yield finer spectra. The processing times for generating the FPS for textures are expected to be improved considerably using fast, optimized algorithms and parallel processing architectures.

Essentially, the fuzzy pattern spectrum can be especially useful in assigning labels to objects from many object classes. Primitive classification in character recognition problems is one of such cases. In a neural network implementation, the fuzzy pattern spectrum may be used in a supervised learning scheme by using the prototypes of known object classes. It is envisaged that future work will be based on developing a complete shape recognition system using morphological decomposition along with the fuzzy pattern spectrum as a classifier for the morphologically primitive shapes. In terms of further extending the theoretical basis of the fuzzy pattern spectrum, extension of the negative pecstrum and the pseudo-pattern spectrum to its fuzzy representation are also fruitful directions for further investigation.

Chapter Six

EPILOGUE

6.1 Recapitulation of the Thesis

Fuzzy mathematical morphology seeks to extend the scope of traditional morphology by accounting for fuzziness inherent in image processing, and in essence has formed the basis for the research work presented in the preceding chapters. In this chapter we recapitulate the contributions and enhancements to the theoretical basis along with the application of these concepts to real world problems. The final section is devoted to discussing possible future direction for research of academic interest as well as industry value.

6.2 Objectives and Accomplishments

6.2.1 Research framework and basis

The research work covering the MPhil tenure was anticipated to encompass theoretical aspects and advances in contemporary mathematical morphology and application of the mathematical basis to practical applications. The objective was to provide a thorough investigation of morphological image analysis, with the final accomplishments being of significance in terms academic value as well as industrial applicability. The literature survey and analysis of contemporary work form a significant portion of perhaps any research undertaking. Indeed, the background research work has played an indispensable role in deciding the focus of this research to be concentrated on fuzzy mathematical morphology, which is by far, one of

the most interesting developments in contemporary mathematical morphology. The ground work for establishing the fundamental basis of fuzzy mathematical morphology can be credited to Sinha, Dougherty [1992] and Bloch, Maitre[1993] which has also been the definition adopted for our proposed developments.

6.2.2 The vehicle license plate segmentation algorithm

The initial study of traditional mathematical morphology formed the basis of the design for the vehicle license plate segmentation algorithm. We employed traditional morphological operation to segment the vehicle license plate segmentation algorithm region based on detecting simple features such as characters and lines. The significant advantage over earlier proposed approaches was the minimal demands of the algorithm in terms of image requirements. The test images consisted of complex images captured by a commercial CCD camera, in natural ambient lighting conditions and tested with images in poor illumination and noise. The algorithm, albeit developed for vehicle licence plate detection, can be used in other similar applications involving detection of text, as it is based on the detection of features present in commonly in characters. Thus this algorithm can be applied to other recognition problems as well without any significant modification to the main algorithm.

In order to supplement the robustness of the algorithm and minimize false detection, the algorithm could be enhanced to detect additional features present in the license plate region. These features could include inner side of corners, which could be detected using the hit or miss transform with suitable structuring elements. Additionally, the hit or miss transform could also be employed to detect fully or partially enclosed areas with varying sizes of structuring elements. A combination of these methods would increase the robustness of the algorithm hence easing the constraints on the image requirements. This research investigation has been published in the form of a conference publication.

6.2.3 The tropical cyclone segmentation algorithm

Fuzzy mathematical morphology served as a more appropriate tool in the case of the problem of automated object segmentation from GMS imagery. The nature of the problem was to design an algorithm which used morphological filtering criteria that would provide a result within the scope of decision making. We designed a novel algorithm combining traditional as well as fuzzy mathematical morphology to segment tropical cyclones from GMS imagery. The key feature of this algorithm was its ability to deal with the ambiguity in the features required to classify a tropical cyclones, using the reasoning process used manually by a human expert.

The proposed algorithm was tested with varied images (single, multiple tropical cyclones)and experimental results were encouraging, in the sense that they were observed to be comparable to those of human experts within the specified limitations. The overall computing requirements were economically feasible as the implementation was entirely based on some efficient and simple morphological and masking operations. Furthermore, some sections can be implemented in parallel, as the algorithm is basically designed to extract features independently, hence these processing steps can be executed simultaneously. The algorithm can be used for detection of other cloud formations by simple modifications to the structuring elements and morphological operations

6.2.4 The Fuzzy Pattern Spectrum

The subsequent direction pursued was predominantly academic nature, aiming to consolidate and enhance the axioms thus far developed in the fuzzy mathematical morphology context. In terms of academic value, the most notable contribution has been introduction of the concept of a fuzzy morphological pattern spectrum based on an intrinsically fuzzy morphological operator. The proposed fuzzy pattern spectrum was aimed at establishing a theoretical framework for fuzzy granulometries, which is an enhancement to the basic theory of fuzzy mathematical morphology. The fuzzy pattern spectrum provides a tools to quantify the spatial ambiguity or fuzziness, which has thus far been solved by heuristic reasoning. The key to the flexibility of the fuzzy pattern spectrum (as opposed to the traditional non-fuzzy

pattern spectra) is the fuzzy opening residue, which essentially serves as the cognitive tool that can be customized based on the nature of the application.

The application of the proposed fuzzy pattern spectrum in multi-level object and texture classification demonstrate its robustness over traditional pattern spectra. It is envisaged that the proposed approach could be used as a sub-system in a complete pattern recognition system for object extraction from complex images. Though the fuzzy pattern spectrum cannot be used in itself as a complete recognition system it however can be used in tandem with other techniques such as morphological shape decomposition. In essence, the fuzzy pattern spectrum provides an understanding of the shape-size distribution within the scope of decision making ,which is vital in a pattern recognition process. To this effect, we have demonstrated its applicability as a primitive shape classifier and texture descriptor. Such concise descriptors would be useful in cataloguing large image databases, to reduce search matching times. Additionally, the descriptors generated using the fuzzy pattern spectrum can be used in a recognition system based solely on morphological operations. A typical system could used morphological shape decomposition algorithms

6.3 Anticipated directions and Perspectives

Mathematical morphology finds a diverse range of applications due to the intrinsic simplicity of operators employed. The basic tools are based merely on min-max operators that are easy to understand even by developers without delving into complex mathematical computations. Additionally, the min-max operators provide practical solutions for real-time applications due to the ease of implementation on pipelined or parallel architectures.

Fuzzy mathematical morphology provides a substantial enhancement over traditional techniques for processing requirements that need to deal with the inherent fuzziness in certain applications. Rather than replace traditional operations, the fuzzy operators can be employed in tandem with their crisp counterparts to provide the right blend of usability and simplicity. It is perceived that there are plentiful areas of applications where such operators would prove indispensable. Some such areas could be extraction of facial features from closed-circuit

imagery, which finds applications in information compression, and can be applicable to security and monitoring systems. The use of the fuzzy pattern spectrum as a feature descriptor which would enable a compact yet comprehensive storage mechanism for textures as also its used in determining faults and irregularities in textures. In a neural network implementation, the fuzzy pattern spectrum may be used in a supervised learning scheme by using the prototypes of known object classes. Future work could be focused on developing a complete shape recognition system using morphological decomposition along with the fuzzy pattern spectrum as a classifier for the morphologically primitive shapes. The extension of the negative pecstrum and the pseudo-pattern spectrum to its fuzzy representation is also a fruitful direction for further investigation.

Experimentation with different renditions of the index function will extend the scope of mathematical morphology. It is envisages that future work will deal with multilevel multishape object extraction, using fuzzifiers such as the π-function and the use of fuzzy logic in edge enhancement and noise filtering combined with the techniques discussed in this is extending these ideas to the negative and pseudo pattern spectrums.

The research work related to the automatic segmentation of Tropical cyclones and tropical storms from remote sensed Geo-stationary Meteorological Satellite images is also under preparation for Journal submission. Enhancements to the basic design could involve extending the implementation as a generic algorithm independent of the size of image features and determining the optimum result accuracy to computation complexity ratio. Better segmentation results can be possible by employing information from other sources in the tracking system which can be used to limit the region of interest. This follows from the fact that once the tropical cyclone is segmented from the initial image, the subsequent images can be reduced to only the possible areas of movement. Other enhancements include an introduction of some post processing steps such as image smoothing to improve segmentation results. Requirement on the tropical cyclone size can be relaxed (at the expense of computation speed) by varying the structuring elements sizes and using the same process iteratively. It should be noted that since this algorithm forms part of an expert system, there will be a certain amount of *a priori* information available. In terms of real-time implementation considerations, the proposed algorithm has been shown to be effectively implemented on standard systems. Another avenue for further development is implementation of the algorithm in hardware. As

this algorithm is based solely on simple morphology operations and image addition or subtraction it can be effectively implemented in hardware which would significantly reduce the processing time, an important factor to be considered in real time recognition systems.

In conclusion, this research work has managed to yield a thorough investigation, striking a balance between theoretical concepts and application oriented problem solving. However, there still vast areas of uncharted waters that remain to be explored. It is hoped that the theoretical foundations proposed in this work will strive to increase the popularity and applicability of morphological image processing in real-world problems.

APPENDIX A

A.1 Overview of the Software

The morphology software "Fuzzymorph", developed by our research group (led by Dr. Joe C. H. Poon) was essentially to satisfy the need for non-commercial software to implement morphological operations. The software development project was aimed at providing a comprehensive yet user friendly package that would be useful to the practicing engineer. The unique feature of this platform is that it can be used to implement traditional as well as fuzzy morphological operations including the fuzzy pattern spectrum.

A.1.1 Introduction

The implementation of some fuzzy morphological operations described in the preceding chapters, was performed using the "Fuzzymorph" platform. The platform was designed to implement fuzzy morphological operations with a view to providing cost effective solutions..

A.1.2 System Requirements

The "Fuzzymorph" platform was targeted to be implemented on most commonly available computer systems. In general the minimum system requirements for this platform are:

A PC compatible system, with at least 80386 or compatible microprocessor, running on DOS 5.0 or higher. A minimum of 4 MB of RAM should be installed, and the program executable code and supporting files require approximately 2 MB of free hard disk space. To visualize images, a VGA color monitor with at least a 256-color display card is recommended.

A.2 Using the Fuzzymorph Platform

A.2.1 Opening Screen

In Figure A.1, the opening screen of "Fuzzymorph" is shown.

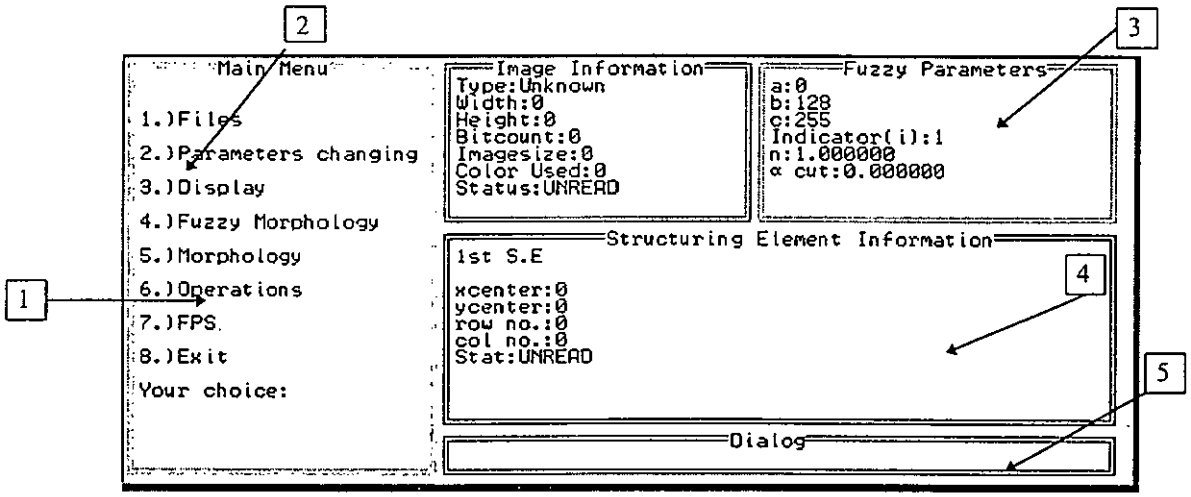

Figure A.1 The opening screen of the Fuzzymorph platform

As shown in the figure, there are several panels visible in the opening screen. Each panel displays specific information or control features to the users. Panel 1 shows the main menu listing all the basic operations provided by the platform, all the procedures available in this platform are shown in this area. Panel 2 displays the image specifics listing all image information such as width, height, size and so on will be displayed in this window. The parameters used in fuzzy morphological operations and in constructing the fuzzy pattern spectrum can be found in panel 3. They include the S function parameters a, b and c which essentially determine the fuzzification and defuzzification of the image, the indicator function parameters i and n and the α level cuts. The actual shape and size of the structuring element described by the number of rows and columns and the coordinates of the origin are shown in panel 4. Additionally, the membership values of each element within the structuring element are also displayed in this panel. However, if the diameter of the structuring is greater than 10 x 10, the its data is not be shown, due to limitation of the panel size. Panel 5 offers a command line for the user as well as the status of the processes and the error messages.

A.2.2 Main Menu

To select the operation or command, the user need only enter the number in front of the command shown in the menu windows to commence the operation. Figure A.2, shows all the sub menus that are available as main menu functions branches. The main menu, provides 8 options in all, and each can be selected by entering the number in front of the displayed command, which show the corresponding sub-menu. When option 8. (Exit) is selected, the program will be terminated and returns to the system prompt. In the following sections, we discuss the use each function in the sub-menus in detail.

In the File menu, there are 5 options viz. 1. Read Image, 2. Write Image, 3. Read S.E., 4. Auto S.E) and 5. Exit to Main.

Option 1. (Read Image) lets the user specify the image which is to be processed, by specifying the input the file name of the bitmap image in the dialog window.

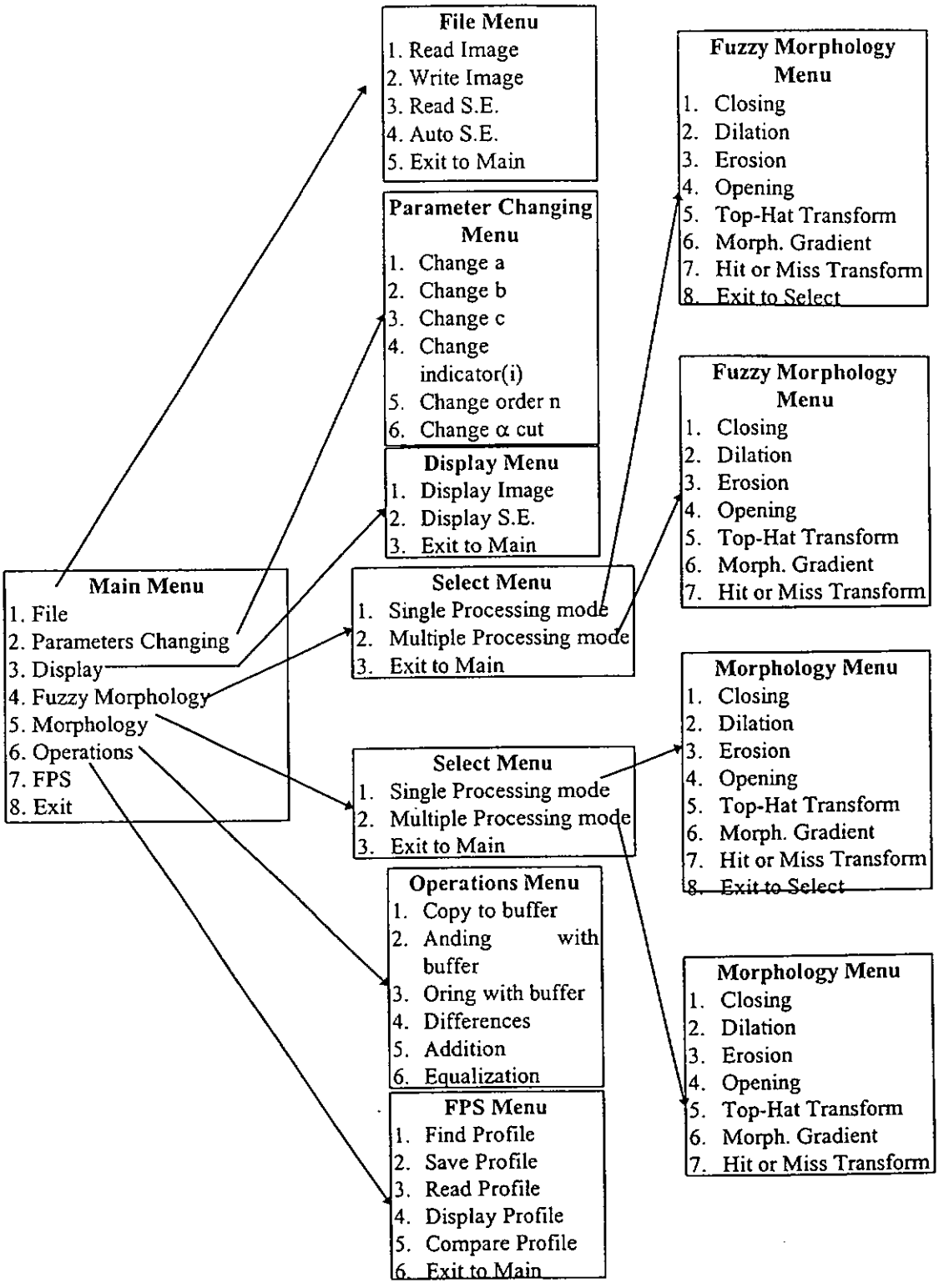

Figure A.2 Branches to sub-menus from the main menu

Option 2. (Write Image) is used to write the processed images into a file. The user will be prompted to input the file name that the result should be saved in.

Option 3. (Read S.E.) is used to read the user defined structuring elements. In the dialog box, the file name of the structuring element is specified. If the structuring element can be read successfully, the detailed configuration of the structuring element is shown in Panel 4. The maximum number of the structuring elements that can be stored is 20 and the platform will assign a number ranged from 1 to 20 to it according to the order in which each the structuring element is specified. User defined structuring elements can be created by using any text editor and the number of rows and columns and the origin of the structuring element must be specified. The system supports function type structuring element, hence the image pixel intensities can be expressed within the range from 0 - 255. An example of a typical structuring element is shown in Figure A.3.

```
11 7 6 4
0 0 255 0 0 -1 -1 -1 -1 -1 -1
-1 0 0 255 0 0 -1 -1 -1 -1 -1
-1 -1 0 0 255 0 0 -1 -1 -1 -1
-1 -1 -1 0 0 255 0 0 -1 -1 -1
-1 -1 -1 -1 0 0 255 0 0 -1 -1
-1 -1 -1 -1 -1 0 0 255 0 0 -1
-1 -1 -1 -1 -1 -1 0 0 255 0 0
```

Figure A.3: An example of structuring element

The first line of the structuring element file describes thesize and location of origin of the structuring element. The first number indicates the number of columns in the structuring element, the second indicates the number of rows and the third and fourth number indicate the x and y co-ordinates of the origin of the structuring element. (We let the horizontal direction be the x axis as it goes from left to right, and let the vertical direction be the y axis as it goes from top to bottom). The value -1 in the elements of the structuring element indicates the "ignore" state of the structuring element which would not be processed by the morphological operators. Thus irregular shaped structuring elements can also be accommodated in this system.

Option 4. (Auto S.E.) provides a standard disk shaped structuring element which is generated by the platform automatically. The diameter of the structuring element need only be specified to generate the structuring element. The element values for such a structuring element range from 0 to 255 with its origin always located at the center.

Specifying Operational Parameters

In the *Parameters Changing Menu*, there are 6 user defined parameters. These parameters give the user enough flexibility to modify each operation to achieve the desired result from the fuzzy morphological operations and the fuzzy pattern spectrum. The parameters that can be changed using this menu are a: 1. (Change a), 2. (Change b), 3. (Change c), 4. (Change indicator(I)), 5. (Change order n) ,6. (Change α-cut) and 7. (Exit to Main).

For image fuzzification we use the *S*-function or π-function as an image fuzzifier and defuzzifier to map the pixel intensities to fuzzy memberships. In an image X of dimension $M \times N$, consisting of a dark background with gray level l_{min} and a bright object region with gray level l_{max}, it would be reasonable to assign membership values, μ_{mn}, using the S function as shown in Eqn. A.1.

$$S(x;a,b,c) = \begin{cases} 0 & \text{if } x \le a \\ S_1 & \text{if } a < x \le b \\ S_2 & \text{if } b < x \le c \\ 1 & \text{if } x > c \end{cases} \qquad \textit{Eqn. A.1}$$

where:

$$S_1(x;a,b,c) = \frac{(x-a)^2}{(b-a)(c-a)}$$

$$S_2(x;a,b,c) = 1 - \frac{(x-c)^2}{(c-b)(c-a)}$$

and

$$b = \frac{a+c}{2}$$

In this example, $a = l_{min}$ and $c = l_{max}$. The membership values are assigned such that pixels closer to l_{max} are assigned values closer to 1, and those closer to l_{min} are assigned values closer to 0. Pixels with gray levels closer to the cross-over point, b, are the *fuzziest* points and are assigned values closer to 0.5.

Option 1. (Change *a)*

This function is used to change the lowest gray-level value of the *S* function. If the gray-level of a pixel is below this value, the *S* function will assigns zero membership to that pixel. By default, its value is *0*.

Option 2. (Change *b)*

This function is used to change the gray-level value of the cross over point of the *S* function which is the mid-point of the *S* function and has the membership value equal to *0.5*. A change in this value will in effect change which gray level should be mapped to the mid-point and hence change the shape of the *S* function. By default, its value is *128*.

Option 3. (Change *c)*

This function is used to change the highest gray-level value of the *S* function. If the gray-level of a pixel is greater than this value, the *S* function will give a *1* membership to that pixel. By default, its value is *255*.

Option 4. (Change *d)*

when this function is selected, the user can change the particular indicator function used in fuzzification prior to the fuzzy morphological operation or to generate the fuzzy pattern spectrum. There are in all three variations of the indicator functions available for the user to choose from based on Eqn A.2 below,

$$I(A,B) = \inf_{x \in U} \min[1, \lambda(u_A(x)) + \lambda(1 - \mu_B(x))] \qquad Eqn.\ A.2$$

The exact definition for λ can be selected by selecting from the three choices which correspond to Eqn. A.3-5. By default, Eqn A.3 is selected.

$$\lambda_n(x) = 1 - x^n, \qquad n \geq 1, \qquad \textit{Eqn. A.3}$$

$$\lambda_n(x) = \frac{1-x}{1+nx}, \qquad 0 \geq n > -1, \qquad \textit{Eqn. A.4}$$

$$\lambda_n(x) = \frac{1}{1+x^n} - \frac{x}{2}, \quad n \geq \frac{Ln(3)}{Ln(2)} = 1.5849... \qquad \textit{Eqn. A.5}$$

Option 5. (Change order *n*)

The user can vary the index value of the indicator function using this option. The range of index value will depend on which indicator function is selected, and are indicated in the prior equations.

Option 6. (Change α - cut)

This option is used to change the α-level cut for image defuzzification. If it is equal to 0, the normal defuzzification will proceed so that the inverse of the S function will be used. If not, it will act as the threshold to defuzzify the processed fuzzy data. In case of the fuzzy pattern spectrum, the α- level will be used to determine the residue following a fuzzy erosion. By default, the α level is set to 0.

Display Menu

This menu offers three options, viz 1. (Display Image), 2. (Display S.E.), and 3. (Exit to Main).

Option 1. (Display Image)

When the user selects this function from the **Display Menu**, the input image and the processed image will be displayed. The original image will be shown in the upper part of the screen while the processed image will be shown in the lower part of the screen.

Option 2. (Display S.E.)

When this function is selected, the user view the parameters of the structuring element. If the size of the structuring element is greater than 10 x 10, the entire screen will is used.

Select Menu

The Main menu options 4. (Fuzzy Morphology) or 5. (Morphology) open the Select menu. This menu offers two processing modes, the Single processing mode, which can process one single operation and the Multiple processing mode which can be used to process a batch file containing a series of operations.

Option 1. (Single process mode)

Option 1 provides the single processing mode and either traditional or Fuzzy Morphological operations can be implemented using the appropriate selection. By default, the first specified structuring element will be used for processing. If the hit or miss transform is selected, the first and second structuring elements will be used.

Option 2. (Multiple processing mode)

Option 2. facilitates the processing of a series of traditional or fuzzy morphological operations sequentially with a maximum of ten operations.

Fuzzy Morphology Menu

The fuzzy mathematical morphology menu offers seven operation viz, 1. (Closing), 2. (Dilation), 3. (Erosion), 4. (Opening), 5. (Top-Hat Transform), A. (Morph. gradient) and 7. (Hit or Miss Transform). Prior to implementing fuzzy morphological operations, the images and structuring elements need to be fuzzified by the fuzzifier described earlier. Subsequently, after processing the resultant image needs to be defuzzified. Two approaches can be employed while defuzzifying. The first one is the simple inversion of the of S function and the other to the threshold the result which will produce a binary image

Morphology Menu

In similar fashion, the morphology operation menu offers all the traditional non-fuzzy counterparts of the above mentioned operations. We apply the function-function operations while implementing gray scale morphological operations.

Image Operations Menu

There are seven image operations provided viz, 1. (Copy to buffer), 2. (Anding with buffer), 3. (Oring with buffer), 4. (Differences), 5. (Addition), A. (Equalization) and 7. (Exit to Main).

Option 1. (Copy to Buffer)

This option is used to copy the current image to the temporary image buffer.

Option 2. (Image Anding)

This operation provides a pixel wise logical "and" with the buffer and is implemented by using the following operation:

$$And(f, g) = min(f(x,y),g(x,y)) \qquad Eqn.\ A.6$$

where f and g are the image and buffered data respectively.

Option 3. (Image Oring)

This operation provides a pixel wise logical "or" with the buffer and is implemented by using the following operation:

$$Or(f,g) = max\ (\ f(x,y), g(x,y)) \qquad Eqn.\ A.7$$

where f and g are the image and buffered data respectively.

Option 4. (Image Difference)

This operation can be used to subtract the buffer by the current image.

Option 5. (Image Addition)

When this function is selected, the buffer will add with the current image.

Option 6. (Image Equalization)

This function can be used to equalize images having poor contrast by using a simple histogram equalization algorithm.

The Fuzzy pattern spectrum processing menu

In this menu, operations relating to the fuzzy pattern spectrum operations are available. In essence, the user has the option to determine the number of iteration of fuzzy operations which are used to generate the fuzzy pattern spectrum. Moreover, one can save the spectrums into file for further analysis. To relate two fuzzy pattern spectra, a comparison function is available to correlate the two spectra. The available options are: 1. (Find Profile), 2. (Save Profile), 3. (Read Profile), 4. (Display Profile), 5. (Compare Profile) and 6. (Exit to Main).

Option 1. (Find Profile)

Using this function is selected the user can calculate the fuzzy pattern spectrum of an image. The number(n) of iterations of a fuzzy opening need to be specified, based on which a set of fuzzy pattern spectrum data is generated. The intermediary images that are generated during each iteration will be saved to files named *resultxxx.bmp* (where *xxx* represents the iteration number of opening). Before the fuzzy pattern spectrum is generated, the user can modify the α-cut using Option 6. (Change α cut) in the Parameter Changing menu to the appropriate desired value.

Option 2. (Save Profile)

This function enables the user to save the generated profile into a file.. The saved files have a specific file format and contain the resulting values of the fuzzy pattern spectrum and the number of opening used to process the fuzzy pattern spectrum. These files can then be used to compare various spectra. An typical file is shown in Figure A.3,

```
5
0.186308
0.187761
0.086526
0.074632
```

Figure A.3: A typical fuzzy pattern spectrum data file

The number in the first line indicates the number of opening used to calculate the spectrum and subsequent numbers are the normalized residues generated after each iteration of the fuzzy pattern spectrum.

Option 3. (Read Profile)

The user can read the fuzzy pattern spectrum data files into a temporary buffer using this option. There are two buffers used to store the spectrum. If the first buffer is occupied, the spectrum will be read into the second buffer. If both are occupied, the spectrum in the second buffer will be removed and then the new spectrum will be read into it.

Option 4. (Display Profile)

The actual profile of the fuzzy pattern spectrum can be viewed using the option.

Option 5. (Compare Profile)

To determine the correlation among two spectrums this option is used. All the correlated values are displayed on the screen and the maximum value is found from the y-axis. Figure A.4 shows a screen shot of a typical correlation between two different spectra.

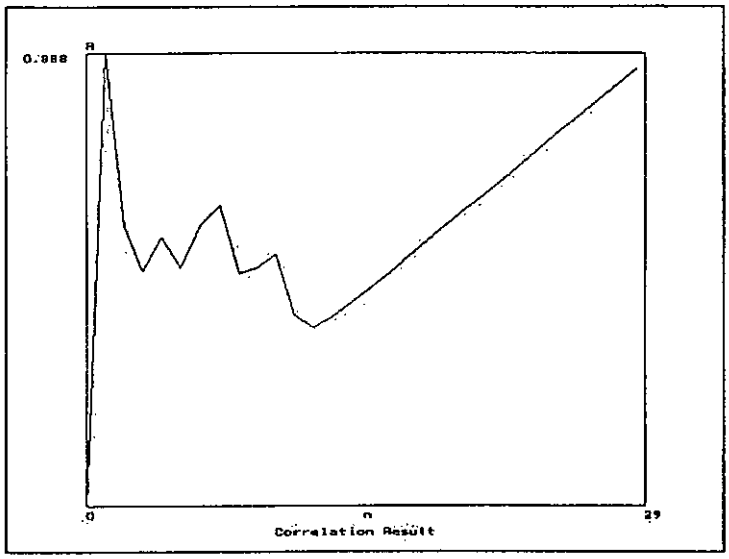

Figure A.4: An example of a typical correlation function.

REFERENCES

- AlShaykh K., Ramaswamy S., Hung H-S., "Fuzzy techniques for image Enhancement and reconstruction", *International Conference on Fuzzy Systems,* vol. 1, pp.582-87, Mar 1993, USA.
- Anastassopuolos A N, Venetsanopuolos A N "The Classification Properties of the Pecstrum and its use for Pattern Identification", *Circuits, Systems and Signal Processing,* vol. 10, pp. 293-326, 1991.
- Arce G. R., Gallagher N. C., "Median Filters: Some modifications and their properties", *IEEE Trans. on Acoustics, Speech and Signal Processing,* vol. ASSP-30, no.5, pp. 739-746, Oct. 1982.
- Arce G. R., Gallagher N. C., Nodes T. A., "Median Filters: Theory for One- and Two-Dimensional Filters", *Advances in Computer Vision and Image Processing,* vol. 2, pp. 89-166, JAI Press Inc., 1986.
- Arregui M. A., Mitxelena J. A., "Automatic Recognition of Number Plates", *Selected papers from the IVth Spanish Symposium,* vol. 1, pp.239-258, 1992.
- Batcher R., "Design of a massively parallel processor", *IEEE Transactions on Computers,* vol. C29, pp. 836-40, 1980.
- Bloch, I.; Maitre, H.," Fuzzy mathematical morphologies: a comparative study" *Pattern Recognition,* vol. 28, iss. 9, pp. 1341-87, Sept. 1995.
- Bender V., "Improvements in tropical cyclone track and intensity forecasts using the GFDL initialization system", *Monthly Weather Review,* vol. 121, pp. 2046-2061, 1993.
- Bolch I., Maitre H., "Constructing a Fuzzy Mathematical Morphology: Alternate ways", *IEEE Conference on Fuzzy Sets,* vol. 2, pp. 1303-1308, 1993.
- Bolch I., Maitre H., "Fuzzy Mathematical Morphology", *Annals of Mathematics and Artificial Intelligence,* vol. 10, pp. 55-84, May 1994.

- Bronskill J. F. Venetsanopuolos A. N., "Multidimensional Shape Description and Recognition using Mathematical Morphology", *Journal of Intelligent and Robotic Systems 1*, pp. 117-143, 1988.
- Bloch, I." Fuzzy connectivity and mathematical morphology", *Pattern Recognition Letters*, vol. 14, no. 6, pp. 483-8, June 1993
- Camps I., Kanungo T., Haralick R., "Gray-Scale structuring element decomposition", *IEEE Transactions on Image Processing*, vol. 5, no. 1, pp. 111-120, January, 1996.
- Cantoni, V., Di Gesu, and Levialdi. S. (editors), *Image analysis and processing II*, Plenum Press, New York, 1988.
- Crimmins T. R., Brown W. M., "Image Algebra and Automatic Shape Recognition", *IEEE Trans. Aerospace and Electronic Systems*, vol. AES-21, no. 1, January 1985.
- Didier D., Prade H. .*Fuzzy sets and systems : theory and applications*. New York, Academic Press, 1980.
- De-Baets B., "Idempotent Opening and Closing Operation in Fuzzy mathematical morphology", *Proceedings of ISUMA-NAFIPS'95*, pp. 228 -233, 1995.
- De Baets, B.; Kerre, E.; Gupta, M.," The fundamentals of fuzzy mathematical morphology. I.", *International Journal of General Systems*, vol. 23, iss. 2, pp. 155-71, 1994.
- Dougherty, E.R.; Sinha, D.," Computational gray-scale mathematical morphology on lattices (a comparator-based image algebra). II. Image operators", *Real-Time Imaging*, vol. 1, iss. 4., pp. 283-95, Oct. 1995.
- Dougherty, E. R., Sinha, D., Sinha, P. (1993). Shape Detection via Fuzzy Morphology, *Proceedings of the SPIE* Vol. 1904 Image Modeling, pp.172-182, 1995.
- Dougherty, E.R., Sinha, D., Sinha, P. (1992). Fuzzy Morphological Filters, *Proceedings of the SPIE Vol. 1825 Intelligent Robots and Computer Vision XI*, pp. 414-426, 1994.
- Sinha D, Dougherty E R, "Fuzzification of Set Inclusion", *Proc. of SPIE*, vol. 1708, pp. 440-449, 1992.
- Djunatan, M.; Mengko, T.," A programmable real-time systolic processor architecture for image morphological operations, binary template matching and min/max filtering" *IEEE International Symposium on Circuits and Systems*, vol.1, pp. 65-8, NY, USA, 1994.
- Dougherty E R, Giardina, C. R *Image processing : continuous to discrete*, Prentice-Hall, 1987.

- Dougherty, E.R., Sinha, D., (1991). An Intrinsically Fuzzy Approach to Mathematical Morphology, *Proceedings of the SPIE - Intelligent Robots and Computer Vision*, vol. 1607, pp.477-488, 1993.
- Dougherty, E. R., *Matrix structured image processing*,. Prentice Hall, 1987.
- Duff M.J.B, Watson D. M., Fountain T. J., Shaw G. K," A cellular Logic Array for image processing", Pattern Recognition, vol.5, pp. 349-56, 1973.
- Ghadiali M. D., Poon J. C. H, Siu W. C.,"Fuzzy Pattern Spectrum as a Texture classifier", *Electronics Letters*, vol 32, no. 19, pp. 1772-3, 1996.
- Gao Z., He H., Liu J., Xi P., The Fuzzy Morphology induced by threshold decomposition, *Proceedings of the SPIE*, vol. 2300, pp. 268-278, 1994.
- Gonzalez R. C., Woods R. E., *Digital image processing*, Reading, Mass. : Addison-Wesley, 1992.
- Golay R.," Hexagonal Parallel transformations", *IEEE transcations on computers*, vol.C19, no 8, August 1969.
- Goetcherian V., "From Binary to Gray Tone Image Processing Using Fuzzy Logic Concepts", *Pattern Recognition*, vol.12, pp. 7-15, 1980.
- Grabisch M., Schmitt M., " Mathematical Morphology, Order Filters and Fuzzy Logic", *4th IEEE Int'l Conf on Fuzzy Systems and the 2nd Int'l Fuzzy Engineering Symposium*, vol4, pp. 2103-8, USA. 1995.
- Gupta M. M., Knopf G. K.," Shape representation using a fuzzy morphological thinning algorithm", *Intelligent Robots and Computer Vision XIII: Algorithms and Computer Vision, SPIE*-vol. 2353, pp. 448-59, 1994.
- Harilick R. M., Chen S., Kanungo. T., "Recursive Opening Transform", *IEEE Computer Society Conference on Computer Vision and Pattern Recognition*, pp. 560-565, 1992.
- Harilick R. M., Stemberg R., Zhuang X, "Image Analysis using Mathematical Morphology", *IEEE Trans. PAMI*, pp. 532-550, July 1987.
- Holland, G. J., Ready Reckoner, *World Meteorological Organization, Geneva*, WMO/TC-No. 560, Report No. TCP-31., 1993
- Hong K. C., Park R-H.," Inspection and subpixel alignment of SMD's using fuzzy morphology", *Journal of the Korean Institute of Telematics and Electronics*, vol. 31B, iss. 9, pp. 112-23, Sept. 1994.

- Huang C.-P., Chaparro, L.F.," Signal representation using fuzzy morphology", *Proceedings of ISUMA - NAFIPS '95 The Third International Symposium on Uncertainty Modeling and Analysis and Annual Conference of the North American Fuzzy Information Processing Society,* pp. 607-12, CA, USA,1995.
- Hyonam J., Haralick R., "Understanding the application of mathematical morphology to Machine Vision", *IEEE Int'l Symposium on Circuits and Systems,* pp.977-982, 1989.
- Jin, X.C.; Ong, S.H., Jayasooriah K.," A domain operator for binary morphological processing", *IEEE Transactions on Image Processing* Vol: 4 Iss: 7 p. 1042-6, July 1995.
- Jin, X.C., Ong, S.H., Jayasooriah K.," Nuclear segmentation using domain operations", *Proceedings of the 16th Annual International Conference of the IEEE Engineering in Medicine and Biology Society,* pp. 1071-2 vol.2 New York, NY, USA, 1994
- Jain, A. K., *Fundamentals of digital image processing* Englewood Cliffs, N.J. : Prentice Hall, 1989.
- Krishnamurthy, P., "Histogram-Based Morphological edge detector", *IEEE Transactions on Geoscience and Remote Sensing,* vol. 32, no. 4, pp. 759-767, 1994.
- Kawamura M, Tsujiko Y., " An approach to geographical Pattern Recognition Using Mathematical Morphology", *International Geoscience and Remote Sensing Symposium,* vol. 2, pp. 872-875, 1994.
- Levine, M. D., *Vision in man and machine,* New York: McGraw-Hill, c1985.
- Lea, L. A. Kellar G., "An algorithm to smooth and find objects in Astronomical Images", *The Astronomical Journal,* vol. 97, no. 4, pp. 1238-1246, 1989.
- Laplante, P.A., Sinha, D.," An architecture for fuzzy morphological operations", *Intelligent Robots and Computer Vision XI- Proceedings of the SPIE,* Vol: 1826 pp. 189-95, 1992.
- Matheron G., *Random Sets and Integral Geometry,* Wiley, New York, 1975.
- Maccarone M. C., Tripiciano M., Di Gesu V., "Mathematical Morphology and Image Analysis: A Fuzzy Approach", *Proc. Of the International Workshop on Knowledge based Systems and Models of Logical reasoning,* Cairo, 1988.
- Maccarone M. C., Tripiciano M., Di Gesu V., 'Fuzzy mathematical Morphology to Analyze Astronomical Images", *IEEE International Conference on Systems, Man and Cybernetics,* pp. 249-251, vol. 1, 1991.

- Maragos P., Schafer R., "Morphological Filters-Part I: Their Set Theoretic Analysis and relations to Linear Shift Invariant Filters ", *IEEE Trans. on Acoustics, Speech and Signal Processing,* pp. 1153-1169, vol. ASSP-35, No.8, 1987.
- Maragos P., Schafer R., "Morphological Filters-Part II: Their relations to Median, Order-Statistic and Stack filters", *IEEE Trans. on Acoustics, Speech and Signal Processing,* pp. 1170-1182, vol. ASSP-35, No.8, 1987.
- Maragos P., "Pattern Spectrum and Multiscale Shape Representation", *IEEE Transactions on Pattern Analysis and Machine Intelligence,* vol. 11, no. 7, pp. 701-716, 1989.
- Maragos P., Schafer R., "Morphological Filters-Part I: Their set-Theoretic Analysis and Relation to Linear Shift-Invariant Filters", *IEEE Transactions on Acoustics, Speech and Signal Processing,* vol. ASSP-35, no 8, 1153-1169, 1987.
- Maragos P., "Pattern Spectrum and Multiscale Shape Representation", *IEEE Transactions on Pattern Analysis and Machine Intellligence,* vol. 11, no. 8, 1991.
- Montgomery B, Farrell F., "Tropical cyclone formation", *Journal of the Atmospheric Sciences,* vol. 50, no.2, pp. 285-310, 1993.
- Pal K., King R. A, "On Edge Detection of X-Ray images using Fuzzy Sets", *IEEE Trans. Pattern Analysis and Machine Intelligence,* pp. 60- 77, vol. PAMI-5, no. 1, Jan. 1983.
- Pal K., Rosenfeld A., " Image Enhancement and thresholding by optimization of fuzzy compactness", *Pattern Recognition Letters,* pp. 77-86, vol. 7, no. 2, Feb. 1988.
- Pitas V. N., Venetsanopoulos A. N., "Morphological Shape Representation", *Pattern Recognition,* vol. 25, no. 6, pp. 555-565, 1992.
- Pitas V. and A. N. Venetsanopoulos, *Nonlinear digital filters : principles and applications,* Kluwer Academic Publishers, 1990.
- Poon J. C. H, Ghadiali M. D., Man G. M., Lau M. S., "A Robust Vision System for Vehicle License Plate Recognition using gray scale Morphology", *International Symposium on Industrial Engineering,* vol. 1, pp. 394-399, Greece, 1995.
- Popov, A. T., "Fuzzy convexity and mathematical morphology", *Vision Geometry IV- Proceedings of the SPIE* Vol: 2573 p. 45-51, 1995.
- Preteux, F., " Advanced mathematical morphology: from an algebraic to a stochastic point of view (image analysis)" *Image Algebra and Morphological Image Processing III Proceedings of the SPIE,* Vol: 1769 p. 44-58, 1992.

- Popev, A. T., " Morphological operations on fuzzy sets", *Fifth International Conference on Image Processing and its Applications* (Conf. Publ. No.410) p. 837-40, London, UK, 1995.
- Rea, J. A., Longbotham, H. G., Kothari H. N.," Stack filters: Relating fuzzy theory to mathematical morphology and order statistics", *Nonlinear Image Processing VI Proceedings of the SPIE* Vol: 2424, pp. 217-27, 1995.
- Rea, J. A., Longbotham, H. G., Kothari H.N, " Fuzzy logic and mathematical morphology: implementation by stack filters" *IEEE Transactions on Signal Processing* Vol: 44, Iss: 1, p. 142-7, Jan. 1996.
- Russ, J. C., *The image processing handbook,* Boca Raton, Fla.,CRC Press, 1992.
- Serra J., "Introduction to Mathematical Morphology", *Computer Vision, graphics and Image Processing,* 35, 283-305. 1986.
- Serra J., *Image Analysis and Mathematical Morphology,* Academic Press, 1987.
- Serra J. and Soille P., *Mathematical morphology and its applications to image processing* (Boston: Kluwer Academic Publishers), 1994.
- Serra J., *Mathematical morphology and its applications to image processing,* Kluwer Academic Publishers, 1994.
- Serra J., Vincent L., "An Overview of Morphological Filtering", *Circuits, Systems and Signal Processing,* vol. 11, no. 1, pp. 47-108, 1992.
- Sinha, D.; Dougherty, E. R.," A general axiomatic theory of intrinsically fuzzy mathematical morphologies", *IEEE Transactions on Fuzzy Systems,* Vol: 3 Iss: 04 p. 389-403, Nov. 1995.
- Sinha D, Dougherty E R," Fuzzy Mathematical Morphology", *Journal of Visual Communication and Image Representation,* pp. 286-302, vol. 3, no. 3, Sept. 1992.
- Sinha, D., Sinha, P., Dougherty, E. R. "Algorithm development for fuzzy mathematical morphology", *Image Algebra and Morphological Image Processing IV - Proceedings of the SPIE,* Vol: 2030 p. 220-30, 1993.
- Sinha D., Dougherty E. R., "Characterization of Fuzzy Minskowski Algebra", *Proceedings of the SPIE,* vol. 1769, pp. 59-69, 1992.
- Srivastava R.; Davidson J.L.," Fuzzy image algebra neural networks for target classification", *Image Algebra and Morphological Image Processing V - Proceedings of the SPIE,* Vol: 2300 p. 145-56, 1994.

- Sternberg, R., "Grayscale Morphology", *Computer Vision, Graphics and Image Processing*, vol. 35, pp. 333-355, 1986.
- Sternberg, R, " Pipeline architectures for image processing", *Multi-Computers and Image processing* (K Preston, L Uhr ed.), Academic Press, NY, 1982.
- Uchida et al, " Low-level Cloud Motion Wind Field Estimated from GMS Short Interval image in Typhoon vicinity", *Geophysical Magazine*, vol. 44, no. 1, 1991.
- Wang, D., He, D-C., Morin D., "Classification of Remote Sensed Images using Mathematical Morphology", *International Geoscience and Remote Sensing Symposium*, vol. 3, pp. 1615-1617, 1994.
- Zadeh L., "Fuzzy Sets", *Information and Control*, pp. 338-353, vol. 8, 1965.